Elsa Daniela Costa Silva

MULTIFUNCTIONAL MAGNETIC-RESPONSIVE HYDROGELS TO ENGINEER TENDON-TO-BONE INTERFACE

Dissertação de Mestrado

Mestrado Integrado em Bioengenharia

Ramo Biotecnologia Molecular

Trabalho efetuado sob a orientação de

Doutora Maria Manuela Estima Gomes

Doutor Pedro Lopes Granja

Setembro, 2016

Agradecimentos

A realização do mestrado em Bioengenharia da Universidade do Porto é algo, que traduz extensas horas de trabalho e reflexão. No entanto na elaboração do trabalho de investigação não seria possível sem os inúmeros contributos daqueles que, de forma direta e/ou indireta contribuíram para a realização desta etapa, pelo que todos merecem o meu público agradecimento. Não obstante, há contributos que não posso omitir pela relevância que possuíram na conclusão desta etapa, como tal utilizo este meio para deixar uma palavra de apreço a algumas pessoas em especial.

Não atribuindo maior ou menor relevância pela ordem de agradecimentos, gostaria de em primeiro lugar agradecer ao Professor Rui Reis pela oportunidade de desenvolver o projeto de dissertação de mestrado neste centro de investigação.

À professora Manuela, que na qualidade de orientadora sempre demonstrou total disponibilidade, dedicação, empenho, celeridade na resposta e auxílio. Ressalvo a sua excelente orientação, competência, sentido crítico, exigência. Mas principalmente a frontalidade com que conduziu a presente investigação. Deste modo, e considerando os demais atributos, revelou-se um pilar essencial nesta investigação. Ao Doutor Pedro Granja, por ter sempre colocado ao meu dispor todo o seu laboratório bem como por toda a disponibilidade e celeridade na resposta.

À minha mentora Márcia Rodrigues, devo o meu profundo e sentido agradecimento pela colaboração, recetividade, companheirismo e atenção demonstrados no desenvolvimento deste trabalho de investigação, que em diversos momentos foram cruciais para a prossecução do mesmo. A inquestionável disponibilidade culminou na resposta a várias incógnitas, inquietações e desorientações. Quero salientar a sua enorme capacidade de em situações de elevada sensibilidade saber levar a bom porto a minha personalidade irreverente e assim potenciar a minha evolução nas mais diversas áreas.

Ao meu amigo e mentor Pedro, deixo aqui o meu sincero agradecimento, a ele devo grande parte do conhecimento adquirido, do desenvolvimento da capacidade crítica e de raciocínio. Muito obrigada pelas horas disponibilizadas, pela pronta disponibilidade e fácil resposta, mesmo enquanto escrevia a sua tese de doutoramento. Ressalvo a tua extraordinária capacidade de absorver conhecimento e a natural predisposição para o expores de forma coerente e explícita.

Não posso deixar de exprimir o meu profundo agradecimento à Raquel, por inúmeras vezes me demonstrar outro ponto de vista sobre as situações e por me ensinar a demonstrar de forma convicta que uma ideia frágil pode ser algo extremamente coeso. E para a minha Anita um muito obrigado por toda a ajuda, compreensão e por me ouvir sempre com tanta atenção durante toda esta caminhada. Assim não esquecendo ninguém, a toda a equipa da Professora Manuela um muito obrigado.

Não poderia deixar de agradecer aos meus meninos e meninas dos 3Bs, a quem devo todos os momentos bem passados, todas as histórias que fizeram com com que esta caminhada fosse realizada com uma imensa alegria, mesmo nos momentos criticos. Cada um com a sua particularidade conseguiu fazer a diferença. Não menos importantes os meus companheiros do Porto, obrigada por estes 5 anos incriveis, um muito obrigado. Em especial ás meninas Joana, Inês e Sara basicamente por tudo. Mesmo entre cidades, continuamos como se não tivesse passado um unico dia. Um especial obrigado para a equipa "achilles" pela infindável luta diária que foi esta última semana passada na Holanda.

Por fim o mais importante, obrigada á minha familia que tão de perto e tão particularmente acompanhou esta evolução e que me fez cair, tantas vezes na real. Tão diferentes e tão iguais fazemos a diferença.

DESENVOLVIMENTO DE HIDROGEIS MAGNÉTICOS MULTIFUNCIONAIS PARAESTRATÉGIAS DE ENGENHARIA DE TECIDOS DA INTERFACE TENDAO/OSSO

Resumo

As limitações das terapias usadas actualmente no restabelecimento completo das funções de um tecido após uma lesão, levaram à criação de novas abordagens de Engenharia de Tecidos e ao desenvolvimento de biomateriais funcionais capazes de guiar a sua regeneração. Entre essas estratégias, a área da Engenharia de Tecidos que aborda o possivel impacto das forças magnéticas propõe, a aplicação de forças e elementos magnéticos como ferramentas multifuncionais melhoradas para aplicações biomédicas. Na verdade, o uso de sistemas magnéticos inteligentes visa o fornecimento de sinais com instruções celulares melhoradas, que podem ser controlados remotamente por elementos magnéticos do sistema dando assim resposta aos requisitos exigidos pelo tecido para as terapias de regeneração.

No caso particular das interfaces de tecidos, como a interface tendão-osso, em que os tecidos são interdependentes complexos, torna-se fundamental a produção de sistemas versáteis com funcionalidades que possam ser remotamente manipuladas sob a actuação de um campo magnético externo.

Assim, o presente estudo propõe o desenvolvimento de um sistema de transporte de células responsivo a um campo magnético, que combina uma matriz fotopolimerizável de sulfato de condroitina, enriquecida com lisado de plaquetas (PL), capaz de gerar blocos de construção ajustáveis, que visam a construção da interface tendão-osso. Este é um sistema versátil que apresenta várias funcionalidades, combinando a modulação das propriedades intrínsecas de um hidrogel com um reservatório de células e libertação de factores de crescimento [1].

De modo a proporcionar uma capacidade de resposta magnética e permitir que o sistema possa ser controlado remotamente ou manipulado ex vivo, foram produzidas nanopartículas magnéticas (MNPs), revestidas com met-CS (met-CS MNPs), possibilitando a sua ligação com o hidrogel. Assim, antes da sua incorporação na matriz do hidrogel de met-CS enriquecida com PL, as Met-CS MNPs foram produzidas e caracterizadas em termos morfológicos, físico-químicos e magnéticos. O impacto da actuação do campo magnético externo nas propriedades intrínsecas do sistema foi também avaliado, revelando que este modula o swelling, a degradação e a libertação

dos factores de crescimentos naturalmente disponíveis na matriz do hidrogel enriquecida com PL. Para além disso, considerando a aplicação do sistema na interface tendão-osso, que é uma zona naturalmente predisposta à lesão e que requer não só uma distribuição espacial das diferentes populações celulares, mas também um ambiente temporal e espacial estável que possibilite o estabelecimento das interacções célula-célula e entre a célula e o seu ambiente, os hidrogéis produzidos foram cultivados quer com pre-osteoblastos diferenciados de células estaminais derivadas do tecido adiposo (pre-Ost), quer com células de tendão humanas (hTCs). Assim, os constructs 3D constituídos apenas por uma unidade (osso ou tendão), ou compostos por duas unidades interconectadas (unidades de osso e tendão) foram unidos e cultivados durante 21 dias sob estimulação de campo magnético. Posteriormente, procedeu-se à sua caracterização em termos de actividade metabólica, proliferação, e expressão proteica dos genes associados ao osso-tendão.

Os resultados obtidos confirmaram que tanto as células hTCs como as pre-Ost cultivadas nos hidrogéis desenvolvidos no âmbito deste projecto, são capazes de proliferar, colonizar e expressar os marcadores associados ao tendão e ao osso, respectivamente, e que MF parece ter um impacto na morfologia e produção matriz extracelular que de alguma forma mimetiza os sistemas muscoesqueléticos como tendão e osso, efeito esse que é melhorado nos sistemas de co-cultura. Em suma, o presente trabalho demostra que os hidrogéis responsivos ao campo magnético apresentam propriedades multifuncionais, que podem ser moduladas externamente através de estimulação MF. Para além disso, o sistema proposto apresenta ainda potencial para diferentes tipos de células e consequentemente diferentes aplicações na área de engenharia de tecidos, tendo demonstrado um especial interesse para interfaces de tecido, nomeadamente para a interface tendão-osso.

Multifunctional Magnetic- Responsive Hydrogels to Engineer Tendon-to-Bone Interface

Abstract

Magnetic tissue engineering is an innovative approach, in the field of tissue engineering that envisions the use of magnetic elements to develop multifunctional systems that can enable remote in vitro and/or ex vivo manipulation, as means to address the demanding requirements to achieve the successful regeneration of tissues. This is particularly important for bioengineering complex tissues and/or tissue interfaces that must use versatile systems, in order to fulfill diverse requisites and enable various functionalities simultaneously. For example, tendon-to-bone interfaces are very prone to injury situations that are not completely solved with currently available techniques. However, engineering these tissues interface and requires the development of systems that can accommodate a proper spatial distribution of different cell populations and provide them an appropriate mechanical and biochemical environment.

Photocrosslinkable natural based hydrogel matrices have received great interest for tissue engineering strategies, especially because they provide versatile systems that can be tailored to diverse applications. The incorporation of magnetic nanoparticles (MNPs) into these systems might enable additional advantages, such as the possibility of being remotely controlled and/or further manipulated both in vitro and ex vivo, throught the application of controlled magnetic stimulus.

Therefore, this work reports on the development of a photocrosslinkable magnetic responsive hydrogel made of a methacrylated chondroitin sulfate (met-CS)-based matrix enriched with platelet lysate (PL), envisioning the generation of tunable hydrogel building blocks to engineer tissue interface such as tendon-to-bone. To provide magnetic responsiveness, magnetic nanoparticles (MNPs) coated with met-CS (met-CS MNPs) were produced to enable their linkage to the hydrogel matrix.

For that met- CS MNPs were produced and characterized physically, morphologically and physicochemically characterized aiming a further incorporation into met-CS hydrogel matrices enriched with PL. The impact of the actuation of an external magnetic in the field into the intrinsic properties of the system was assessed, revealing that through the use of this mechanical stimuli it is possible to modulate the swelling, degradation and release of growth factors naturally present

PL. Moreover the potential use of this versatile hydrogel in tendon-to-bone and the possible impact of EMF was assessed in in hydrogels units laden with either pre-osteoblasts differentiated from human adipose derived stem cells (pre-Ost) or human tendon derived cells (hTDCs), cultured in single units or in co-cultures. The obtained results confirmed that both hTDCs and pre-Ost cells are able to proliferate, colonize and express tendon and bone related markers in the developed hydrogels. Moreover, EMF seems to impact cell morphology and synthesize a tendon- and bone-like ECM, being this effect highlighted in co-culture systems. Together, these results suggest that developed hydrogel represents a potential cell laden system for tissues interface engineering in which the properties can be externally modulated through EMF stimulation

Table of Contents

List of Abbreviations

A	
ADH	Adipic Acid Dihydrazide
AKT	Protein kinase B
AMF	Alternating Magnetic Field
ASCs	Adipose Stem Cells
B	
BBB	Blood-Brain Barrier
BCL-2	B-cell protein 2
C	
COLAI	Collagen I
Ch	Chitosan
Cryo-SEM	Low Temperature Scanning Electron Microscopy
CS	Chondroitin Sulfate
CS-A	Chondroitin Sulphate A
CSses	Chondroitinases
D	
DCN	Decorin
Dm	Degree of Methacrylation
DMA	Dynamic mechanical analysis
DMSA	Dimercaptosuccinic Acid
E	
E	Young's Modulus
E'	Storage Modulus
ECM	Extracellular Matrix
EDCI	1-Ethyl-3-(3-dimethylaminopropyl)carbodiimide
ELISA	Enzyme-linked Immunosorbent Assay
EMF	External Magnetic Field
EOEOVE	(2-ethoxy)ethoxyethyl Vinyl Ether
F	
FDA	Food and Drug Administration
FTIR	Fourier transform infrared spectroscopy
G	
GAG	Glycosaminoglycan
GAPDH	Glyceraldehyde 3-phosphate dehydrogenase
GFs	Growth Factors
H	
HASCs	Human Adipose Stem Cells
HAses	Hyaluronidases
HTDCS	Human Tendon Derived Stem Cells
Hsp25	Heat shock protein 25
HCl	Hydrochloric acid
Hz	Hertz
J	
JNK	C-Jun N-terminal Kinases
L	
LbL	Layer-by-Layer
M	
magTE	Magnetic Force-based Tissue Engineering
Met-CS	Methacrylated Chondroitin Sulphate
Met-CS	Methacrylated Chondroitin Sulphate
MNPs	Nanoparticles
MAGPL	Magnetic Responsive Hydrogels Enriched with Platelet Lysate
MLs	Magnetic Liposomes
MPs	Magnetic Particles
MRI	Magnetic Resonance Imaging
N	
NGF	Nerve Growth Factor
NMR	Nuclear Magnetic Resonance
NPs	Nanoparticles

O

ODVE	Octadecyl Vinyl Ether
OPN	Osteopontin

P

PBS	Phosphate Buffered Saline
PC	Platelet Concentrate
PCL	Poly(L-lysine)
PDMS	Polydimethylsiloxane
PDGF-BB	Platelet Derived Growth Factor
PEG	Polyethylene glycol
PEMF	Pulsed Electromagnetic Field
PL	Platelet Lysate
Pre-ost	Pre-osteoblastic
PRF	Platelet-rich Fibrin
PRHds	Platelet-rich Hemoderivates
PRP	Platelet-rich Plasma

R

ROS	Reactive Oxygen Species
RT-PCR	Real-Time Polymerase Chain Reaction

S

SPIONs	Superparamagnetic Iron Oxide Nanoparticles
SVF	Stromal Vascular Fraction

T

Tan δ	Loss factor
TEM	Transmission electron microscopy
TGA	Thermogravimetric analysis
TEN-C	Tenascin-C
TERM	Tissue Engineering Regenerative Medicine
TF	Transferrin

LIST OF FIGURES

LIST OF TABLES

CHAPTER I GENERAL INTRODUCTION

This chapter is based on the following publication:

Silva ED, Gonçalves AI, Santos LJ, Rodrigues MT, Gomes ME (2016) "Magnetic-responsive Materials for Tissue Engineering" in Fundamental Principles of Smart Materials for Tissue Engineering (Qu Wang, Editor), RSC Smart Materials Series, accepted.

MAGNETIC-RESPONSIVE MATERIALS FOR TISSUE ENGINEERING AND REGENERATIVE MEDICINE

Abstract

Novel tissue engineering approaches are emerging to meet regenerative medicine demands and challenges towards successful therapies to completely restore the function in damaged or degenerated tissues. Among them, magnetic tissue engineering envisions the development of complex systems in which magnetic elements are exploited as remotely controlled multidimensional tools with potential for diagnostic and therapeutic actions.

This chapter provides an overview of the latest developments on the design and assessment of magnetic tissue engineering strategies with particular emphasis on smart magnetic materials and its relevance for tissue regeneration. Special attention will be given to the fabrication of sophisticated systems from nano to macro scale, and to the role of magnetic smart materials for providing alternative approaches to address the demanding tissue requirements and meet successful alternative strategies for regenerative medicine. The cellular response to the presence of magnetic elements will be also considered in this chapter, including internalization and clearance mechanisms as well as the relevance of magnetic stimulation for cell proliferation and differentiation among other biological processes.

1. INTRODUCTION

1.1 Magnetic Forces in Living Systems

All living organisms are daily exposed to the influence of external forces characterized by distinct physical parameters, including the stimuli provided by magnetic fields. Magnetic forces reveal a fundamental influence in processes as different as the seasonal migration of bird and mammal species, or the homeostasis and equilibrium of endogenous biological processes.[2]

Indeed, living organisms, namely the rainbow trout and some species of bacteria, align themselves with Earth´s North Pole. In bacteria, the biological response is due to the presence of magnetosome, an organelle that contains magnetite, the principal element involved in their magnetic responsive capacity, which orients magnetotactic bacteria towards the direction of the magnetic field.[3],[4]

The discovery of these intriguing features in living organisms renewed interest in the relevance of magnetic forces application to the human body and the potential action of magnetic properties in diagnostics and therapies. Biomedical applications of magnetic elements, for instance, as contrast agents in magnetic resonance imaging[5] have been explored and established as successful screening platforms while others as biosensors are steadly arising into the clinical scenario.[5], [6]

Considering the potential effect of magnetic forces in biological systems and promising outcomes in the diagnosis and therapeutic fields, magnetic stimulation may significantly influence wound healing and tissue regeneration. Magnetic forces have been described to act at the cellular level, enhancing the rate of survival of cells, including H9C2 cells after ischemia,[7] and influencing the differentiation process towards the osteogenic and chondrogenic phenotype of adipose derived stem cells.[8] Furthermore, cellular mechano-sensing and mechano-stimulation provided by external magnetic forces may play an important role in appropriate tissue formation by inducing intracellular processes via signaling pathways.[9] The exposure time and the intensity of the applied magnetic field also impacts different cell types including bone mesenchymal stem cells[10] and hippocampal neurons[11] in terms of cell processes as proliferation and differentiation.[10, 11]

Mechanical forces can be therapeutically administrated to assist the regeneration of musculoskeletal tissues. Pulsed electromagnetic field (PEMF) therapy is an FDA-approved treatment for orthopedics commonly utilized to encourage bridging of delayed or non-union bone defects since 1979.[12]

1.2 Magnetic Force Tissue Engineering

The capacity to successfully mimic a complex tissue, providing the essential microenvironment to the cells and stimulate the formation of functional tissues in order to ultimately promote the regeneration of damaged

or degenerated tissues remains one of the biggest challenges in the tissue engineering regenerative medicine field.[13] This challenge has inspired the development of stimuli-sensitive systems, also known as "smart" materials that sensibly and reversibly respond to a stimulus and, to some extent, have the capacity of adaptation. The stimulus can be achieved by external regulation using magnetic and electromagnetic forces, alterations in the temperature, light or through internal regulation by local changes in pH, ionic strength or by specific interactions.[14],[15], [16],[17],[18],[19] As a response, the material can change its shape, alter surface characteristics or solubility, go through molecular assembly or into a sol-to-gel transition.[20] If efficiently applied, the stimulus provides essential cues that assist the interaction among the biomaterial surface, extracellular matrix and cells, with potential to enhance vital functions such as adhesion, proliferation, migration, and tissue differentiation. Moreover, smart materials can be designed and fabricated to meet multi-functional parameters and still be precisely controlled (e.g. respond to multiple stimuli, in a time-spatial manner).[20] Unlike pH or temperature, the actuation of magnetic forces offers the advantage of being externally monitored and triggered over implanted scaffolds, cells or constructs to stimulate a therapeutic action, as often as desired, with different intensities during treatment or even under a continuous or interrupted manner.[20] Moreover, it is simultaneously, a highly precise and non-invasive tracking, guiding and monitoring system that can be easily and fastly turned on or off.

The increasing number of studies with reference to novel applications of magnetic nanoparticles and magnetic stimulation gave risen to a new concept of magnetic force-based tissue engineering (magTE) proposed by Ito and colleagues in 2004.[21] Since then, great possibilities were offered to TERM strategies from cell selection, monitoring and guidance to cellular assemble into 3D structures or towards the development of multi-functional and sophisticated 3D architectures to recapitulate native tissues.[21]

1.3 Magnetic Particles for TERM Applications

The responsiveness of materials to magnetic forces is based on the fact that certain magnetic elements such as iron, cobalt, nickel and manganese within the material attract or repel each other through the movement of charged particles. These elements are frequently found in nature as particulate matter in volcanic eruptions, in minerals or as part of cell metabolism in the form of ferritin in the heart, spleen and liver in humans.[2],[22] Magnetic materials can be found with different dimensions and shapes as tubes, rods or spherical components like magnetic nanoparticles (MNPs) that can be further arranged into higher complex systems to form micro- and macro-scale structures of increased complexity. The magnetic nanoparticles (MNPs) in particular, are quite versatile and combine unique physicochemical properties with a large surface area that can be properly modified to bond to biological agents. MPs studies based on cobalt, nickel and manganese suggest some level of cytotoxicity and susceptibility to oxidation which may limit their use for biomedical applications.[23] Alternatively, iron MPs have been more investigated for biomedical

purposes because of their lower cytotoxicity in comparison to other MPs, including cell tracking, cell sorting, drug release or gene therapy, suggesting a relevant role in theranostic strategies.[24],[25]

1.3.1 Properties of Magnetic Particles

The magnetic properties of MPs are commonly defined by magnetization, coercivity and saturation magnetization. The frequency of the external magnetic field applied to a solution of MPs is often low; around few kHz or less, and mostly influences MPs rotation movement which will affect MPs magnetization alignment, and afterwards influence MPs to move along the direction of the magnetic forces. Saturation magnetization is the maximum magnetization value of a nanoparticle under a high magnetic field while coercivity refers to the ability of a particular material to have magnetization without the application of a magnetic field. Zero coercivity, that is no residual magnetization, is essential in magnetic platforms for biomedical applications as well as appropriate and uniform MPs dimensions in combination with high magnetization values and colloidal stability.[25]

Moreover, MPs have the intrinsic capacity to be heated, and thus increase the temperature in the nearby environment by the actuation of an alternating magnetic field (AMF). Under the actuation of an AMF the magnetic moments of the MPs rotate, and heat is released when the MPs relax back to their original magnetic orientation.[25] This property of MPs has been explored in hyperthermia cancer treatments and can be further combined with thermo-responsive materials for bioagent delivery to be released upon magnetic stimulation.[1]

1.3.2 Superparamagnetic Iron Oxide Nanoparticles (SPIONs)

One particularly interesting subset of MNPs are superparamagnetic iron oxide nanoparticles (SPIONs), once they possess robust magnetic nature under the influence of an external magnetic field. SPIONs rotate to align themselves along the field and do not retain any reminiscent magnetism, with zero coercivity after removal of the magnetic force. The superparamagnetic behavior of MNPs is achieved when the particles dimensions are below the critical size (Rc). Below the Rc threshold it is energetically favorable for the magnetic particle exist with a single domain which happens typically in the range of a few nanometers.[26] SPIONs core normally consists of ferromagnetic magnetite (Fe3O4) and magnetite (Fe2O3), but sometimes results from combinations with other elements like copper, cobalt, and nickel. The low-toxic nature of SPIONs and the superparamagnetic features highlight their promising outcomes for biomedical and tissue engineering applications.[27] Like other types of MNPs, SPIONs can be remotely controlled and concentrated in a target *in vivo* location by the application of magnetic forces. However, the most distinguishable characteristic of SPIONs is the capability to be magnetized only when a magnetic field is applied, presenting the possibility of being “turned off” upon removal of the magnetic field. This singularity

of SPIONs avoids superparamagnetic particles to clog and potentially eliminates the threat of embolism within small capillaries as the risk of agglomeration is negligible.

1.3.3 Coating and Functionalization of MPS

Under physiological conditions (pH=7.4 and ionic strength= 150mM), iron oxide nanoparticles tend to aggregate once the stability of magnetic particles depends on a balance between attractive and repulsive forces.[25] Furthermore, MPs properties as effective surface charge, degree of dispersion, degree of aggregation or hydrodynamic size are directly influenced by the MNPs suspending media.[25] In order to overcome the low stability in physiological conditions, protect MNPs against aggregation and promote better biocompatibility and improved functionality, the surface of MNPs can be coated with materials as, for instance, polyethylene glycol (PEG),[25] dextran, chitosan, hyaluronic acid, or chondroitin sulfate.[28] MPs coated with hydrophilic polymers (e.g. PEG, dextran) have shown higher half-life in biological fluids in comparison with uncoated magnetic particles.[25] A hydrophilic coating results in fewer interactions with the components of blood, because they sterically hinder the interactions between the MPs and the opsonization proteins through a shielding process, and also due to the phenomenon of solvation resultant from the interaction with water molecules. Consequently these MPs have a slower clearance rate and evidence higher life span in the host.[25] Particles mainly constituted of hydrophobic domains at the surface are rapidly and efficiently coated with plasma components, and consequently more rapidly removed from blood circulation by the mononuclear phagocyte system (also called reticuloendothelial system or macrophage system).[29],[30] If desired, protection from interactions with blood elements can be assured using amphiphilic copolymers that spread in contact with aqueous solutions leading to a sterically diminution of probability of contact with these elements.[31]

Lipid-like coatings of the magnetic core forming liposomes and lipid NPs are a potential alternative to polymer coatings due to their versatile and tailorable structure and biocompatibility, being considerably explored in drug delivery mainly because of their intrinsic capacity to accommodate and release a wide range of therapeutic agents.[32]

Inorganic metals like gold are also used for the MNPs coating but the process itself is difficult and demanding.[33] Coatings with nonmetallic materials as graphite, or silica have also been strategically applied to provide chemical stability against oxidation.[34],[35] The type of coating and its conformation will influence not only the degree of aggregation of MPs but also the surface charge, hydrodynamic size and will play an important role regarding MNPs biological fate.

The functionalization via coating will tune the response of the particle itself with biological elements and will determine the surface properties of the MNP.[36] The nature and the thickness of the coating influence the magnetic properties and act as a protective barrier against the interaction and eventual collision among MNPs, keeping them apart from one another, thus leading to stable magnetic formulations.[25] The surface

coating, independently of the type of materials used, can be further functionalized with a vast range of complex and highly efficient molecules, including antibodies,[37] lectins, proteins,[38], hormones,[39] charged molecules and some low molecular weight ligands.[40] These molecules allow to target, monitor and track in real time a specific process with precise recognition from the cellular level (surface molecules and intracellular organelles of a desired cell type) to the macro scale of tissues and organs.

The type of coating and its conformation will influence not only the degree of aggregation of MPs but also the surface charge, hydrodynamic size and will play an important role regarding MNPs biological fate.

The surface charge of a coated magnetic particle is influenced by electrolytic solutions like blood, which will influence MPs affinity for adsorption of ions, proteins and natural organic materials. The charge and the type of coating have a relevant effect on the type of proteins adsorbed, on the strength of the interaction and on the hydrodynamic diameter of MNPs.[41]

The influence of surface charge in the rate of internalization has been studied with dimercaptosuccinic acid (DMSA) coated MNPs (17.3 ± 4.8 nm, negative surface charge), chitosan coated MNPs (16.5 ± 6.1 nm, positive surface charge) and agglomerates of both (DMSA/Ch, 85.7 ± 72.9 nm, highest positive surface charge) cultured with oral squamous carcinoma cell KB at physiological conditions. DMSA MNPs showed the lowest cellular uptake while the agglomerates of DMSA/Ch exhibited the highest cellular uptake.[42]

1.3.4 Dimension oriented Applications of Magnetic Particles

The magnetic properties of the MPs can be tailored by controlling the size of MPs. As referred before the MNPs dimensions will impact on the responsiveness to the magnetic field through the saturation of magnetization that was shown to diminish with the decrease of the magnetic particle size.[43] Thus, the choice for the optimal size is fundamental to target a desired function. Smaller particles have a larger surface area to volume ratio and higher magnetization density in comparison with magnetic microparticles. Due to their small size, nanoparticles are normally selected for cell recognition or specific capture of a biological entity, diagnosis or even for the treatment of diverse diseases like cancer, taking advantage of their intrinsic capacity to extravasate through the endothelium in inflammation sites, epithelium, and tumors in combination with their high stability in solution.[44] Moreover, the release of a molecule can also be tuned by controlling the size of the MPs.[45]

Sub-micron MPs can theoretically generate heat and thus induce an increase in the temperature in the surroundings when an alternating magnetic field (AMF) is applied.[25] Magnetic hyperthermia has been used in cancer treatment since tumor cells are hypersensitive to higher temperatures in comparison with healthy cells. The intensity of generated heat can be tuned through the manipulation of magnetic features like the size of MPs or by the manipulation of the actuation parameters of the external magnetic field.[46]

Moreover, internalized magnetic particles were described to kill cancer cells simply by exposure of the cells to an AMF without perceptible temperature rise, which led to the new terminology "Magnetically mediated energy delivery".[47]

Moreover, SPIONs offer the possibility to be conjugated with MRI techniques to localize the tumor and subsequently induce a hyperthermia treatment.[48] For example in a work developed by Jain and colleagues MRI was combined with liposomal iron oxide nanoparticles to treat glioblastoma multiform, a primary malignant tumor of the brain.[49] This nanoparticulate system was also found to be promising as drug delivery carriers across the blood-brain barrier (BBB), which has been a severe limitation of currently available treatments. MPs have been produced with different physico-chemistry properties and coating shells to improve their biocompatibility, reduce aggregation and to acquire specific functionalities which are envisioned to influence and direct the final application of MPs. In this sense, MPs have been explored as referred before for hyperthermia and diagnosis such as contrast agents in magnetic resonance imaging [5], and more recently for bio-agent delivery, tissue engineering and biosensing (Figure 20.1). [25],[43],[50] Also the combination of multiple functionalities in a single MP can lead to the development of "theranostics" to address diagnosis and therapy simultaneously, which represents an important route of MP technology toward clinical therapies (Figure 1.1). For biosensing applications in particular, MNPs have been used to enhance the sensitivity and the stability of biosensors for the detection of several biomolecules. An example is the work developed by Li and colleagues in which a magnetoresistive biosensor with nanoparticles (approximately 12.8 nm) was used as a detection platform for rapid quantification of biomolecules such as interleukin-6 from body fluids.[51]

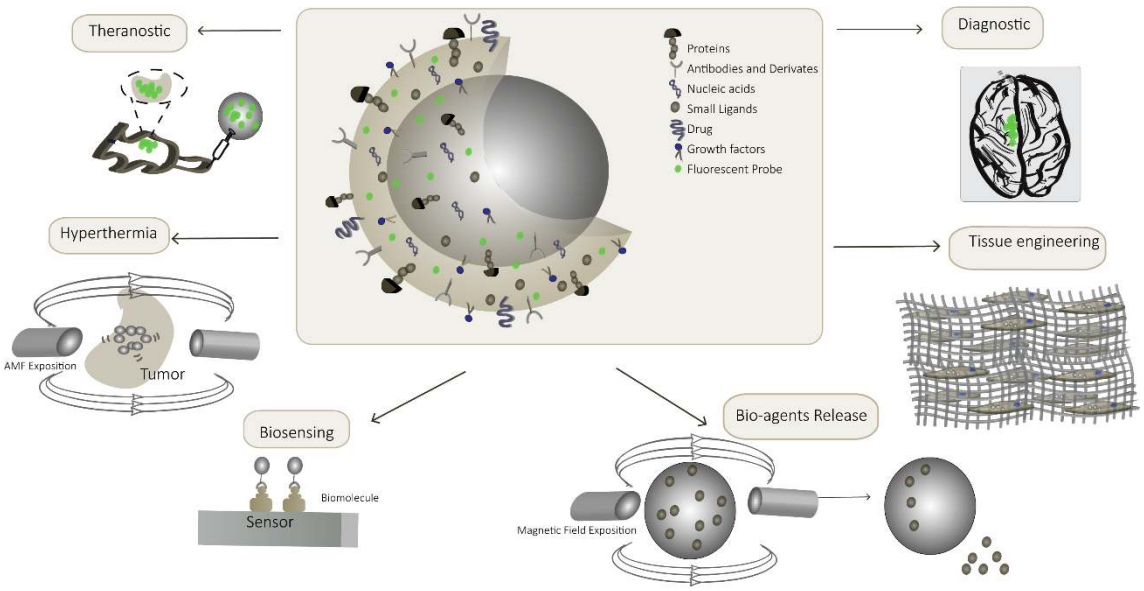

Figure 1.1: Magnetic Particles for biomedical applications. The surface coating and functionalization of MPs will ensure biocompatibility, prevent aggregation and provide cues for the isolation, sorting and tracking of

cells or biomolecule through bonding of highly specific antibodies or proteins, for cell and drug delivery and cell imaging. These properties assist the use of MPs for promising biosensor technologies, tissue engineering strategies and as effective diagnostic tools. Furthermore, the ability of MPs to generate heat has also motivated their use in hyperthermia studies aiming at cancer treatments or at controlling the release profile of incorporated drugs or growth factors. Another interesting feature of MPs is that these properties can be combined into multifunctional MPs with potential to synergistically act with diagnosis and therapeutic actions and thus as complex theranostic instruments for the clinical field.

1.4 Cell Response to Magnetic Elements

1.4.1 Cytotoxicity, Internalization and Clearance

There are several parameters of considerable importance that can influence the biocompatibility of the magnetic particles, including the type of raw biomaterial, dimensions, shape, concentration, route and local of administration.[52],[23]

Not only is biosafety assurance a key parameter for clinical applications but it is also crucial to understand the bio-transformation of the MPs within the body and the mechanisms that determine their course of action and elimination.

The interaction of MPs with the biological systems, more specifically how the particles react with cells, proteins, hormones, and plasma constituents is important for predicting the biodistribution of by-products resultant from particles biodegradation and bioresorption.[29] MNPs with iron cores have been described to be more biocompatible and non-cytotoxic than cobalt, nickel or manganese MNPs. In a study by Karlsson and colleagues the toxicity of metal oxides of nano- (<100 nm) and micro- particles (<5 μm) of Fe2O3, Fe3O4, TiO2 and CuO was evaluated using a human alveolar type II-like epithelial cell line.[23] The iron oxides particles showed very low cytotoxicity levels in comparison to CuO and TiO2 particles for concentrations up to 100 μg/ml, without significant differences among particles of different dimensions.[23] Iron oxide MNPs uptake by different cells showed no evidence of a pejorative cellular response. Furthermore, Ferumoxides (Ferridex®)[53] and Ferucarbotran (Resovist®),[54] which are also iron oxide MNPs, have been FDA approved for clinical applications in MRI imaging. This data suggests the applicability of these particles for tissue engineering and regenerative medicine approaches.[14],[55],[56] However, each and newly developed MP presents a unique combination of features and properties, which implies that MPs should be individually considered and evaluated regarding their functionality and biocompatibility. Besides particle dimensions, the physicochemical properties may also influence the potential outcomes of using MPs in living entities.[29] Although MPs are expected to bring great benefits into therapeutics and biomedicine, the *in vivo* response needs to be assessed so that limitations and drawbacks can be safely

overcome. Magnetic targeting of MPs specifically to a tissue/organ can rise the local iron concentration disturbing iron homeostasis. Additionally, because of the large surface area to mass ratio, MNPs may diffuse across biological membranes and tissues barriers which could potentially induce cytotoxicity (DNA damage, oxidative stress) in a concentration dependent manner.[29] Furthermore, free iron released upon MPs degradation can produce reactive radicals and consequently may cause cellular deterioration, death or carcinogenesis.[57] The application of an AMF in combination with MPs can also impact on the cellular homeostasis and increase the production of reactive oxygen species (ROS).[58]

Despite these possible risks, it is generally accepted that in a concentration dependent manner, iron oxides are non-toxic to cells since they can be degraded via endogenous iron metabolism and metabolized into its basic elements.[59] For instance, Pisanic and colleagues have demonstrated that SPIONs coated with dimercaptosuccinic acid have elicited a dose-dependent cytotoxicity ([Fe] = 0.15-15 mM) when cultured with a neuronal cell line. They found that the particles diminished the ability of the cells to either survive or demonstrate normal biological responses and morphologies.[60] In another work, Jeng and colleagues have shown that high concentrations of metal oxide particles ([Fe] ≈ 2.5 mM) have a statistically significant negative effect upon mitochondrial function in Neuro-2A (mouse neuroblastoma, CCL-131, ATCC) cell lines. [61]

Iron is a metal but also an essential and highly conserved nutrient involved in several systemic and cellular functions. Macrophages and hepatocytes play an important role for the systemic storage of iron that is not needed for immediate use. Iron is stored in liver and available in blood circulation where it is required for the production of hemoglobin in hema-groups of red blood cells.[62]

Human iron metabolism refers to a balance between iron uptake, storage and excretion/loss, which is challenged by iron homeostasis. Iron in circulation bounds to transferrin [63], an abundant plasma protein that binds to iron atoms with extremely high affinity.[64] At this stage iron can be taken up by tissues with transferrin receptors.[65] However if iron is not bounded (free iron form), it can lead to several damages in the organism. Thus, iron homeostasis aims to avoid the potential detrimental effects of free-iron without losing its benefits. To maintain the balance, iron absorption, storage and excretion are meticulously controlled, being a small fraction of iron intake absorbed and the remaining excess eliminated by cellular excretion through skin, urine or blood loss.[64]

MPs can be recycled or cleared in a relatively short-term through regular excretion routes (Figure 1.2). The MP coating undergo progressive degradation and predominant renal elimination while iron in its elementar form can be eliminated, predominantly via the faeces.[66] Their clearance from the body has been described to occur through a model of lysosomal metabolism of iron oxide nanoparticles and mechanisms of nanoparticle degradation. [67],[68],[69]

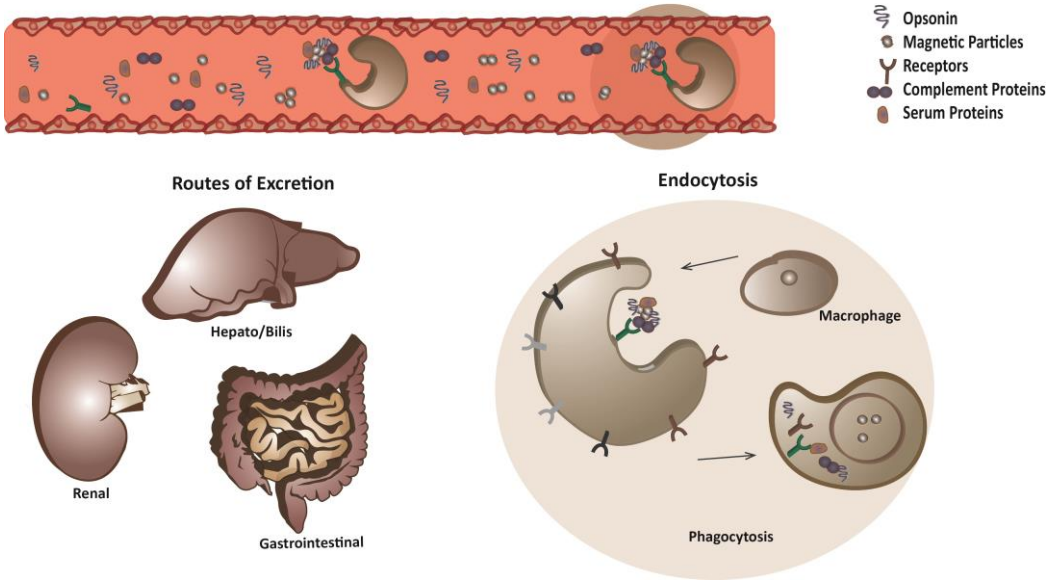

Figure 1.2: Clearance and elimination routes of MPs. Independently of the administration route it is likely that MP will ultimately reach the vascular system. Depending on the surface properties of MNPs like charge, size, coating or functionalization, the MPs may undergo adsorption or opsonization by serum proteins that will further mediate macrophage intervention and MNP phagocytosis and lysosomal elimination. The MPs can be cleared from the organism through different routes; mainly by kidney, liver or gastro-intestinal excretion. The kidney rapidly removes 5–6 nm particles from the vascular compartment via renal filtration and urinary excretion. When kidney excretion is not possible, the hepatobiliary system becomes the primary route of excretion for MPs before the release of MPs into the gastrointestinal tract for elimination through faeces.

Another important aspect to be considered in MP-body dynamics is the complex interactions between cells and MPs. Considering the size, the physicochemical characteristics and the biological entities that decorate the MPs, MPs can be effectively internalized by cells. This interplay of cues results in different mechanisms of cellular uptake and consequently intracellular sorting toward different compartments.[70] Studies of co-incubation of cells and MPs evidenced that the particles are commonly internalized through spontaneous endocytosis pathways or by phagocytosis.[71]

As the cellular membrane is negatively charged, positively charged particles are more efficiently and rapidly endocytosed. Although the rate and the type of endocytosis also depend on the type of cell, MNP dimensions influence the rate of internalization and the internalization route.[72] In fact, all particles with size ranging from 10 nm to 500 nm and limited up to 5 μm can be internalized through different pathways depending on the cell type and other properties but the larger particles of approximately 5 μm are the most likely to be

engulfed via micropinocytosis.[73] MNPs up to 2 nm can pass through passive diffusion by cell membranes, capillaries, and even through the blood-brain barrier, which may interfere with cell metabolism and lead to several damages.[74]

The shape of MPs also influences the biocompatibility and bio-distribution. Rod-based NPs have shown an increased cellular uptake in comparison with spherical NPs for sizes over 100nm.[43] This outcome may be associated to the position of rod NPs that evidence different length and width dimensions, to present themselves to the cell. However, when the spherical MNPs have sizes up to 100 nm, cell uptake behavior is just the opposite.[75] Thus, the versatility of MPs in terms of particle design and consequently their intrinsic characteristics as well as MPs interaction and functionality with the environment and biological entities, should be carefully considered and investigated to address a particular need and TERM application.

1.4.2 Mechanosensing & Mechanotransduction Pathways

Interactions between the cell and its microenvironment are crucial for triggering endogenous mechanisms fundamental for morphogenesis, tissue homeostasis, remodeling and pathogenesis. Magnetic fields *per se* influence the activation of mechanotransduction signaling pathways, stem cell differentiation and the presence of anti- and pro-apoptotic molecules. Cells are endowed with the capability of sensing these external mechanical stimuli and translating them into a biochemical response, a process termed as mechanotransduction.[76]

Although the mechanisms underlying the therapeutic action of pulsed electromagnetic field (PEMF), that can be viewed as the combination of an electric field (stationary charges) and a magnetic field (moving charges), remain to be entirely understood, it is increasingly evident that cells are able to perceive electromagnetic fields as any other source of environmental stress and react accordingly. This is mediated via the mechanotransduction signaling pathway MAPK, a pathway classically activated upon osmotic shock, radiation or any other kind of environmental stress. It contains 3 branches, ERK, p38 and JNK and the active form of p38 (phosphorylated) and ERK 1/2-cbfa1 signaling has been proposed to accelerate osteogenesis.[7],[77] This may actually help understanding why PEMF is successfully at encouraging bone regeneration. Besides stem cell commitment, magnetic fields also influence the expression of stress proteins and influence the expression of pro-survival and apoptotic genes. In example, pre-stimulation of rat heart-derived cells with a 60 Hz magnetic field enhance the levels of the heat shock protein 25 (Hsp25), increase the levels of Bcl-2, an anti-apoptotic protein, and reduce activity of apoptotic caspase 3, 8 and 9.[78]

Magnetic fields in combination with magnetic responsive biomaterials present further advantages. This is supported by a number of recent studies addressing the potential of magnetically actuated biomaterials in angiogenesis and bone TE. Endothelial cells cultured in magnetite-impregnated alginate scaffolds and alginate scaffolds (control) formed tube-like structures after 7 days of magnetic stimulation at 40 Hz and 10-15 Oe. Although both materials supported the formation of such primordial blood vessels, the number

of lumens was significantly higher in the magnetically actuated alginate suggesting a synergistic effect between the magnetic field and the magnetic biomaterial.[79] Cardiac cells cultured in a similar material caused significant activation of AKT, a promoter of cell hypertrophy and survival, but also troponin-T, a pro-survival contractile protein, after 6 days of stimulation at 5 Hz and 10-15 Gauss.[79] Only cells from the magnetically actuated alginate presented these patterns of protein expression. As referred above, magnetically actuated materials have been showing great promise in bone TE. Magnetic polylactic acid and hydroxyapatite scaffolds implanted in lumbar transverse defects of New Zealand white rabbits have evidenced a positive effect in bone regeneration upon the establishment of static magnetic field.[80] Twenty days post implantation osteoblasts and the bone protein osteocalcin were found in greater abundance in tissue sections from the magnetically actuated scaffold group, resulting overall in better organized collagen fibers and more newly formed bone at day 30.[81] Magnetic actuation concomitantly combined with magnetic responsive have been successfully utilized to accelerate osteogenesis, promote the formation of new blood vessels and encouraging the presence of pro-survival molecules or activation of pro-survival signaling pathways.

Thus, it is critical to continue exploring the mechanisms behind cell magnetic stimulation to fully understand and characterize the actuation of magnetic forces in each tissue or organ, and how these forces can be combined with smart magnetic materials as a mean to improve TERM strategies.

1.5 Magnetic Responsive 3D Systems

Tissue engineering (TE) strategies rely on multiple combinations of cells, scaffolds and bioactive agents, some of them with therapeutic action, in order to provide the most suitable environment and promote regeneration in detriment of repair. The improvements in TE are intimately associated with the biomaterials to assist tissue formation and regeneration.

TE approaches which provide a bioengineered product that stimulates regeneration while simultaneously enabling real-time follow up will be a major advance in clinical therapies. Magnetic smart materials offer such new perspectives in TE (Figure 1.3).

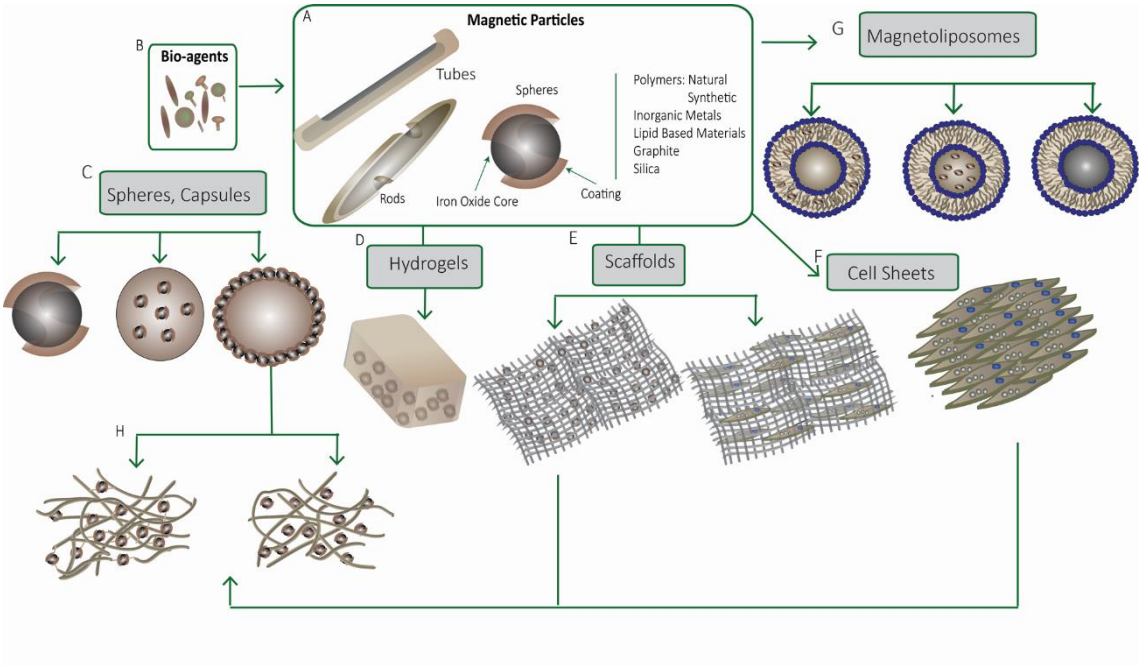

Figure 1.3: Magnetic smart-materials for tissue engineering applications. A) Iron oxide particles (MPs) can be found with different dimensions and shapes as tubes, rods or spherical components. B) These MPs can be functionalized via coating in order to have a better biocompatibility and improved functionality with biomolecules, including antibodies, lectins, proteins, hormones, charged molecules and some low molecular weight ligands. Functionalized/ non-functionalized MPs can be incorporated in a non-magnetic matrix originating magnetic responsive systems (C, D, E, F and G); C) Magnetic responsive spheres or capsules produced through the dispersion/synthetization of MPs within the polymeric matrix, magnetic particle core coated with non-magnetic material or by the fabrication of spheres with a polymeric matrix core coated with MPs. D) Magnetic responsive hydrogels where MPs are dispersed/synthetized within the polymeric matrix. E) Magnetic scaffolds where MPs can be directly incorporated within the non-magnetic matrix matrix or in the cells through cell labeling, if cells are intended to be seeded or cultured on a scaffold prior implantation. F) Cell sheets with magnetically pre-labelled cells. G) Magnetoliposomes (MLs) in which MPs can be coated with a phospholipid bilayer, embedded in the lipid bilayer or being encapsulated in the internal aqueous space of unilamellar vesicles. These MLs can be further used to produce cell sheets (H). In the case of spheres (C), hydrogels (D) and scaffolds (E) in which MPs are dispersed/synthetized within the non-magnetic matrix, the MPs can be either cross-linked to the matrix or dispersed through the pores.

The most common fabrication procedures for magnetic materials, either as particulate systems, gels, scaffolds or others, are based on the incorporation of magnetic particles in a non-magnetic matrix.[29]

The non-magnetic matrix complements MPs functionality preventing the aggregation of the MNPs, protecting them against oxidation and allowing the bond of functional groups.[25] This matrix will also improve the stability of the tissue engineered construct and can assist the inclusion of new physical and biological properties, and consequently multifunctional behavior.

The selection of the non-magnetic matrix with appropriate composition and architectural features is thus a critical step envisioning a successful tissue engineered substitute. Distinct materials have been applied for the production of these matrices, including natural and synthetic polymers as well as ceramics materials. Each type of materials, used alone, blended or combined as composite materials, present specifications than can be more advantageous considering the application they are intended to.

The incorporation of magnetic nanoparticles within 3D architectures constitutes an attractive approach to achieve magnetically responsive systems enabling remote control and stimulation of cell laden constructs.[76] Diverse templates of smart magnetic materials from spheres, liposomes, gels to 3D hierarchical structures have been explored for TERM strategies (Figure 1.3).[28],[82],[83],[84]

MNPs can be integrated within 3D scaffolds directly or by previous association with (stem) cells (Figure 1.3E).[85] After incorporation, the application of an external magnetic field may induce scaffold structure deformation. The matrix structure and properties will relate to their application and on the fabrication methodologies that include bottom-up methods through the assembly of building blocks (Figure 1.4) and 3D printing technologies.[86]

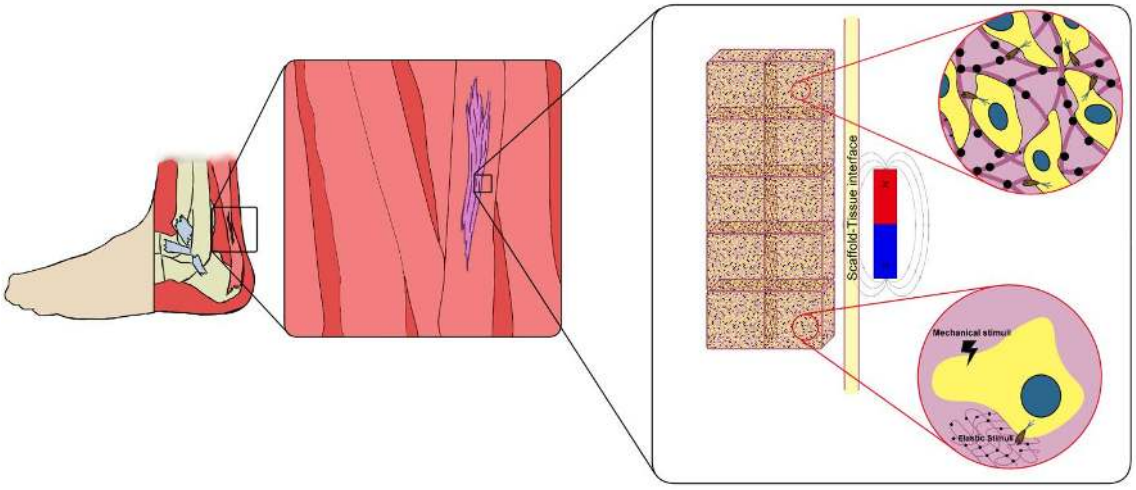

Figure 1.4: Smart Magnetic Hydrogels as building blocks for tissue engineering applications. Hierarchical and complex systems can be achieved incorporating magnetic nanoparticles in a 3D porous hydrogel, conferring magnetic responsiveness capacity. The application of a magnetic field will potentially promote self-assembly of the hydrogels originating complex and well-defined 3D- architectures combined or not with encapsulated cells. These constructs can be further implanted and potentially promote cellular mechano-

stimulation under the actuation of a magnetic field that may influence appropriate tissue formation by inducing intracellular processes via signaling pathways.

1.5.1 Magnetic Systems: Spheres, Capsules and Liposomes

Magnetic spheres, capsules, and lipid layered vesicles as liposomes and water-in-oil droplets, can be produced from combinations of different biomaterials, often polymeric matrices or lipid based materials incorporated with MPs (Figure 1.3C,G).

The strategies to produce magnetic spheres are the encapsulation of MPs in a biodegradable polymeric matrix that usually rely on either i) uniformly disperse MPs within the polymeric matrix; ii) induce the formation of a MPs core within the sphere; or iii) the fabrication of spheres with a polymeric matrix core coated with MPs (Figure 1.3 C).[87],[88]

These magnetic spherical-shape structures are envisioned for a wide range of applications including controlled delivery, diagnostic MRI, tissue regeneration and cancer therapies mediated by hyperthermia.[5] Several biofabrication techniques have been exploited to produce magnetically responsive spheres, being the layer-by-layer (LbL) deposition, the most commonly used. LbL consists in the preparation of a multi-layered film by the sequential deposition of alternating layers of oppositely charged materials, in which MPs can be easily integrated between the layers through surface modification.[89]

Their versatile intrinsic properties enable their use in encapsulation/release systems since they serve as protective carriers of pharmaceutical agents, genes, cells and growth factors (GFs) to be delivered at specific sites.[1] For effectiveness, the bioactive agent should be released on demand and at tunable rates. In this aspect, magnetic responsiveness is fundamental once magnetic forces are very well suited to control the rate of drug release and biomolecules in biological systems and because the human body has a great acceptability to static and alternating magnetic fields.[90]

Particularly in drug delivery, magnetic spheres are a useful tool due to their small size that leads to large surface/volume ratio, great loading efficiency, high diffusibility, motility and excellent capacity to rapidly respond to the stimuli of the surrounding environment.[1],[91],[92] For example under the influence of an electromagnetic field (EMF), the release of an anticancer drug, doxorubicin, co-encapsulated with magnetic nanoparticles (Fe3O4) in polylactide spheres was prolonged without a burst effect which ensures minimal exposure for the healthy cells, and locally increases drug release.[93] Another work [94] reported the feasibility of the encapsulation of hybrid chitosan/hyaluronic acid nanoparticles by spray drying into microspheres with an aerodynamic diameter of approximately 2.6 μm for lung delivery. The homogeneously distribution of MNPs in this carrier resulted in a dry powder with appropriate aerodynamic properties.[94]

Magnetic alginate microspheres have also been used in another study to deliver neuron growth factor [1] in a control manner assisted by the application of EMF targeting PC12 cells, a cell line derived from a rat

pheochromocytoma.[56] The NGF release in combination with the magnetic field was able to promote cellular differentiation of these cells towards neuronal regeneration.[56]

Unlike magnetic spheres, magnetic capsules are hollow vesicles commonly produced from combinations of polymeric solutions and MPs. Magnetic capsules can offer advantages in comparison with microspheres depending on the final application or drug delivery strategy. In spheres the bio-agent is entrapped within the polymeric matrix while in microcapsules, the bio-agent can be encapsulated within the core that can be in liquid phase. Of course that the core features can influence the bio-agent to be more susceptible to oxidation and degradation.[1]

Ma *et al.* produced thermo-stable magnetic capsules by LbL assembly. Spherical structures were polymerized with melamine and formaldehyde, and surface coated with silica where different layers of negatively charged SPIONs were deposited by polyelectrolyte LbL assembly. [95]

The magnetic spheres can be incorporated into a continuous matrix in order to improve the physicochemical and biological characteristics of the final system. Thus, magnetic nano- and micro-spheres are obvious candidates as building block units in order to fabricate constructs with increasing levels of organization using bioengineering techniques like random packing, rapid prototyping or directed assembly. The latter has been more deeply investigated since this method takes advantage of attractive inter-particle forces generated by MPs.[96] Yoon and colleagues reported the production of protein microspheres using an ultrasonic method where magnetic nanoparticles of approximately 25nm were embedded inside and outside the sphere to yield nano-functionalization. Another work reported the directed assembly of magnetic nanoparticles using a commercial compact template covered with PDMS to obtain cylindrical microstructures.[97] These magnetic microspheres were further used as building blocks to produce complex TE structures.

Liposomes are widely studied in the TERM field due to their chemical and physical versatility, amphiphilic properties, low toxicity, fluidity and surface functionalization. Magneto-liposomes (MLs) are liposome vesicles in which MPs are surrounded by an artificial self-assembled phospholipid bilayer.

In MLs, iron oxide MPs can be either coated with a phospholipid bilayer, embedded in the lipid bilayer (limited embedding efficiency associated with the particle size) or encapsulated in the internal aqueous space of unilamellar vesicles (Figure 1.3 G).[98],[99] Their utility resides in several applications as for MRI contrast agents, cell sorting, drug delivery, gene delivery and tissue engineering.

Indeed, liposomes are perhaps the first carriers which have succeeded in translating from bench to bedside.[50] Depending on the final application, the location of the MPs within lipid based systems may be a determinant factor. For example, in MRI applications it is better to have NPs within the core of the MLs, while for drug delivery the MPs should be between the bilayer, as the core may impact the drug even before the membrane became permeable. Additionally the energy required to permeate the membrane is lower when the MPs are between the bilayer.[100]

The combination of MPs with liposome technologies is envisioned to result in a promising system for innovative therapeutic solutions. MLs can host hydrophilic and hydrophobic cargoes in their aqueous compartments and bilayer structure, respectively or even in their bilayer/aqueous medium interfaces for amphiphilic drugs, being possible to deliver large amounts of a drug to the specific target site. Additionally they offer a great possibility to maintain the levels of several drugs in a therapeutic desirable range, and they allow to increase the half-life, stability and permeability of several drugs without associated toxicity for the neighboring tissues.[101],[102]

MLS may be designed to be thermosensitive since the *in situ* generation of heat allows the manipulation of liposome permeability and consequently drug release rate.[24] As mentioned before, MPs exhibit remarkable heating effects when exposed to an AMF. Combining these systems may provide an excellent platform for drug delivery, hyperthermia treatment and MRI tracking.

Magnetic hybrid liposomes synthetized with liposomal membranes, thermosensitive block copolymers of (2-ethoxy)ethoxyethyl vinyl ether (EOEOVE), octadecyl vinyl ether (ODVE) and MNPs have shown to enhance the release rate of a model drug when exposed to an AMF (360 kHz, 234Oe), without significant drug release after the AMF was turned off.[103] Studies with thermosensitive magneto liposomes encapsulated with drugs as methotrexate also showed that the agent release was faster at higher temperatures (41°C) when exposed to an EMF.

In respect to drug targeting for specific tissues, the presence of an additional trigger like pH together with the magnetic core of the ML offer great advantages. This is because a magnet can be used to guide MLs after an endovenous administration of the drug to the local of action where alterations in the pH can control the rate of release.[104] Magnetoliposomes can also be used for tracking using imaging techniques like MRI. In a work developed by Soenen *et al*, cationic MLs were used to magnetically label human blood outgrowth endothelial cells in order to follow their homing and integration capacity within the host.[105]

The cell internalization of magnetoliposomes can also enable to position cells accordingly to a suitable pattern stimulated by the actuation of magnetic forces even in 3D template-free approaches. These magnetically labeled cells will act as building blocks to be accumulated and distributed accordingly to a specific pattern using the magnetic field. This Mag-TE approach using magnetoliposomes has been utilized for a number of applications that includes preparation of artificial blood vessels,[13] skeletal muscles,[21] and bone tissue formation., [106]

Magnetic responsive liposomes can be efficiently internalized through electrostatic interactions between the ML and the cell membrane, increasing the MNPs accumulation in the target cells.[21] Because cell membranes are constituted by a phospholipid membrane, cationic liposomes (with approximately 10 nm) can be internalized and further use ML internalized cells to produce cell sheets (Figure 1.3F). Yamamoto *et al* used this system to produce artificial skeletal muscles tissues based on the use of multilayered sheet-like

constructs with mouse C2C12 myoblast cells, whose experiment assisted the creation of the magnetic force-based TERM concept[106].

1.5.2 Smart Magnetic Gels

The similarities of the mechanical and compositional characteristics of hydrogels with soft tissues like cartilage and their applications in cell or biochemical agent delivery, increases their potential for TERM applications as a therapeutic tool for general and personalized medicine.[37],[14]

The conjugation of hydrogel matrices with inorganic components like MPs can possibly overcome the difficulty to accurately control the release rate of an incorporated factor as a response to alterations in the environment.[29],[107] In fact, a hydrogel-MPs system has also the advantage of gathering the synergistic properties of both elements including the mechanical reinforcement, and site-specificity.[108] Furthermore, magnetic hydrogels provide suitable semi-wet, 3D environments for molecular-level biological interactions.

Methods such as blending-,[109] *in situ* precipitation[110] and grafting-onto- , [111] have been described to produce magnetic hydrogels (Figure 20.3 D, H). The limitation of the blending method relies in a non-uniform distribution of the MPs within the gel with the risk of losing MNPs from the hydrogel in contact with the liquid solutions.[109] In the *in situ* preparation method, the hydrogels are firstly produced and immersed in an aqueous solution containing the ferrous ions, and concentrated into an alkaline solution to produce the MNPs. Although MPs can be uniformly distributed into the hydrogel, it is difficult to determine the precise MPs concentration. Furthermore, this method is only suitable for stable polymers in alkaline conditions in which iron oxides MPs have a tendency to oxidize, and with significant limitations for cell studies.[110]

The grafting onto method is based on the establishment of a crosslinking between the precursor hydrogel and the surface of MPs, that requires functional groups to guarantee the efficiency of the process.[109] Because of the presence of covalent bonds, MPs are unlikely to diffuse out of the hydrogel network.

Blending and *in situ* precipitation methods normally result in magnetic hydrogels with weak interactions leading to a minimal mechanical force reinforcement.[112] In contrary, crosslinking MPs directly to the matrix would enhance the mechanical properties of the system, transforming a rather soft, brittle hydrogel into an elastomeric material that upon a magnetic field stimulation, may quickly deform with no heat evolution or exhaustion.[113]

Magnetic hydrogel matrices with tunable properties like stiffness, degree of wettability or even surface functionalization with bioactive molecules, are interesting templates aiming to achieve specific cell or tissue response for TERM applications. Smart magnetic hydrogels have the ability to incorporate and assist the release of a multitude of bioactive agents and remotely control the release of these agents through external magnetic actuation. Thus, these hydrogels constitute an interesting platform to study the release profiles as

well as the control of cell behavior and processes such as angiogenesis in response to mechano-magnetic stimuli.[79] Chondroitin sulfate-A (CSA) and carrageenan in combination with iron oxide MNPs and CSA coated -iron oxide MNPs demonstrated "on-demand" drug delivery upon the application of an oscillating magnetic field.[114] *In situ* produced magnetic gelatin hydrogels were shown to assist the release of vitamin B12 upon EMF of 400 Oe.[115] With this system the vitamin B12 release can be programmably controlled. Other magnetic hydrogels as hemicellulose-based hydrogels, also produced by an *in situ* process, evidenced a great potential for controlled drug delivery.[84] Moreover, the Fe3O4 nanoparticles in this system tuned the thermal stability, macrostructure, swelling behavior and magnetization of the hybrid hydrogels.

In another study, the rate of deformation of macroporous alginate ferrogels containing iron oxide NPs associated to the presence of an external magnetic field led to a higher release rate of mitoxantrone drug after exposure to moderate AMF (every 2 h for a total of 14 hours).[116] Despite these interesting results from magnetic hydrogels, only a few systems were proposed for TERM applications.[14],[28],[108] Hydrogels with magnetic gradients can also resolve several challenges that exist with the localization of the implanted material.[80] For instance, magnetic gelatin membranes crosslinked with MNPs were fabricated with a non-uniform magnetization upon AMF application. The spatial variation of the magnetization within the scaffold causes the magnetic objects to move, and target delivery is possible by bonding bio-agents to the MNPs, without impairing the biocompatibility and others essential properties.[80] Additionally, the gelatin membranes have thermic properties tunable by AMF, which unlocks new possibilities for the production of biomaterials with thermal gradients.[80] In the work of Campbell and colleagues injectable gelling magnetic hydrogels were produced with aldehyde-functionalized dextran SPIONs cross-linked to poly (Nisopropylacrylamide) (pNIPAM) and assessed in a mouse model.[14] No chronic inflammation or evidence of fibrous capsule formation was observed after a subcutaneous injection combined with an AMF. The release rate of bupivacaine hydrochloride, an anesthetic drug, was assessed to be higher in the presence of AMF. Thus, smart magnetic hydrogels constitute an advantageous choice for tissue engineering and drug delivery since they can resolve the limitations and side effects currently associated with the systemic route of administration, including the bio-distribution of the bioactive agent to deliver, the lack of specificity towards a particular local, and the necessity of overdosing to achieve proper concentration at a specific location.[117] Furthermore, the system can be easily controlled in a spatiotemporal manner through the application of a magnetic field.

The development of tissue-like functional magnetic hydrogels building blocks (Figure 20.4) can be obtained through the use relatively simple methodologies and technologies involved in their fabrication, such photolithography and molding.[14],[82],[118] Various assembling approaches have been used including microfluidics, nanotextured surfaces, and surface tension.[119],[120],[121] These techniques allow microtissues scale-up into larger tissues and permit the creation of complex and well-defined 3D-architectures.

The work developed by Liu and colleagues is an interesting example that took advantage of the robustness and the magnetic controllability of microtissues formed with gelatin based materials.[121] Using a microfluidic device, individual microtissue units were assembled into larger scale tissue constructs under an external magnetic field. With this system, it was also possible to establish a separable co-culture system with human hepatocyte cells, which incorporated MNPs and the supporting cells, NIH/3T3 cells, without MNPs. Hepatic cells were then separated from the supporting cells through the application of the external magnetic field and further implanted in a nude mice. As a magnetic system, these microtissues, in particular the MNPs incorporated in the hepatic cells, could be tracked by MRI.

Building blocks of magnetic hydrogels can also be applied for cell patterning using a simple and low cost method.[122] Hydrogels produced with PEG and iron oxide microparticles were placed in a culture plate and the cell lines seeded over the hydrogels. The hydrogels prevent the cellular adhesion in the areas they were inserted and can be further removed using magnets without affecting the cells. In another work, magnetic microparticles were combined with a fibrinogen solution in order to produce a fibrin gel that manipulated with magnetic forces produced a defined architecture that could mimic the fibrin fibrils.[123] The assembling of soluble fibrin monomers coated with magnetic microbeads into fibrin fibers upon magnetic forces stimulation showed that human microvascular endothelial cells were capable to adhere and spread along the fibers, suggesting a potential role of magnetic templates in angiogenesis strategies.[123]

1.5.3 Magnetic Responsive 3D Scaffolds

As described in previous sections, MNPs can be directly incorporated into a 3D scaffold matrix or in the cells through cell labeling, if cells are intended to be seeded or cultured on a scaffold prior implantation (Figure 1.3 E,H).[124]

Under the actuation of magnetic forces, an implanted magnetic scaffold adjusts the magnetic force distribution leading to a higher concentration of magnetic flux in the surroundings. As a consequence, the magnetic elements, as MPs, within a scaffold produce magnetic gradients that generate significant magnetic attractive forces in the proximities of the scaffold, which acts as a trapping center, for instance, for magnetized cells and with potential to improve the scaffold bioactivity.[80]

Scaffolds produced from commercial hydroxyapatite, collagen and magnetic nanoparticles, in which RGD peptides were incorporated, were shown to respond to a magnetic field with magnetization values as high as 15 emu g-1 at 10 kOe.[55] Therefore, the release of pre-loaded biological agents could be triggered when a magnetic field was turned on. The actuation of a magnetic field is a dynamic parameter that can be applied in both *in vitro* and *in vivo* environments, and is preferentially directed to target cells which recognize these forces rather than to template structures, like the scaffold and tissue extracellular matrices. Magnetic

responsive scaffolds made of polycaprolactone (PCL) were shown to stimulate the migration and odontogenesis of human dental pulp cells. [125] The incorporation of MNPs into a scaffold may help the proliferation and differentiation rate of bone cells and thus bone regeneration as bone tissue is capable of converting mechanical stress provoked by, for instance, magnetic forces into induced voltage across the bone, known as "the piezoelectric effect of bone".[126] This effect is mainly responsible for the great capacity of bone to adapt under impressive mechanical forces.

The nanofibrous films of poly lactide,- hydroxyapatite and iron oxide NPs were shown to induce a higher proliferation rate, faster differentiation and ECM secretion of pre-osteoblast cell line under exposure to static magnetic field.[81] The developed scaffold was later implanted in a bone defect model of New Zealand white rabbits.[81] The study aimed at assessing osteogenesis upon the application of an external static magnetic field. The scaffolds under the external magnetic field promoted higher osteocalcin expression in the bone defect, faster achievement of cortical bone and medullar cavity continuity when compared to scaffolds without magnetic stimulation.

The development of a polymeric magnetic scaffold made of starch and PCL fibers (SPCL) with aligned structural features in which MNPs were incorporated, was recently described by Gonçalves *et al.* for tendon tissue engineering. These magnetic scaffolds were shown to assist the tenogenic differentiation of human adipose-derived stem cells under magneto-stimulation conditions. Afterwards, the magnetic scaffolds were implanted in an ectopic rat model, evidencing good biocompatibility and integration within the surrounding tissues. [86]

Mimicking the natural alignment and orientation of tissues has been a challenge in scaffold design and fabrication, including in magnetic responsive scaffolds. Highly oriented PLGA/SPIONs fibrous bundles were fabricated by electrospinning with oriented fibers to guide cell growth and distribution.[127] Upon the application of an EMF, the cell seeded bundles were magnetized, and thus able to be magnetically rearranged in order to build a 3D cell-dense engineered tissue with a highly oriented architecture. Cells proliferated along the direction of fibers in a similar manner to the native skeletal muscle tissues.

1.6 Conclusions and Future Perspectives

With the progress in nanomedicine and in the technological field, several advances have been made that highlight the interest and relevance of using magnetic elements like MPs for achieving therapeutic benefits in a multitude of TERM strategies from drug delivery, tissue augmentation and replacement to gene and cell based therapies.

Although MPs are already available in the market for diagnosis purposes, the design and manipulation of MPs alone or integrated in smart magnetic materials through different processing methodologies to render them multi-functional properties, may result in different outcomes on the system biocompatibility and safety.

This chapter gathers the most promising features and hot topics on magnetic materials that evidence the promisor future of magnetically responsive materials in different areas of TERM. MPs combined with a non-magnetic 3D template have been proposed as building blocks for tissue engineering constructs to mimic tissue structures and morphologies, as agents to mechanically enhance the 3D template properties and as controlled delivery agents of cells, drugs, GFs and other biomolecules towards successful tissue regeneration instead of assisting repair.

Smart magnetic systems can be easily controlled through remote actuation and *ex vivo* stimulation directly applied to the organism via magnetic devices, providing potential means to significantly augment the performance of magnetic tissue substitutes. Moreover, since the effect of electromagnetic energy is local and limited to the site of application, remote control of cell or construct fate through external stimulation offers new opportunities for non-invasive clinical therapies with potential for long-term control over the release rate of single or multiple drugs during treatment follow up. The most promising features of MP based approaches are likely associated to the long term, non-invasiveness and continuous tracking by the use of imaging techniques like MRI.

Future developments will alike focus on increasing the complexity of these systems, making them more effective and functional accordingly to biological requirements, using current and state-of-the-art technological tools. Additionally, improvements and insights on the mechanisms associated to the actuation and stimulation provided by an external magnetic field will be made to precisely control over the intrinsic properties of smart magnetic materials like swelling, porosity and structure. In consequence, this will lead to well-controlled drug delivery and successful tissue-like substitutes for assisting tissue and organ regeneration.

Besides the design and fabrication of new smart magnetic materials, it is also important to continue exploring the biological mechanisms at the cell and organism levels that respond to magnetic elements and to the magnetic forces necessary to activate or stimulate cell responses. This dynamic interaction among cell/tissue-magnetic system/magnetic forces may be tissue- or cell-specific, may depend on the regenerative potential of cell/tissue and on the purpose of the developed system (e.g. therapeutic agent release, augmentation device...). Furthermore studies should be performed to understand and determine how magnetic forces can safely impact cells and tissues in terms of exposure time, intensity of the field without prejudice to the patient and how deep into the tissues layers can local topic magnetic stimulation actuate in between the magnetic field and the tissue to regenerate .

The successful application of smart magnetic materials as biomedical tools for diagnosis and in clinical therapies can impact the quality of life of patients worldwide. Furthermore, TERM approaches that provide a real-time monitoring system with therapeutic action allowing the follow-up of patients after medical intervention without requiring further surgical procedures, through physical contact with medical devices

that generate magnetic forces and manipulate their intensity and duration stimulating local tissues, will be a major advance in clinical therapies aiming at the treatment of a wide range of injuries and related diseases.

1.6. References

[1] Lohmann KJ. Q&A: Animal behaviour: Magnetic-field perception. Nature. 2010;464:1140-2.

[2] Jogler C, Schüler D. Genetic Analysis of Magnetosome Biomineralization. In: Schüler D, editor. Magnetoreception and Magnetosomes in Bacteria: Springer Berlin Heidelberg; 2007. p. 133-61.

[3] Yan L, Zhang S, Chen P, Liu H, Yin H, Li H. Magnetotactic bacteria, magnetosomes and their application. Microbiological Research. 2012;167:507-19.

[4] Jaiswal MK, De M, Chou SS, Vasavada S, Bleher R, Prasad PV, et al. Thermoresponsive Magnetic Hydrogels as Theranostic Nanoconstructs. ACS applied materials & interfaces. 2014;6:6237-47.

[5] Kneipp J, Kneipp H, McLaughlin M, Brown D, Kneipp K. In Vivo Molecular Probing of Cellular Compartments with Gold Nanoparticles and Nanoaggregates. Nano letters. 2006;6:2225-31.

[6] Yuge L, Okubo A, Miyashita T, Kumagai T, Nikawa T, Takeda S, et al. Physical stress by magnetic force accelerates differentiation of human osteoblasts. Biochemical and biophysical research communications. 2003;311:32-8.

[7] Lima J, Gonçalves AI, Rodrigues MT, Reis RL, Gomes ME. The effect of magnetic stimulation on the osteogenic and chondrogenic differentiation of human stem cells derived from the adipose tissue (hASCs). Journal of Magnetism and Magnetic Materials. 2015;393:526-36.

[8] Henstock JR, Rotherham M, Rashidi H, Shakesheff KM, El Haj AJ. Remotely Activated Mechanotransduction via Magnetic Nanoparticles Promotes Mineralization Synergistically With Bone Morphogenetic Protein 2: Applications for Injectable Cell Therapy. Stem cells translational medicine. 2014;3:1363-74.

[9] Bai WF, Xu WC, Feng Y, Huang H, Li XP, Deng CY, et al. Fifty-Hertz electromagnetic fields facilitate the induction of rat bone mesenchymal stromal cells to differentiate into functional neurons. Cytotherapy. 2013;15:961-70.

[10] Ma J, Zhang Z, Su Y, Kang L, Geng D, Wang Y, et al. Magnetic stimulation modulates structural synaptic plasticity and regulates BDNF-TrkB signal pathway in cultured hippocampal neurons. Neurochemistry international. 2013;62:84-91.

[11] Trock DH, Bollet AJ, Markoll R. The effect of pulsed electromagnetic fields in the treatment of osteoarthritis of the knee and cervical spine. Report of randomized, double blind, placebo controlled trials. The Journal of rheumatology. 1994;21:1903-11.

[12] Perea H, Aigner J, Heverhagen JT, Hopfner U, Wintermantel E. Vascular tissue engineering with magnetic nanoparticles: seeing deeper. Journal of tissue engineering and regenerative medicine. 2007;1:318-21.

[13] Campbell SB, Patenaude M, Hoare T. Injectable Superparamagnets: Highly Elastic and Degradable Poly (N-isopropylacrylamide)–Superparamagnetic Iron Oxide Nanoparticle (SPION) Composite Hydrogels. Biomacromolecules. 2013;14:644-53.

[14] Servant A, Methven L, Williams RP, Kostarelos K. Electroresponsive polymer-carbon nanotube hydrogel hybrids for pulsatile drug delivery in vivo. Advanced healthcare materials. 2013;2:806-11.

[15] Glassman MJ, Olsen BD. Arrested Phase Separation of Elastin-like Polypeptide Solutions Yields Stiff, Thermoresponsive Gels. Biomacromolecules. 2015.

[16] Gao L, He J, Hu J, Wang C. Photoresponsive Self-Healing Polymer Composite with Photoabsorbing Hybrid Microcapsules. ACS applied materials & interfaces. 2015;7:25546-52.

[17] Lu J, Li Y, Hu D, Chen X, Liu Y, Wang L, et al. Synthesis and Properties of pH-, Thermo-, and Salt-Sensitive Modified Poly(aspartic acid)/Poly(vinyl alcohol) IPN Hydrogel and Its Drug Controlled Release. BioMed Research International. 2015;2015:12.

[18] Brahim S, Narinesingh D, Guiseppi-Elie A. Polypyrrole-hydrogel composites for the construction of clinically important biosensors. Biosensors & bioelectronics. 2002;17:53-9.

[19] Kumar A, Srivastava A, Galaev IY, Mattiasson B. Smart polymers: Physical forms and bioengineering applications. Progress in Polymer Science. 2007;32:1205-37.

[20] Ito A, Takizawa Y, Honda H, Hata K, Kagami H, Ueda M, et al. Tissue engineering using magnetite nanoparticles and magnetic force: heterotypic layers of cocultured hepatocytes and endothelial cells. Tissue engineering. 2004;10:833-40.

[21] Grassi-Schultheiss PP, Heller F, Dobson J. Analysis of magnetic material in the human heart, spleen and liver. Biometals : an international journal on the role of metal ions in biology, biochemistry, and medicine. 1997;10:351-5.

[22] Karlsson HL, Gustafsson J, Cronholm P, Moller L. Size-dependent toxicity of metal oxide particles–a comparison between nano- and micrometer size. Toxicology letters. 2009;188:112-8.

[23] Qiu D, An X. Controllable release from magnetoliposomes by magnetic stimulation and thermal stimulation. Colloids and surfaces B, Biointerfaces. 2013;104:326-9.

[24] Reddy LH, Arias JL, Nicolas J, Couvreur P. Magnetic Nanoparticles: Design and Characterization, Toxicity and Biocompatibility, Pharmaceutical and Biomedical Applications. Chemical Reviews. 2012;112:5818-78.

[25] Chen L, Zhang H, Li L, Yang Y, Liu X, Xu B. Thermoresponsive hollow magnetic microspheres with hyperthermia and controlled release properties. Journal of Applied Polymer Science. 2015;132:n/a-n/a.

[26] Kittel C. Physical Theory of Ferromagnetic Domains. Reviews of Modern Physics. 1949;21:541-83.

[27] Weissleder R, Elizondo G, Wittenberg J, Rabito CA, Bengele HH, Josephson L. Ultrasmall superparamagnetic iron oxide: characterization of a new class of contrast agents for MR imaging. Radiology. 1990;175:489-93.

[28] Tóth IY, Veress G, Szekeres M, Illés E, Tombácz E. Magnetic hyaluronate hydrogels: preparation and characterization. Journal of Magnetism and Magnetic Materials. 2015;380:175-80.

[29] Nel AE, Madler L, Velegol D, Xia T, Hoek EMV, Somasundaran P, et al. Understanding biophysicochemical interactions at the nano-bio interface. Nature materials. 2009;8:543-57.

[30] Lobatto ME, Fuster V, Fayad ZA, Mulder WJM. Perspectives and opportunities for nanomedicine in the management of atherosclerosis. Nat Rev Drug Discov. 2011;10:835-52.

[31] Huynh KA, Chen KL. Aggregation Kinetics of Citrate and Polyvinylpyrrolidone Coated Silver Nanoparticles in Monovalent and Divalent Electrolyte Solutions. Environmental science & technology. 2011;45:5564-71.

[32] Jiang S, Eltoukhy AA, Love KT, Langer R, Anderson DG. Lipidoid-Coated Iron Oxide Nanoparticles for Efficient DNA and siRNA delivery. Nano letters. 2013;13:1059-64.

[33] Gréget R, Nealon GL, Vileno B, Turek P, Mény C, Ott F, et al. Magnetic Properties of Gold Nanoparticles: A Room-Temperature Quantum Effect. ChemPhysChem. 2012;13:3092-7.

[34] Sanaee MR, Bertran E. Synthesis of Carbon Encapsulated Mono- and Multi-Iron Nanoparticles. Journal of Nanomaterials. 2015;2015:10.

[35] Santra S, Tapec R, Theodoropoulou N, Dobson J, Hebard A, Tan W. Synthesis and Characterization of Silica-Coated Iron Oxide Nanoparticles in Microemulsion: The Effect of Nonionic Surfactants. Langmuir. 2001;17:2900-6.

[36] Nel A, Xia T, Mädler L, Li N. Toxic Potential of Materials at the Nanolevel. Science. 2006;311:622-7.

[37] Cheng K, Shen D, Hensley MT, Middleton R, Sun B, Liu W, et al. Magnetic antibody-linked nanomatchmakers for therapeutic cell targeting. Nat Commun. 2014;5.

[38] Cova M, Oliveira-Silva R, Ferreira JA, Ferreira R, Amado F, Daniel-da-Silva AL, et al. Glycoprotein enrichment method using a selective magnetic nano-probe platform (MNP) functionalized with lectins. Methods in molecular biology (Clifton, NJ). 2015;1243:83-100.

[39] Majouga A, Sokolsky-Papkov M, Kuznetsov A, Lebedev D, Efremova M, Beloglazkina E, et al. Enzyme-functionalized gold-coated magnetite nanoparticles as novel hybrid nanomaterials: Synthesis, purification and control of enzyme function by low-frequency magnetic field. Colloids and Surfaces B: Biointerfaces. 2015;125:104-9.

[40] Yuen AKL, Hutton GA, Masters AF, Maschmeyer T. The interplay of catechol ligands with nanoparticulate iron oxides. Dalton Transactions. 2012;41:2545-59.

[41] Nel AE, Madler L, Velegol D, Xia T, Hoek EM, Somasundaran P, et al. Understanding biophysicochemical interactions at the nano-bio interface. Nature materials. 2009;8:543-57.

[42] Ge Y, Zhang Y, Xia J, Ma M, He S, Nie F, et al. Effect of surface charge and agglomerate degree of magnetic iron oxide nanoparticles on KB cellular uptake in vitro. Colloids and surfaces B, Biointerfaces. 2009;73:294-301.

[43] Shubayev VI, Pisanic TR, 2nd, Jin S. Magnetic nanoparticles for theragnostics. Adv Drug Deliv Rev. 2009;61:467-77.

[44] Panyam J, Sahoo SK, Prabha S, Bargar T, Labhasetwar V. Fluorescence and electron microscopy probes for cellular and tissue uptake of poly(d,l-lactide-co-glycolide) nanoparticles. International Journal of Pharmaceutics. 2003;262:1-11.

[45] Redhead HM, Davis SS, Illum L. Drug delivery in poly(lactide-co-glycolide) nanoparticles surface modified with poloxamer 407 and poloxamine 908: in vitro characterisation and in vivo evaluation. Journal of Controlled Release. 2001;70:353-63.

[46] Gonzales-Weimuller M, Zeisberger M, Krishnan KM. Size-dependant heating rates of iron oxide nanoparticles for magnetic fluid hyperthermia. Journal of magnetism and magnetic materials. 2009;321:1947-50.

[47] Creixell M, Bohorquez AC, Torres-Lugo M, Rinaldi C. EGFR-targeted magnetic nanoparticle heaters kill cancer cells without a perceptible temperature rise. ACS nano. 2011;5:7124-9.

[48] Kokot G, Zemljič Jokhadar Š, Batista U, Babič D. Magnetically Self-Assembled Colloidal Three-Dimensional Structures as Cell Growth Scaffold. Langmuir. 2015;31:9576-81.

[49] Jain KK. Use of nanoparticles for drug delivery in glioblastoma multiforme. Expert review of neurotherapeutics. 2007;7:363-72.

[50] Zhang L, Gu FX, Chan JM, Wang AZ, Langer RS, Farokhzad OC. Nanoparticles in medicine: therapeutic applications and developments. Clinical pharmacology and therapeutics. 2008;83:761-9.

[51] Li Y, Srinivasan B, Jing Y, Yao X, Hugger MA, Wang J-P, et al. Nanomagnetic Competition Assay for Low-Abundance Protein Biomarker Quantification in Unprocessed Human Sera. Journal of the American Chemical Society. 2010;132:4388-92.

[52] Soenen SJ, Himmelreich U, Nuytten N, De Cuyper M. Cytotoxic effects of iron oxide nanoparticles and implications for safety in cell labelling. Biomaterials. 2011;32:195-205.

[53] Arbab AS, Yocum GT, Rad AM, Khakoo AY, Fellowes V, Read EJ, et al. Labeling of cells with ferumoxides-protamine sulfate complexes does not inhibit function or differentiation capacity of hematopoietic or mesenchymal stem cells. NMR in biomedicine. 2005;18:553-9.

[54] Kim HS, Choi Y, Song IC, Moon WK. Magnetic resonance imaging and biological properties of pancreatic islets labeled with iron oxide nanoparticles. NMR in biomedicine. 2009;22:852-6.

[55] Bock N, Riminucci A, Dionigi C, Russo A, Tampieri A, Landi E, et al. A novel route in bone tissue engineering: magnetic biomimetic scaffolds. Acta Biomater. 2010;6:786-96.

[56] Ciofani G, Raffa V, Menciassi A, Cuschieri A, Micera S. Magnetic alginate microspheres: system for the position controlled delivery of nerve growth factor. Biomedical microdevices. 2009;11:517-27.

[57] Toyokuni S. Iron-induced carcinogenesis: the role of redox regulation. Free radical biology & medicine. 1996;20:553-66.

[58] Wydra RJ, Rychahou PG, Evers BM, Anderson KW, Dziubla TD, Hilt JZ. The role of ROS generation from magnetic nanoparticles in an alternating magnetic field on cytotoxicity. Acta biomaterialia. 2015;25:284-90.

[59] Markides H, Rotherham M, El Haj AJ. Biocompatibility and Toxicity of Magnetic Nanoparticles in Regenerative Medicine. Journal of Nanomaterials. 2012;2012:11.

[60] Pisanic TR, 2nd, Blackwell JD, Shubayev VI, Finones RR, Jin S. Nanotoxicity of iron oxide nanoparticle internalization in growing neurons. Biomaterials. 2007;28:2572-81.

[61] Jeng HA, Swanson J. Toxicity of metal oxide nanoparticles in mammalian cells. Journal of environmental science and health Part A, Toxic/hazardous substances & environmental engineering. 2006;41:2699-711.

[62] Munro HN. Iron regulation of ferritin gene expression. Journal of cellular biochemistry. 1990;44:107-15.

[63] Andrews NC. Molecular control of iron metabolism. Best practice & research Clinical haematology. 2005;18:159-69.

[64] Cheng Y, Zak O, Aisen P, Harrison SC, Walz T. Structure of the human transferrin receptor-transferrin complex. Cell. 2004;116:565-76.

[65] Weissleder R, Nahrendorf M, Pittet MJ. Imaging macrophages with nanoparticles. Nature materials. 2014;13:125-38.

[66] Arbab AS, Wilson LB, Ashari P, Jordan EK, Lewis BK, Frank JA. A model of lysosomal metabolism of dextran coated superparamagnetic iron oxide (SPIO) nanoparticles: implications for cellular magnetic resonance imaging. NMR in biomedicine. 2005;18:383-9.

[67] Levy M, Lagarde F, Maraloiu VA, Blanchin MG, Gendron F, Wilhelm C, et al. Degradability of superparamagnetic nanoparticles in a model of intracellular environment: follow-up of magnetic, structural and chemical properties. Nanotechnology. 2010;21:395103.

[68] Schulze E, Ferrucci JT, Jr., Poss K, Lapointe L, Bogdanova A, Weissleder R. Cellular uptake and trafficking of a prototypical magnetic iron oxide label in vitro. Investigative radiology. 1995;30:604-10.

[69] Sahay G, Alakhova DY, Kabanov AV. Endocytosis of nanomedicines. Journal of controlled release : official journal of the Controlled Release Society. 2010;145:182-95.

[70] Marion S, Wilhelm C, Voigt H, Bacri JC, Guillen N. Overexpression of myosin IB in living Entamoeba histolytica enhances cytoplasm viscosity and reduces phagocytosis. Journal of cell science. 2004;117:3271-9.

[71] Zhang S, Li J, Lykotrafitis G, Bao G, Suresh S. Size-Dependent Endocytosis of Nanoparticles. Advanced materials (Deerfield Beach, Fla). 2009;21:419-24.

[72] Benmerah A, Lamaze C. Clathrin-coated pits: vive la difference? Traffic (Copenhagen, Denmark). 2007;8:970-82.

[73] Soo Choi H, Liu W, Misra P, Tanaka E, Zimmer JP, Itty Ipe B, et al. Renal clearance of quantum dots. Nat Biotech. 2007;25:1165-70.

[74] Chithrani BD, Ghazani AA, Chan WCW. Determining the Size and Shape Dependence of Gold Nanoparticle Uptake into Mammalian Cells. Nano letters. 2006;6:662-8.
[75] Santos LJ, Reis RL, Gomes ME. Harnessing magnetic-mechano actuation in regenerative medicine and tissue engineering. Trends in biotechnology. 2015;33:471-9.
[76] Hsu S, Chang JC. The static magnetic field accelerates the osteogenic differentiation and mineralization of dental pulp cells. Cytotechnology. 2010;62:143-55.
[77] Kurian MV, Hamilton L, Keeven J, Mehl P, Mullins JM. Enhanced cell survival and diminished apoptotic response to simulated ischemia-reperfusion in H9c2 cells by magnetic field preconditioning. Apoptosis : an international journal on programmed cell death. 2012;17:1182-96.
[78] Sapir Y, Cohen S, Friedman G, Polyak B. The promotion of in vitro vessel-like organization of endothelial cells in magnetically responsive alginate scaffolds. Biomaterials. 2012;33:4100-9.
[79] Samal SK, Goranov V, Dash M, Russo A, Shelyakova T, Graziosi P, et al. Multilayered Magnetic Gelatin Membrane Scaffolds. ACS applied materials & interfaces. 2015;7:23098-109.
[80] Meng J, Xiao B, Zhang Y, Liu J, Xue H, Lei J, et al. Super-paramagnetic responsive nanofibrous scaffolds under static magnetic field enhance osteogenesis for bone repair in vivo. Scientific Reports. 2013;3:2655.
[81] Tasoglu S, Yu CH, Liaudanskaya V, Guven S, Migliaresi C, Demirci U. Magnetic Levitational Assembly for Living Material Fabrication. Advanced healthcare materials. 2015;4:1469-76, 22.
[82] Yanase N, Noguchi H, Asakura H, Suzuta T. Preparation of magnetic latex particles by emulsion polymerization of styrene in the presence of a ferrofluid. Journal of Applied Polymer Science. 1993;50:765-76.
[83] Zhao W, Odelius K, Edlund U, Zhao C, Albertsson A-C. In situ synthesis of magnetic field-responsive hemicellulose hydrogels for drug delivery. Biomacromolecules. 2015;16:2522-8.
[84] Santo VE, Rodrigues MT, Gomes ME. Contributions and future perspectives on the use of magnetic nanoparticles as diagnostic and therapeutic tools in the field of regenerative medicine. Expert review of molecular diagnostics. 2013;13:553-66.
[85] Goncalves AI, Rodrigues MT, Carvalho PP, Banobre-Lopez M, Paz E, Freitas P, et al. Exploring the Potential of Starch/Polycaprolactone Aligned Magnetic Responsive Scaffolds for Tendon Regeneration. Advanced healthcare materials. 2015.

[86] Luo B, Song X-J, Zhang F, Xia A, Yang W-L, Hu J-H, et al. Multi-Functional Thermosensitive Composite Microspheres with High Magnetic Susceptibility Based on Magnetite Colloidal Nanoparticle Clusters. Langmuir. 2010;26:1674-9.

[87] Gao Q, Wang C, Liu H, Chen Y, Tong Z. Dual nanocomposite multihollow polymer microspheres prepared by suspension polymerization based on a multiple pickering emulsion. Polymer Chemistry. 2010;1:75-7.

[88] Decher G. Fuzzy nanoassemblies: toward layered polymeric multicomposites. science. 1997;277:1232-7.

[89] Schenck JF. Safety of Strong, Static Magnetic Fields. Journal of Magnetic Resonance Imaging. 2000;12:2-19.

[90] Zhang B, Zhang H, Fan X, Li X, Yin D, Zhang Q. Preparation of thermoresponsive Fe3O4/P(acrylic acid-methyl methacrylate-N-isopropylacrylamide) magnetic composite microspheres with controlled shell thickness and its releasing property for phenolphthalein. J Colloid Interface Sci. 2013;398:51-8.

[91] Habraken WJ, Wolke JG, Mikos AG, Jansen JA. Injectable PLGA microsphere/calcium phosphate cements: physical properties and degradation characteristics. Journal of biomaterials science Polymer edition. 2006;17:1057-74.

[92] Mhlanga N, Sinha Ray S, Lemmer Y, Wesley-Smith J. Polylactide-based Magnetic Spheres as Efficient Carriers for Anticancer Drug Delivery. ACS applied materials & interfaces. 2015;7:22692-701.

[93] Al-Qadi S, Grenha A, Remuñán-López C. Microspheres loaded with polysaccharide nanoparticles for pulmonary delivery: Preparation, structure and surface analysis. Carbohydrate Polymers. 2011;86:25-34.

[94] Ma J, Wu Y, Zeng Y, Li Y, Wu D. Thermo-stable hollow magnetic microspheres: preparation, characterization and recyclable catalytic applications. Journal of Materials Chemistry A. 2015;3:16762-73.

[95] Toprak MS, McKenna BJ, Mikhaylova M, Waite JH, Stucky GD. Spontaneous Assembly of Magnetic Microspheres. Advanced Materials. 2007;19:1362-8.

[96] Ozdemir T, Sandal D, Culha M, Sanyal A, Atay NZ, Bucak S. Assembly of magnetic nanoparticles into higher structures on patterned magnetic beads under the influence of magnetic field. Nanotechnology. 2010;21:125603.

[97] Xulu PM, Filipcsei G, Zrínyi M. Preparation and Responsive Properties of Magnetically Soft Poly(N-isopropylacrylamide) Gels. Macromolecules. 2000;33:1716-9.

[98] Martina MS, Fortin JP, Menager C, Clement O, Barratt G, Grabielle-Madelmont C, et al. Generation of superparamagnetic liposomes revealed as highly efficient MRI contrast agents for in vivo imaging. J Am Chem Soc. 2005;127:10676-85.

[99] Monnier Christophe A, Burnand D, Rothen-Rutishauser B, Lattuada M, Petri-Fink A. Magnetoliposomes: opportunities and challenges. European Journal of Nanomedicine2014. p. 201.

[100] Mohammed AR, Weston N, Coombes AGA, Fitzgerald M, Perrie Y. Liposome formulation of poorly water soluble drugs: optimisation of drug loading and ESEM analysis of stability. International Journal of Pharmaceutics. 2004;285:23-34.

[101] Barenholz Y. Doxil(R)–the first FDA-approved nano-drug: lessons learned. Journal of controlled release : official journal of the Controlled Release Society. 2012;160:117-34.

[102] Katagiri K, Imai Y, Koumoto K, Kaiden T, Kono K, Aoshima S. Magnetoresponsive on-demand release of hybrid liposomes formed from Fe3 O4 nanoparticles and thermosensitive block copolymers. Small (Weinheim an der Bergstrasse, Germany). 2011;7:1683-9.

[103] Simoes S, Moreira JN, Fonseca C, Duzgunes N, de Lima MC. On the formulation of pH-sensitive liposomes with long circulation times. Adv Drug Deliv Rev. 2004;56:947-65.

[104] Soenen SJ, De Meyer SF, Dresselaers T, Vande Velde G, Pareyn IM, Braeckmans K, et al. MRI assessment of blood outgrowth endothelial cell homing using cationic magnetoliposomes. Biomaterials. 2011;32:4140-50.

[105] Yamamoto Y, Ito A, Kato M, Kawabe Y, Shimizu K, Fujita H, et al. Preparation of artificial skeletal muscle tissues by a magnetic force-based tissue engineering technique. Journal of bioscience and bioengineering. 2009;108:538-43.

[106] Brulé S, Levy M, Wilhelm C, Letourneur D, Gazeau F, Ménager C, et al. Doxorubicin Release Triggered by Alginate Embedded Magnetic Nanoheaters: A Combined Therapy. Advanced Materials. 2011;23:787-90.

[107] Daniel-da-Silva AL, Lóio R, Lopes-da-Silva JA, Trindade T, Goodfellow BJ, Gil AM. Effects of magnetite nanoparticles on the thermorheological properties of carrageenan hydrogels. Journal of colloid and interface science. 2008;324:205-11.

[108] Shin MK, Kim SI, Kim SJ, Park SY, Hyun YH, Lee Y, et al. Controlled Magnetic Nanofiber Hydrogels by Clustering Ferritin. Langmuir. 2008;24:12107-11.

[109] Beaune G, Ménager C. In situ precipitation of magnetic fluid encapsulated in giant liposomes. Journal of Colloid and Interface Science. 2010;343:396-9.

[110] Liang Y-Y, Zhang L-M, Jiang W, Li W. Embedding Magnetic Nanoparticles into Polysaccharide-Based Hydrogels for Magnetically Assisted Bioseparation. ChemPhysChem. 2007;8:2367-72.

[111] Schexnailder P, Schmidt G. Nanocomposite polymer hydrogels. Colloid Polym Sci. 2009;287:1-11.

[112] Meid J, Dierkes F, Cui J, Messing R, Crosby AJ, Schmidt A, et al. Mechanical properties of temperature sensitive microgel/polyacrylamide composite hydrogels?from soft to hard fillers. Soft Matter. 2012;8:4254-63.

[113] Hoare T, Santamaria J, Goya GF, Irusta S, Lin D, Lau S, et al. A magnetically triggered composite membrane for on-demand drug delivery. Nano letters. 2009;9:3651-7.

[114] Hu S-H, Liu T-Y, Tsai C-H, Chen S-Y. Preparation and characterization of magnetic ferroscaffolds for tissue engineering. Journal of Magnetism and Magnetic Materials. 2007;310:2871-3.

[115] Cezar CA, Kennedy SM, Mehta M, Weaver JC, Gu L, Vandenburgh H, et al. Biphasic Ferrogels for Triggered Drug and Cell Delivery. Advanced healthcare materials. 2014;3:1869-76.

[116] Torchilin VP. Drug targeting. European journal of pharmaceutical sciences : official journal of the European Federation for Pharmaceutical Sciences. 2000;11 Suppl 2:S81-91.

[117] Liu W, Li Y, Feng S, Ning J, Wang J, Gou M, et al. Magnetically controllable 3D microtissues based on magnetic microcryogels. Lab on a chip. 2014;14:2614-25.

[118] Chen C-H, Abate AR, Lee D, Terentjev EM, Weitz DA. Microfluidic Assembly of Magnetic Hydrogel Particles with Uniformly Anisotropic Structure. Advanced Materials. 2009;21:3201-4.

[119] Khademhosseini A, Langer R. Microengineered hydrogels for tissue engineering. Biomaterials. 2007;28:5087-92.

[120] Gurkan UA, Tasoglu S, Kavaz D, Demirel MC, Demirci U. Emerging technologies for assembly of microscale hydrogels. Advanced healthcare materials. 2012;1:149-58.

[121] Fu CY, Lin CY, Chu WC, Chang HY. A simple cell patterning method using magnetic particle-containing photosensitive poly (ethylene glycol) hydrogel blocks: a technical note. Tissue engineering Part C, Methods. 2011;17:871-7.

[122] Alsberg E, Feinstein E, Joy MP, Prentiss M, Ingber DE. Magnetically-guided self-assembly of fibrin matrices with ordered nano-scale structure for tissue engineering. Tissue engineering. 2006;12:3247-56.
[123] Ino K, Ito A, Honda H. Cell patterning using magnetite nanoparticles and magnetic force. Biotechnology and bioengineering. 2007;97:1309-17.
[124] Yun HM, Lee ES, Kim MJ, Kim JJ, Lee JH, Lee HH, et al. Magnetic Nanocomposite Scaffold-Induced Stimulation of Migration and Odontogenesis of Human Dental Pulp Cells through Integrin Signaling Pathways. PloS one. 2015;10:e0138614.
[125] Fukada E, Yasuda I. On the Piezoelectric Effect of Bone. Journal of the Physical Society of Japan. 1957;12:1158-62.
[126] Lee WY, Cheng WY, Yeh YC, Lai CH, Hwang SM, Hsiao CW, et al. Magnetically directed self-assembly of electrospun superparamagnetic fibrous bundles to form three-dimensional tissues with a highly ordered architecture. Tissue engineering Part C, Methods. 2011;17:651-61.

CHAPTER II Materials and Methods

2. MATERIALS AND METHODS

This chapter aims to offer a detailed description of the materials, reagents, cell types and experimental techniques used in the work that has been developed under the scope of this Master Thesis.

2.1 Materials

In this project, magnetic responsive chondroitin sulfate hydrogels enriched with human platelet lysate were produced envisioning their application for interfacial tissue engineering (TE) strategies. As a proof of concept, we investigated the functionality of developed hydrogels as a construct for tendon-to-bone interface (Figure 2.1).

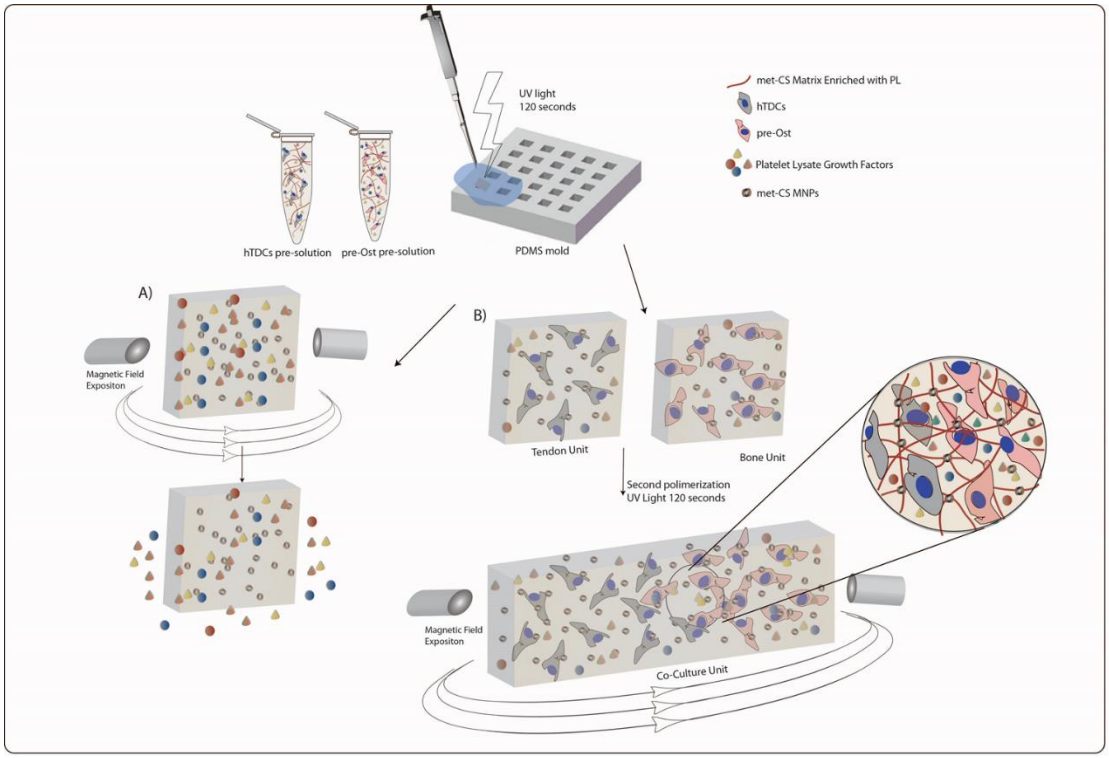

Figure 2.1: Schematic representation of the work developed in this Master Thesis. Production of met-CS MAGPL hydrogels for A) modulation of the release of bioagents present in PLs through the use of an external magnetic field (EMF); B) assemble of met-CS MAGPL Hydrogels as single tendon

or bone units and co-culture units aiming at a tendon-to-bone interface model. The impact of EMF was also investigated in single and co-culture units.

The selection of the elements to develop such system as well as their methods of production and characterization is described in detail in the following sections.

2.1.1 Chondroitin sulfate

Chondroitin sulfate (CS) is a sulfated glycosaminoglycan composed of a repeating disaccharide unit resulting from the copolymerization of D-glucoronic acid with N-acetyl-D-galactosamine, usually sulfated in carbon 4 and 6[1]. It is one of the major components of the extracellular matrix (ECM) of several connective tissues including bone and tendon, playing a crucial function in the maintenance of the structural integrity of the ECM, and for instance in the establishment of interactions with collagen[2],[3]. In the ECM, CS is largely associated with glycoproteins, forming proteoglycans through covalent bonding. Moreover, CS is capable of absorbing large quantities of water due to their polyelectrolyte nature without sacrificing its mechanical properties[4], which renders CS great potential to be used as an ECM-mimicking natural material. The presence of sulfate (pKa ~ 1) and carboxyl (pKa ~3.3) groups confers to this polymer a strong negative charge even at low pH (<3)[5], and thus an inherent ability to attract positively charged molecules like growth factors (GFs) through electrostatic interactions. Indeed, CS has been shown to have a significant role in intracellular signaling pathways, by binding and mediating the regulation of GFs and other bioactive molecules[5]. CS also plays a fundamental role in modulating the stability, activity, release, and spatial localization of these GFs, which has been associated with the sulfation of the CS molecule[6]. Furthermore, it has been reported to participate in tissue regeneration tuning biological properties such as the modulation of anti-inflammatory response, water and nutrient absorption and improved wound healing[4]. As a natural polymer, CS evidences interesting properties namely biodegradability, chemical versatility and biological performance for tissue engineering applications[4]. CS is biodegradable by hyaluronidases (HAses)[7] and chondroitinases (CSses)[8], naturally available in the human body, by hydrolysis in the hexosaminidic β(1→4) linkages between N-acetyl d-glucosamine and d-glucuronic acid[1]. The chemical structure of CS offers multiple modification sites, including carboxyl and hydroxyl groups, which are involved in the chemical modification of CS with methacrylate groups. Methacrylated

derivatives are versatile and can be more easily converted into matrices with different shapes, such as scaffolds, hydrogels or other 3D structures by radical polymerization using photo-initiators, such as Irgacure 259 in the presence of UV light[4].

In this work, chondroitin sulfate was obtained from chondroitin sulfate A sodium salt from bovine trachea purchased from Sigma and chemically modified with functional methacrylated groups as described in section 2.2.1.

2.1.2 Superparamagnetic Iron Oxide Nanoparticles (SPIONs)

Superparamagnetic nanoparticles (SPIONs) are widely used in biomedical applications, essentially due to their high magnetization in combination with the capacity of not retaining magnetization after removal of the magnetic field, thus avoiding aggregation [9]. In fact, these properties make SPIONs excellent candidates to provide magnetic responsiveness to non-magnetic tridimensional (3D) supportive matrices, such as scaffolds or hydrogels for tissue engineering applications [9]. In the particular case of mechano-sensitive tissues like tendon and bone, magnetic stimulation has been shown impact the activation of mechanotransduction signaling pathways[10]. Moreover, SPIONs incorporated in 3D biomaterials can be further stimulated through the application of an external magnetic field (EMF), static or alternating, that cells sense as being mechanical (compressive and tensile) forces, replicating the effect of mechanical loading essential for the normal functionality of these tissues[11]. Furthermore, the application of SPIONs in the field of tissue engineering (TE) has the potential to stimulate and control sub-cellular interactions that are not possible using conventional macro and micro scale TE approaches [11]. Moreover, SPIONs can render biomaterials the possibility of being manipulated using magnets and thus enabling their controlled assembly towards the generation of structures with increasing complexity [12]. In fact, the incorporation of SPIONS allows the development of novel and sophisticated biocompatible materials with additional features, such as magnetic manipulation, while influencing the cellular processes contributing to the creation of tissue-like constructs with improved functionality.

In this work, magnetic nanoparticles (MNPs) with superparamagnetic behaviour (SPIONs) were produced using Fe^{3+} and Fe^{2+} salts purchased to Sigma by a co-precipitation method and further functionalized with a methacrylated chondroitin sulphate (met-CS) coating. Nevertheless in this work SPIONs were referred as MNPs.

2.1.3 Platelets Lysate (PL)

The use of platelet-rich hemoderivates (PRHds), like platelet lysates (PL), platelet-rich plasma (PRP) or platelet rich fibrin (PRP), has a vast potential for regenerative strategies[13]. The PRHds have been proposed as an alternative cost-effective source of GFs and other molecules with biological activity at physiological concentrations[14]. Among PRHds, PL offers several advantages namely the removal of platelet debris, thus the possibility of retraction is limited, and the donor to donor variation can be minimized using pooled samples obtained from several donors and frozen until needed [13].

PL can be easily prepared by mechanical disruption of platelet membranes in platelet concentrates via thermal shock through cycles of freezing and thawing. Subsequent centrifugation separates the platelet debris from the supernatant containing bioactive platelet factors. Among the GFs derived from PL, PDGF-BB has been shown to have a role in fundamental stages of the regenerative process and in the processes of osteogenesis[15] and tenogenesis[16]. PL comprises also structural proteins involved in the formation of blood clot, such as fibrin, fibronectin and vitronectin [13] acting as provisional ECM matrix during coagulation and providing cues for cell adhesion and migration[14].

PL was prepared from platelet concentrate (PC) obtained by plasma apheresis from volunteer blood donors, following a previous established cooperation protocol with Hospital de São João (Porto, Portugal). PC with a platelet count of 10^6 platelets/µL were biologically selected according to the Portuguese legislation (Decreto Lei nº 185/2015) and processed as previously described [17],[18]. Briefly, PC samples were pooled using 9 donors and subjected to three freeze/thaw cycles. Each cycle consisted in a quick freezing by immersion in liquid nitrogen (-196 °C) and thawing in a water bath at 37°C. These steps enabled platelet lysis and promoted the release of their protein content. In order to eliminate platelet debris, PL was centrifuged at 1400 g for 10 minutes. Finally, the PL was aliquoted and stored at -80°C upon needed. Prior to use, PL aliquots were defrosted and centrifuged at 2000 rpm for 5 min.

2.2 Methods

2.2.1 Synthesis of Methacrylated Chondroitin Sulfate

Hydrogel matrices are typically formed by chemical or ionic crosslinks. Covalently crosslinked hydrogels have become more attractive in TE strategies as their structural stability, mechanical properties and degradation can be tuned[19]. In order to generate mechanically and chemically robust materials, native chondroitin sulfate can be modified through covalent derivatization of the carboxylic acid or hydroxyl group, as occurs in the methacrylation process.

In the methacrylation process, the hydroxyl group of CS is nucleophilically attacked by the carbonyl groups present in the methacrylic anhydride in order to form an ester bond, originating methacrylated chondroitin sulfate (met-CS) [20] (Figure 2.2). The methacrylate substitution on CS can occurs by a simple and reproducible reaction of CS with methacrylic anhydride in basic conditions (ph ~ 8.5). Additionally, the degree of substitution on CS can be controlled by several parameters, including the reaction time, reaction temperature, concentration of methacrylic anhydride and the pH. [20]

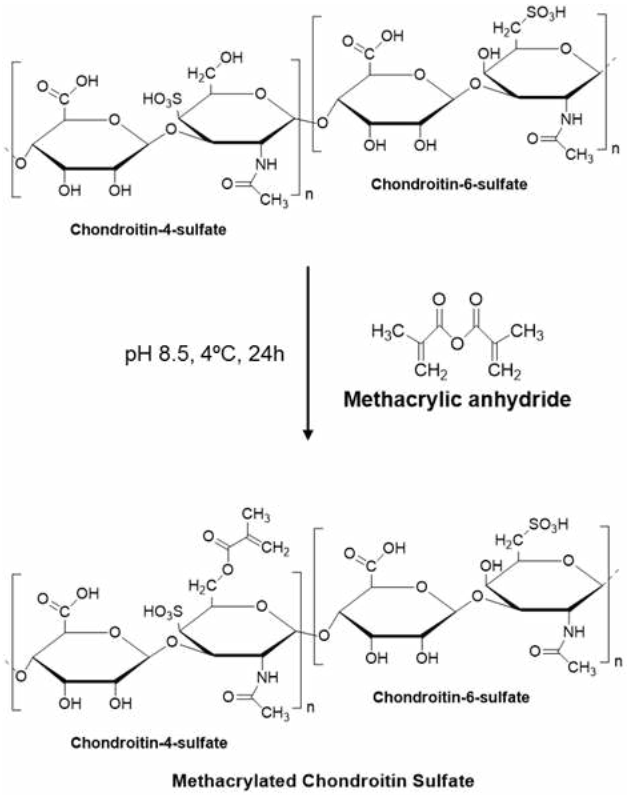

Figure 2.2: Methacrylation process of Chondroitin sulfate (CS) using methacrylic anhydride in basic conditions.

CS methacrylation was performed following a procedure previously described elsewhere [21]. In brief, a 1% (w/v) solution of CS was prepared in distilled water and the pH of the solution was adjusted to 8.5 using a 5 M NaOH solution. The methacrylation process was performed at 4°C with the slowly addition of 10-fold excess molar of methacrylic anhydride (276685, Sigma) to the CS solution. The pH was continuously adjusted to 8-8.5 by dropwise addition of NaOH for 24h. Then, the resulting solution was precipitated by adding 3-fold reaction volume of cold ethanol (absolute ethanol at -20°C, E/0650DF/17, Enzymatic). Three subsequent washing and centrifugation steps (6154 g, once for 10 minutes and twice for 5 minutes) using absolute ethanol were performed to eliminate unreacted reagents and reaction by-products. The methacrylated chondroitin sulfate (met-CS) was then dissolved in distilled water and purified by dialysis (cellulose dialysis membranes, average flat width 33 mm, Mw cut-off 14 kDa, Sigma) against distilled water for one week, with water renewal three times a day. Finally, the solution was filtered (180µm, Millipore), frozen at -80°C and freeze-dried (LyoALfa 10/15 Telstar) for one week.

2.2.2 Production of Methacrylated-Chondroitin Sulfate Nanoparticles (met-CS MNPs)

2.2.2.1. Production of Magnetic Nanoparticles (MNPs) by Co-Precipitation Method

Magnetic nanoparticles (MNPs) developed for biomedical applications have been synthesized using different chemical methods including co-precipitation microemulsions and hidrotermal synthesis, among others[9]. In particular, the co-precipitation method allows to produce a large amount of MNPs with high purity and excellent magnetic properties in a simple and efficient manner[9]. Thus, MNPs were prepared by co-precipitation of Fe^{2+} and Fe^{3+} with ammonium hydroxide (NH_4OH) (05002, Sigma). The chemical reaction of iron oxide nanoparticles formation is described by Equation 2.1.

$$Fe^{2+} + 2Fe^{3+} + 8OH \rightarrow Fe_3O_4 + 4H_2O \quad \textbf{(Equation 2.1)}$$

Briefly, $FeCl_3.6H_2O$ (31232, Sigma) and $FeCl_2.4H_2O$ (220299, Sigma) were mixed to form a 50 mL aqueous solution (Millipore water) at a molar ratio of 2:1 (2.25 mmol Fe^{3+}: 1.125 mmol Fe^{2+}) inside a triple bottleneck under magnetic stirring and in a nitrogen environment. The mixture was heated up to 80 °C and 25% (v/v) of NH_4OH was added to the salt solution until the pH of the solution

became 10.5. After the addition of NH_4OH, the mixture developed a dark color, indicating the formation of the MNPs. The solution was further cooled at room temperature for 15 min and the dark precipitate was separated from the solution using a permanent magnetic (0.6 T). These particles were washed 3 times with Millipore water and 3 times with absolute ethanol by centrifugation at 8322 rcf for 15 min in order to remove the unadsorbed Fe^{2+}, Fe^{3+} cations and the NH_4OH.

2.2.2.2. Functionalization of MNPs with a met-CS Coating

Since iron nanoparticles are easily oxidized in the presence of oxidant agents as oxygen and it is important to obtain physically and chemically stable colloidal systems, the MNPs should be protected[9]. A common and quite effective strategy is to coat MNPs with a polymer. Polymeric coatings may also be used as multifunctional tools to improve the biocompatibility [9], favor water-dispersibility, prevent both *in vitro* and *in vivo* MNP aggregation and, for instance, can be further used as a carrier of GF or drugs[22][23]. Since electrostatic repulsion may occur between charged particles, the coating may also provide an electrosteric stabilization effect.

In this work, MNPs were coated with CS modified with methacrylate groups (met-CS) to chemically bind MNPs to a methacrylated CS hydrogel matrix, assisting the development of multifunctional 3D matrices (Figure 2.3). With this strategy it is possible to overcome a fast loss of MNPs from the matrix upon contact with liquid systems, which has been described as a major limitation of magnetic hydrogels[24]. Moreover, the met CS will also provide stabilization of MNP, as uncoated MNPs tend to aggregate when they are mixed with polymer solutions yet without interfering with the magnetic responsiveness of MNPs.

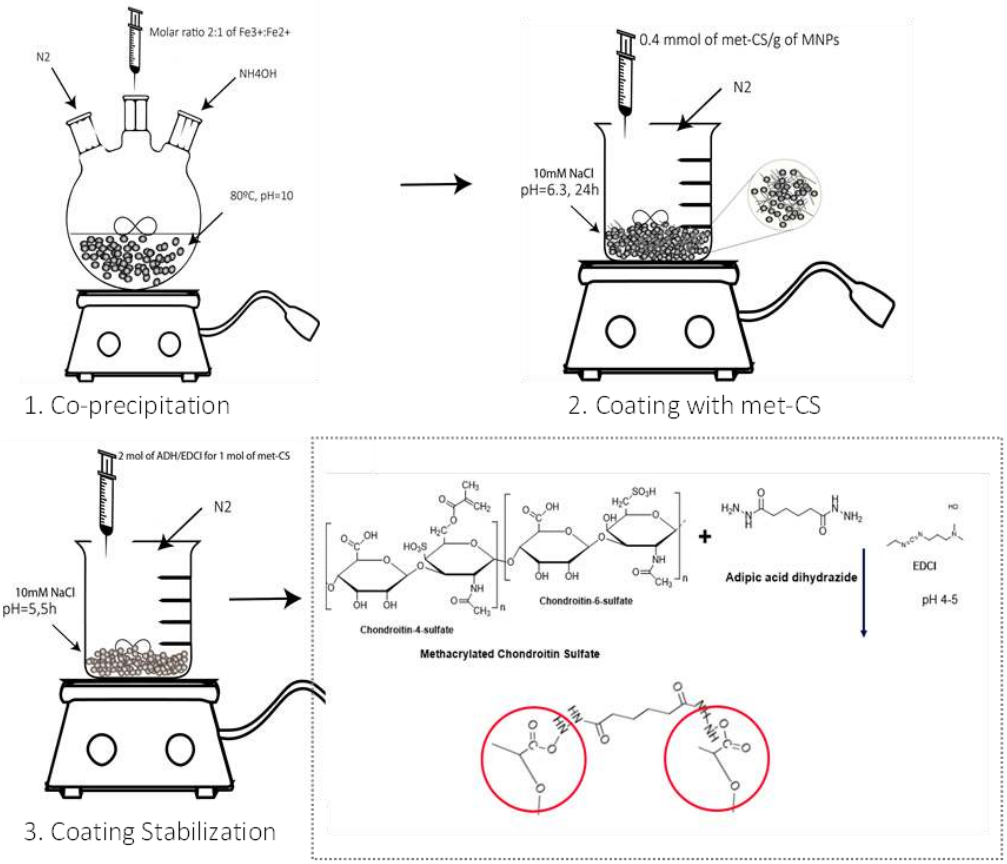

Figure 2.3: Schematic representation of the production steps of methacrylated chondroitin sulfate (met-CS MNPs). Carbodiimide (EDCI), Adipic Acid Dihydrazide (ADH), Sodium Chloride (NaCl).

In this work, the coating of the MNPs with methacrylated CS (met MNPs) was performed by suspending MNPs (3.3 mg/mL) in a solution of 10mM of NaCl and the pH adjusted to 6.3 ± 0.3. Afterwards, a 2% (w/v) met-CS solution was added dropwise at a solid/liquid ratio of 20 g/L (which means 0.4 mmol of met-CS per gram of MNPs). The pH was re-set to 6.3±0.3 and the coating process was carried out for 24h under magnetic agitation in a nitrogen environment.

The stabilization of the met-CS coating was performed by chemical crosslinking of the carboxylic acid moieties of the glucoronic acid with adipic acid dihydrazide (ADH) using a well-established carbodiimide (EDCI)-based chemistry[25] (Figure 2.3). Briefly, the pH of the met-CS MNPs suspension was set to 4.75 and a solution containing ADH (A0638, Sigma) and EDCI (424331, Sigma) corresponding to a molar excess of 2:1 (2 mol of ADH/EDCI for 1 mol of met-CS) was added dropwise to the suspension. The pH was continuously adjusted to 4.5 with 0.1 M of HCl and the reaction was allowed to proceed at room temperature until no pH variation was observed.

The solution was then washed 3 times by centrifugation (8322 rcf, 10 min) with Milipore water. Afterwards, the solution was dialyzed (cellulose dialysis membranes, average flat width 33 mm, Mw cut-off 14 kDa, Sigma) for one week against Milipore water.

2.2.3 Photopolymerization

Radical photopolymerization is one of the most common methods to produce hydrogels by combining the irradiation of a given wavelength and light-sensitive compounds, the photoinitiators. The photoinitiator is decomposed into free radicals leading to the formation of covalent bonds between precursor molecules in a fast reaction which results in the formation of a hydrogel matrix. Particularly, in materials with methacrylated groups under exposure to a light source, free radicals react with the C=C present in the methacrylate group creating new radicals called primary propagating radicals that initiate polymerization. The reaction is propagated until radical molecules are no longer available. UV light-activated polymerization is often used to produce hydrogels for biomedical applications [4], allowing spatial and temporal control of the reaction. In addition, UV light activated systems allow a fast curing rate and the capacity to initiate the reaction without extreme temperatures or environments without oxygen, thus allowing the encapsulation of cells without a significantly impact on their viability [26]. Moreover these systems require a UV sensitive photoiniatior like Irgacure 2959, commonly used due to a well-established cytocompatibility in concentrations below 0.25 % (w/v) [27].

To prepare the hydrogels Irgacure 2959 was used in combination with a UV light curing system (EXFO OmniCure S2000) with a range wavelength of 320-500 nm and a potency of 1.2 mW/cm^2 to establish a stable network between produced met-CS MNPs and the met-CS matrix in order to obtain magnetic responsive met-CS hydrogels.

2.2.4 Development of Magnetic Responsive Hydrogels Enriched with Platelet Lysate (met-CS MAGPL Hydrogels)

Methacrylated chondroitin sulfate was used to produce photocrosslinkable met CS hydrogel matrices using Irgacure 2959 [2-hydroxy-4'-(2-hydroxyethoxy)-2-methylpropiophenone 98%] (410896, Sigma) in the presence of UV light. For that, Irgacure 2959 was dissolved either in phosphate buffered saline (PBS) or in PL solutions to a final concentration of 0.25 % (w/v). Then, 8% (w/v) met-CS was dissolved into these solutions of PBS or PL, vortex and centrifuged for 3

minutes at 5000 rpm to remove the oxygen and air bubbles. Afterwards, different concentration of met-CS MNPs (100, 200 and 400 µg/mL) were added to the met-CS solution of PBS (met-CS MAG, experimental control) or PL (met-CS MAGPL) and sonicated to homogenize the met-CS MNPs. Hydrogels without met-CS MNPs were also produced as controls also prepared with a PBS or a PL solution and described as met-CS and met-CS PL, respectively (Table 2.1).

Table 2.1: Met CS hydrogel formulations prepared with met-CS MNPs in different solutions used in the proposed study.

	Met-CS MNPs (µg/ml)		
Solvent of met-CS	0	200	400
PBS	met-CS	Met-CS_{200} MAG	Met-CS_{400} MAG
PL	met-CS/PL	Met-CS_{200} MAGPL	Met-CS_{400} MAGPL

After assessing the most promising formulation with met-CS MNPs (200µg/mL) for cellular studies, met CS hydrogels enriched with PL were produced in the form of single and double hydrogel units. The single and double hydrogel units were envisioned to assess cell behavior in single and co-culture systems to better understand cell response to the developed hydrogels and also to evaluate their potential for interfacial tissue applications.

The single hydrogel units were produced by injecting 50 µL of a solution with the met-CS PL and met-CS MNPs into customized polydimethylsiloxane (PDMS, Sylgard® 184 Silicone Elastomer kit, Dow Corning) molds with a square shape of approximately 5×5 mm and 1 mm of height and after polymerization by exposure to UV light (320-500 nm, 1.2 mW/cm2, EXFO OmniCure S2000) for 120 seconds.

In the case of double hydrogel units, the first hydrogel unit was prepared as describd for the single units and placed on the left side of a a PDMS mold with 10mm×10mm and another 50 µL of solution was added to the right side of this mold. The hydrogels units were physically attached into a double hydrogel unit by UV light polymerization for 120 seconds.

2.3 Characterization of met-CS by ^{1}H Nuclear Magnetic Resonance (NMR)

NMR spectroscopy is a technique commonly used to acquire information regarding physical, chemical and electronic properties of atoms and molecules. Thus, the degree of modification of CS after reaction with methacrylic anhydride was determined by the analysis of ^{1}H NMR spectrum. For that, met-CS as well as unmodified CS were dissolved in deuterium oxide ($^{2}H_2O$, D-020-100, Laborspirit) at a final concentration of 5mg/mL and their spectra were recorded (Varian Inova 500) at 70ºC with a frequency of 400.13 MHz and a delay of 1s.

The degree of methacrylation (Dm) was calculated based on the ratio between the relative area of the peaks corresponding to vinyl protons of methacryloyl moiety (at 5.8 and 6.2 ppm) and the methyl protons of the acetyl moiety of CS (at ~2.1 ppm). Data on the quantification of the degree of methacrylation is presented in Annex I.

2.4 Physicochemical characterization of met CS MNPs

2.4.1 Fourier Transform Infrared (FTIR) Spectroscopy

Infrared spectroscopy allows the study of the interaction of infrared light with matter to withdraw chemical and structural information from a sample. In this work, Fourier transform infrared spectroscopy (FTIR) was used to qualitatively analyze the coating layer of met-CS MNPs and the successful crosslinking between the met-CS with ADH/EDC. Uncoated MNPs were also analyzed as experimental controls. The infrared spectra of met-CS MNPs and uncoated MNPs were recorded on an IR-Prestige 21 spectrometer (Shimadzu, Scientific Instruments, USA) by averaging 32 scans at a resolution of 4 cm^{-1} over the wavenumber range between 4000 cm^{-1} and 400 cm^{-1} at room temperature. Samples were prepared using the potassium bromide (KBr) (221864, Sigma) pellet technique. Briefly, uncoated MNPs and met-CS MNPs were dried at 105 °C for 24h. Afterwards, these formulations of MNPs were mixed with KBr and processed into pellets before acquisition.

The regions of the spectra at 1550–1650 cm^{-1} (corresponding to asymmetric vibration of R-COO), 1515–1570 cm^{-1} (corresponding to NH bending of the amides II), 1630–1680 cm^{-1} (correspondent to amides II, C=O stretching, NH bending), 1715 cm^{-1} (correspondent to C=O stretch of the ester group) and at 1250 cm^{-1} (the stretch of the SO group) were analyzed.

Electrokinetic Measurement (Zeta Potential)

The pH-dependent and ionic strength surface charge of MNPs impact MNPs aggregation in aqueous suspension. In suspensions of uncoated MNPs the surface charge of the iron core that

can lead to the formation of positive Fe-OH_2^+ and negative Fe-OH^- while in the case of met-CS MNP suspensions, the charge depends on the groups present in the met-CS [22].

Thus to maximize the electrostatic interactions of MNPs before the met CS coating and to assess the stability of both met-CS MNPs and uncoated MNPs suspensions, the zeta potential was verified at different pH (3, 5, 7, 10).

Zeta Potential evaluation was assessed in 0.005% (w/v) solutions of met-CS MNP and uncoated MNPs in ultrapure water. The pH of the solutions was adjusted with 0.5 mM of NaOH or HCl. Then the resultant suspension was sonicated for 1 minute at room temperature and 1 mL of suspension was transferred into a Universal 'dip' cell kit (Malvern). The zeta potential was measured at room temperature using a ZetaSize Nano-ZS (Malvern Instruments Ltd.). Triplicate samples were considered and analyzed for a minimum of 10 scans.

2.4.2 Determination of the Hydrodynamic Size

The dimensions of produced met-CS MNPs were measured using a ZetaSizer Nano dynamic light scattering equipment (Malvern Instruments Ltd.). The measurements were carried out using a He-Ne laser with 633nm at 90° scattering angle. Samples were analyzed at a concentration of 0.05mg/mL and temperature was maintained at 37°C. Immediately before the analysis, the pH of the solutions was adjusted to 7.4 with 0.5 mM of NaOH or HCl, and then sonicated for 1 minute at room temperature. The mean diameter was evaluated using the Stokes-Einstein equation. Triplicate samples were considered and analyzed for a minimum of 10 scans.

2.4.3 Thermo Gravimetric Analysis (TGA)

The percentage of met-CS coating at the surface of the MNPs was assessed by thermal gravimetric analysis (TGA) with a simultaneous thermal analyzer (model STA7200, Hitachi). To perform the analysis, 2-4 mg of met-CS MNPs were placed in a stainless steel crucible. An empty stainless steel crucible was used as reference. The sample was exposed to a rising temperature up to 105°C at a rate of 10°C/min under a nitrogen atmosphere. After reaching 105°C, the temperature was isothermally held for 10 min in order to remove the water content. To burn the organic part (met-CS coating) available in the met-CS MNPs under an oxygen environment, the temperature was increased to 600°C at a rate of 20°C/min and isothermally maintained during 20 min. The mass was recorded as function of the temperature. The weight percentage of met-CS in the MNPs was calculated comparing the mass loss after water removal and the remaining mass (Equation 2.2).

Uncoated MNPs were used as experimental (negative) controls. Five replicates per condition were analyzed.

$$\%\ metCS = \frac{mass\ after\ water\ removal - mass\ loss\ after\ water\ removal}{mass\ after\ water\ removal} \times 100\%$$ **(Equation 2.2)**

2.4.4 Assessment of the Magnetic Properties of Produced MNPs

The magnetic behavior of MNPs produced in section 2.2.2 was investigated in order to confirm their magnetic responsiveness and the superparamagnetic behavior, including magnetic remanescence and intrinsic magnetization (magnetic moment) by measuring the magnetization curve as function of the applied magnetic field (hysteresis loop). The magnetization measurements of met-CS MNPs and uncoated MNPs were assessed in a superconducting quantum interference device (SQUID-VSM) magnetometer from Quantum Design, under an applied magnetic field between −20.0 and 20.0 kOe at room temperature. Before the analysis, met-CS MNPs and MNPs were freeze dried (LyoALfa 10/15 Telstar) for three days.

2.4.5 Transmission Electron Microscopy (TEM)

The size of the uncoated MNPs and met-CS MNPs were assessed by Transmission Elecron Microscopy TEM (Jeol JEM 1400, Zeiss model EM 10C), upon preparation of solutions with 0.05% of uncoated MNPs and met-CS MNPs in Millipore Water. The Electron Microscopy Service of I3S (Instituto de Investigação e Inovação em Saúde) prepared and performed the analysis.

2.5 Characterization of developed met-CS MAGPL Hydrogels

2.5.1 Low Temperature Scanning Electron Microscopy (cryo-SEM) and TEM

Scanning electron microscopy is commonly used to determine the microstructure of different types of 3D matrices, but fails to recreate the highly hydrated hydrogel structure once it must be dried before the analysis[28]. Thus low temperature scanning electron microscopy (cryo-SEM) is an alternative technique to analyze the native structure of a hydrogel once the sample is quickly frozen in liquid nitrogen thus preserving the intrinsic microstructure.

In this work the microstructure of magnetic hydrogels enriched with PL (met-CS MAGPL) with 200 and 400 μg/mL of met-CS MNPs (met-CS_{200} and met-CS_{400} MAGPL) were assessed by cryo-SEM. Hydrogels without MNPs (met-CS and Met-CS PL hydrogels were used as control.

The cryo-SEM analysis was performed using a high resolution scanning electron microscope with X-ray Microanalysis with a JEOL JSM 6301F/ Oxford INCA Energy 350/ Gatan Alto 2500 equipment. For that, the hydrogels were rapidly cooled (plunging it into sub-cooled nitrogen, slush nitrogen) and transferred under vacuum to the cold stage of the preparation chamber. Further the specimen was fractured, sublimated ('etched') for 120 sec. at -90°C, and coated with Au/Pd by sputtering for 45 sec. The sample was then transferred into the cryo-SEM chamber and the analysis was performed at a temperature of -150°C.

In order to assess the distribution within the met-CS MAGPL hydrogels, TEM analysis was performed. It was used met-CS PL hydrogels as control. Hydrogels were fixed with TEM-Fix. The Histology preparation and TEM analysis was performed by theElectron Microscopy Service of I3S.

2.5.2 Dynamic Mechanical Analysis

Dynamic Mechanical Analysisis commonly used to study the viscoelastic parameters and thus assess mechanical parameters of 3D materials such as the storage modulus (E') that illustrates the polymer's ability to store energy elastically, and the loss modulus (E") which characterizes the polymer's ability to dissipate energy as heat[29]. The mechanical properties are normally assessed when an oscillatory stress is applied to the sample and the response of the material is measured.

In this work, DMA was used to measure the mechanical/viscoelatic properties of magnetic met-CS hydrogels enriched with PL with different concentrations of met-CS MNPs (0, 200, 400 µg/mL) using a ATRITEC8000B DMA (Triton Technology, UK) equipped with a compressive mode. Hydrogels were immersed in α-MEM culture medium (12000-063, Alfagene) for 15 hours supplemented with 10% of fetal bovine serum (FBS) (10270106, Alfagene) and 1% of antibiotic/antimitotic (A/A) (15240062, Alfagene) overnight at 37°C. Hydrogel dimensions were accurately measured before analysis. Hydrogels with approximately 5 × 5 mm and a thickness of 1 mm were assayed. The experiment was performed by applying compression cycles of increasing frequency (0.1-10 Hz) under constant strain amplitude (0.1 µm) using a preload of 0.1 % of the sample thickness. The assays were performed under simulated physiological conditions by immersion of the samples in a Teflon reservoir with α-MEM medium at 37°C. At least three hydrogels per formulation were tested.

2.5.3 Effect of magnetic stimulation in the Properties of developed met-CS MAGPL Hydrogels

The influence of magnetic stimulation as well as magnetic activation of met-CS MNPs incorporated in the met CS PL hydrogel matrix is an important parameter to be assessed in the developed hydrogels. Thus, the impact of a magnetic field in the degradation profile and in the GF release from the PL and in the behavior of cells were performed.

External magnetic stimulation (EMF) was provided by a magnefect nano device (nanoTherics Ltd, Keele, UK) under an oscillation frequency of 2 Hz and 0.2 mm of displacement conditions composed by an oscillating magnet array system (0.35 T per magnet per hydrogel). These EMF conditions were selected based on previous works developed in our group, which demonstrated the application of a magnetic field enhanced the biological performance of hASCs in terms of cell proliferation [30] and have also shown to reduce the inflammation and fibrotic tissue formation in a rodent model[31].

The magnetic stimulation induced by the oscillation frequency was maintained without interruption during the experimental setup. Samples under in static non stimulating conditions were used as experimental negative controls of the influence of magnetic actuation.

2.5.3.1. Swelling and Weight variation upon magnetic Stimulation

The swelling is an important characteristic of a hydrogel defined as the amount of aqueous solution that the hydrogel can uptake. It is, therefore an indicator of the polymer network hydrophilicity[32]. The stability and degradability of met-CS MAGPL hydrogels upon implantation depends of several factors, including erosion, hydrolysis, and enzymatic degradation of the polymeric matrix [32]. Thus, hydrogel degradation is another relevant parameter to consider as it can lead to changes in mechanical and swelling properties overtime. Ultimately hydrogel matrix degradation impacts the structure, stability and the release rate of GFs, as the ones present in PL solution, or cells laden in the hydrogel[32]. The magneto-mechanical stimulation resultant from the actuation of an external magnetic field may impact the properties of met-CS MAGPL hydrogel as well as the magnetic activation of met-CS MNPs present within the met-CS MAGPL hydrogels.

Thus, in this work, the influence of the actuation of an external magnetic field (EMF) in the swelling and degradation profile of the developed met-CS_{200} MAGPL hydrogels was assessed. The hydrogels

were prepared into 5 mm diameter and 5 mm height cylindrical-shaped molds and individually placed in the wells of a 24 well plate. Hydrogels were then subjected to magnetic stimulation as described in section 2.2.7.3. Hydrogels were retrieved after 3 and 6 hours, 1, 7, 14 and 21 days and hydrogels cultured in static non stimulating conditions were used as experimental controls.

For the swelling assay each sample was incubated in 1.5 mL of PBS at 37°, pH 7.4. After each time point, the wet samples were removed from the well and weighted in an analytical balance (Denver Instrument, Germany) after the removal of excess surface liquid (wet weight, m WET). Then samples were freeze dried during 3 days before measuring the dry weight of the samples (m dry). The swelling percentage of the samples was calculated according to equation 2.3:

$$\frac{m\,WET}{m\,dry} \times 100 \quad \textbf{(Equation 2.3)}$$

For the enzymatic degradation assay, the hydrogels were incubated at 37°C in 1.5 ml of a solution of 2.6 U/mL of hyalurodinase (HAse) (H2126, Sigma) in PBS or in PBS alone (experimental control). This concentration corresponds to values naturally present in the blood plasma and thus this enzymatic value directly relates to human physiological concentrations[33]. In the case of weight loss assessment, the procedure was similar to the one described for swelling assay. Briefly, the formulations were weighed after each determined time point (m WET) using an analytical balance after removal of excess surface liquid. Then, the enzymatic solution or PBS where the samples were incubated into, were replaced by fresh solutions until the end of the experimental setup.

The weight loss was calculated based on water uptake, following the equation 2.4:

$$\frac{m\,WET}{m\,dry} \times 100 \quad \textbf{(Equation 2.4)}$$

Where m WET is the weight of the swollen sample and the m Initial the weight of the sample in the t=0.

Samples under static non stimulating conditions were used as experimental controls. The experiments were performed using in a minimum of 3 samples of each condition.

2.5.3.1. Assessment of Growth Factors Release from Platelet Lysate upon Magnetic Stimulation

PL were used as a soluble pool of growth factors (GFs) and adhesion molecules under the hypothesis of occurrence of electrostatic interactions, exploring the attraction between the strongly negatively charged polymer (met-CS) and the positively charged GFs to form a biochemical enriched hydrogel matrix in which cells can be encapsulated. Moreover, the incorporation of met CS MNPs within the CS matrix enriched with PL is expected to allow a remote control over the developed system, thus on the GF release, by the application of an external magnetic field (EMF). The enzyme-linked immunosorbent assay (ELISA) assay is an analytic enzymatic assay to detect the presence of a substance, usually an antigen in solution. The release of specific GFs present in PL, namely platelet derived growth factor (PDGF-BB) from hydrogels subjected to EMF stimulation and/or enzymatic degradation was assessed by ELISA. PDGF-BB was selected as one of the most relevant proteins for TE present in PL, and shown to promote tendon fibroblast proliferation and matrix remodeling during tendon healing[34]. Briefly, the technique consists in the immobilization of a specific antibody (capture antibody) to the solid surface of a 96-well plate that will bind to the interest molecule. Then, a specific antibody (the detection antibody) is applied and will bind to the molecule of interest. Then, a solution containing the substrate of the enzyme is added to produce a detectable signal (color change) that will be used to quantify the antigen available in the solution. The content of PDGF-BB was assessed according to the manufacturer's instructions (Pepro Trech). For this, met-CS_{200} MAGPL hydrogels were prepared incubated in PBS or in a HAse solution (2.6 U/ml) at 37°C under the stimulation of EMF (section 2.2.7.3.). PDGF-BB was quantified in the incubation medium after 15, 45 and 90 minutes, 3 and 6 hours, 1, 2, 4, 7 and 10 days . Samples in static non EMF conditions were considered experimental controls. The PDGF-BB was quantified using a minimum of 3 samples per condition.

2.6 Biological assays

2.6.1 Isolation and culture of cells

Cells used in the present work were isolated from human tissues. For this purpose, human lipoaspirates and tendon tissue samples were collected under an established protocol with Hospital da Prelada (Porto, Portugal). All samples were obtained under informed consent, according to the Declaration of Helsinki and the protocols were approved by the ethical committee of the Hospital.

Samples were transported in a 10% (v/v) A/A in PBS solution inside a sterile container and processed as described below.

2.6.1.1. Human Tendon Derived Cells (hTDCs)

Human tendon derived cells (hTDCs) isolated from tendon tissues are a heterogeneous population of cells which have shown to assist the regeneration of tendon-to-bone interface in animal models [35], and thus a promising source to be used in tissue interface of tendon-to-bone. Human TDCs will be used in this work to colonize the tendon hydrogel unit in both single and double unit systems [36].

Human TDCs were collected from tendon samples from patients undergoing orthopedic reconstructive surgeries. Briefly, samples were firstly washed with DPBS containing 10% (v/v) of A/A and surrounding non-tendon tissue was removed using a surgical blade. Afterwards, samples were minced and digested with a solution of 0.1% (w/v) collagenase type I solution (Z56.LS004196, Sigma) during 1 hour at 37°C under agitation (200 rpm). The digested tissue was filtered with a cell strainer (100 μm), centrifuged (1200 rpm, 5min, 5°C) and the resultant cellular suspension was expanded in basal medium composed by α MEM with 10% (v/v) FBS, 1% A/A (v/v) and Na_2CO_3 at 37°C, 5% CO_2.

Cells were cryopreserved until usage. Human TDCs in 2D cultures were further characterized by flow cytometry analysis (data not shown). In all experimental assays, hTDCs were used in passage 2 to 4. Cells used during these experiments were characterized by flow cytometer (data not shown).

2.6.1.2. Human Adipose Stem Cells (hASCs)

In recent years, adipose tissue has been gaining attention as a stem cell source with therapeutic potential for a wide range of pathologies due to the high self-renewal and multilineage differentiation potential of adipose derived stem cells (ASCs), including their commitment and differentiation towards osteoblastic like cells under appropriate stimulation. Moreover, human ASCs (hASC) are obtained using less invasive procedures and in larger quantities in comparison with bone marrow derived stem cells[37].

Thus, hASCs that will be osteogenically stimulated with standard osteogenic inductive medium, were envisioned to colonize the bone hydrogel units in single and double unit systems.

Human ASCs used during the experimental setup were isolated from lipoaspirate samples of female donors. In order to disrupt the connective tissue to release the cells, the sample was

digested with a solution of 0.05% (w/v) collagenase type I in PBS under mild agitation during 45min at 37°C. Then, the suspension was filtered (100µm, Sigma), centrifuged (2587rpm, 10 minutes) to separate the stromal vascular fraction (SVF) and washed with lysis buffer for removal of the red blood cells. Further the solution was centrifuged at 2587rpm for 10 min and the resultant cellular suspension was expanded in basal medium as described in the previous section at 37°C, 5% CO_2. Cells were cryopreserved and expanded upon needed. Experimental assays were performed with hASCs in passage 3 to 5.

2.6.1.3. Pre Osteogenic differentiation of hASCs

Human ASCs were pre-differentiated into pre-osteoblastic like cells (pre-Ost) before laden in the met-CS MAGPL hydrogels. Human ASCs were cultured in osteogenic medium to induce the osteogenic phenotype, that was composed of α-MEM, 10% FBS, 1%A/A supplemented with osteogenic factors, namely dexamethaxone (10^{-8} M, Sigma-Aldrich), ascorbic acid (50µg/mL, Sigma-Aldrich) and β-glycerophosphate (10mM, Sigma- Aldrich) for 14 days before being cultured in the developed hydrogel units. To assess hASC commitment toward the osteogenic phenotype flow cytometry was performed after 14 days in osteogenic culture. In the following assays, pre-osteoblastic like cells were designed as pre-Ost cell.

2.7 Assessment of the Cytocompatibility of Developed MNPs in the presence of HASCs

To assess the influence of met CS MNPs in cellular processes, namely metabolic activity and proliferation rate, hASCs were seeded in 24-well tissue culture plates at a density of 10^3 cells per cm^2 in basal medium. After 24 h in culture, the culture medium was replaced with 1 mL of α MEM medium containing different concentrations of MNPs (200, 400 µg/mL). Then, hASCs cultured with MNPs for 1, 3 and 7 days and characterized for metabolic activity by Alamar Blue (BUF012B, Arium) and for cellular proliferation using a dsDNA quantification kit (P7589, Alfagene). Met-CS MNPs were compared to uncoated MNPs. Cells cultured in the absence of MNPs were used as controls of the experiment.

2.8 Encapsulation of hTDCs and/ or Pre-Ost in the met-CS MAGPL hydrogel tendon and bone units

After reaching the sufficient cell number for encapsulation in the met-CS MAGPL hydrogels, hTCs and pre-Ost cells were detached using tripLE Express (126905-028, Alfagene) and counted using a hemocytometer. Cells were then centrifuged at 1200rpm for 5 minutes and suspended in a density of 2×10^6 /mL in basal culture medium.

The behavior of cells laden in met-CS_{200} MAGPL hydrogels was assessed in single (tendon or bone units) and co-cultures of hTCs and Pre-Ost cells (tendon-bone interface units).

To prepare the tendon, bone and co-culture units, hTDCs and pre-Ost cells were gently mixed with met-CSPL solution containing the photoinitiator as described in section 2.2.3.1. Afterwards, 200 µg/mL of met-CS MNPs (prepared as described in section 2.2.2.) was added and vortex to homogenize the met-CS MNPs.

In the case of tendon and bone single units, 50 µL of the prepared solution containing hTCs or pre-Ost cells was injected into a PDMS mold with 5mm×5mm and UV light polymerized for 120 seconds.

In the case of co-culture units, 50 µL of the solution containing hTDCs was injected in the PDMS mold and UV light polymerized for 120 seconds. Then, the formed hydrogel (tendon unit) was placed into the left side of another PDMS mold (10mm×10mm) and 50 µL of a solution containing pre-Ost cells was added to the right side of the 10mm×10mm mold. The hydrogels units were physically attached through polymerization of the bone and tendon units by UV light for 120 seconds, forming a co-culture tendon-bone interface unit.

Both single and co-culture units were gently removed from the mold and cultured in 24 well plate in basal medium during 1, 7, 14 and 21 days in EMF conditions . Formulations cultured in non-stimulating conditions were used as experimental control of magnetic actuation.

Single Met-CS MAGPL hydrogel laden with hTDCs or pre-Ost cells (single cell-hydrogel units) were used as controls.

2.9 Characterization of the Cell Behavior in the Developed Systems

2.9.1 Alamar Blue Assay

Alamar Blue cell viability reagent is a non-toxic colourimetric assay that quantitatively permit the assessment of cell viability. This method uses a cell permeable compound, resazurin that after cell membrane penetration is reduced to resorufin resulting in a fluorescent molecule. Metabolically active cells continuously convert resazurin to resorufin thus giving information about the viability and cytotoxicity [38].

The metabolic activity of hASCs in the presence of met-CS MNPs (cytocompatibility assay) and in cell laden met-CS_{200} MAGPL hydrogels were verified after 1, 3 and 7 days. Regarding the cell-laden met-CS MAGPL hydrogels, the metabolic activity of single and co-culture units was assessed in the day 1, 7, 14 and 21. Briefly, a solution of 10 % (V/V) of Alamar Blue in α-MEM medium was prepared and incubated for 15 minutes at 37°C. Before the analysis, the cells cultured in the presence of different concentrations of met-CS MNPs and encapsulated in the single and co-culture units were washed 2 times in PBS and 800 µL of the solution previously prepared was added to the samples. The samples were then, incubated for 5 hours at 37°C in 5% CO_2 protected from the light. The fluorescence was read in a microplate reader (Synergy HT, BIO-TEK) with an excitation of 530 nm and an emission of 590 nm. Six biological replicates were considered for each condition per timer point.

2.9.2 Cellular Content assay (dsDNA quantification)

The cellular content assay is a quantitative technique that uses an ultra-fluorescence compound, Picogreen, that binds to double-strand DNA to quantitatively determine the dsDNA concentration of a given sample measured by a Microplate reader.

The proliferation rate of hASCs cultured with different concentrations of met-CS MNPs was assessed after 1, 3 and 7 days. The cellular proliferation in the single (bone or tendon) and co-culture (tendon-bone units) was performed after 1, 7, 14, 21 days in culture.

To perform the analysis, the samples of interest were washed two times with DPBS and 1 mL of ultra-pure water was added in order to induce cellular lysis. Then the cellular suspension was mixed and each sample was frozen at -80°C. Prior to the analysis, the samples were thawed and milled in an ultrasonic processor (VCX-130PB-220, Sonics) to rupture the cell membrane. Experimental samples and standards (concentrations from 0-2 µg/mL) were gently mixed with a PicoGreen

solution (1:200 dilution, P7589, Alfagene), placed in a white opaque 96 well-Plate (734-1662, VWR) and incubated for 10 minutes protected from light. The experimental setup was followed accordingly with manufacturer´s instructions. The fluorescence was read in a microplate reader with an excitation of 485 nm and an emission of 530 nm. The concentration of dsDNA was assessed by comparing the fluorescence intensity of a sample with the generated standard curve (obtained with the DNA standards). At least 3 biological replicates were considered for each condition per time point.

2.9.3 Immunolabeling of tendon and bone related proteins

Immunolabeling for Collagen I (ab34710), Osteopontin (ab14175) and Tenascin-C (ab6393) was performed in single units after 7 and 21 days and in co-culture units after 21 days in culture. All primary antibodies were purchased to Abcam. To perform the analysis, the antibodies were diluted in ratio of 1:200, 1:100 and 1: 200 for collagen I, osteopontin and tenascin-C respectively, and incubated 1 hour at room temperature. Alexa Fluor 488 was used as fluorescent secondary antibody from rabbit (1754421, Alfagene) for collagen I and mouse (1741782, Alfagene) for tenascin-C and osteopontin. Moreover DAPI (4', 6-diamidino-2-phenylindole) (40009, VWR) and Phalloidin red stains (Phalloidin–Tetramethylrhodamine B isothiocyanate) were used in dilutions 1:1000 and 1:200 respectively. After, the samples were analyzed in an inverted confocal microscope (TCS SP8, LEICA) equipped with argon/He-Ne laser sources.

2.9.4 Gene Expression Analysis by Real-Time Polymerase Chain Reaction (RT-PCR)

The expression of the genes tenascin, decorin, osteopontin, collagen I was quantitatively assessed by real-time polymerase chain reaction (RT-PCR) on RNA isolated from pre-Ost cells and hTCs, and co-cultures 7, 14 and 21 days after the encapsulation in met-CS MAGPL hydrogels. In the case of the co-culture tendon bone interface units, each hydrogel was sectioned in three parts as illustrated in the Figure 2.4. Four independent biological replicates for each time point were analyzed.

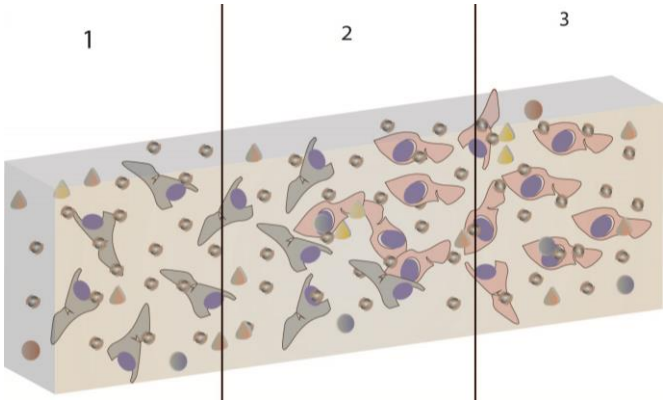

Figure 2.4. Representative scheme of the sections part of the co-culture system for gene expression analysis by real-time polymerase chain reaction (RT-PCR). The section one represents the part of the hydrogel encapsulating hTDCs, the second part the interface between the hydrogel encapsulating hTDCs and pre-Ost and the third section relates to the hydrogel encapsulating pre-Ost cells.

Total RNA was isolated from cells using the TRI Reagent® RNA Isolation Reagent (Sigma-Aldrich) according with the manufacturer's instructions. The yield and purity of RNA isolation was determined by spectrometry using the NanoDrop 1000 Spectrophotometer (ThermoScientific). The cDNA was synthesized using 100 pg of RNA as template and the qScript™ cDNA Synthesis Kit (Quanta BioSciences). The primers, listed in Table 2.2 were designed using the primer-BLAST tool available at http://www.ncbi.nlm.nih.gov/tools/primer-blast. To avoid the amplification of genomic DNA or pre-RNA (non-spliced RNA), the primers were designed in order to span the exon-exon junctions. Target genes were normalized to the reference housekeeping GAPDH gene according to Livack's method [39]. The analysis was performed on a real time Polymerase Chain Reaction (RT-PCR) Mastercycler (Realplex, Eppendorf).

Table 2.2. List of primers used for RT-PCR expression analysis of osteogenic and tendon related genes. The primers were designed using the primer-BLAST web tool

NCBI Reference Sequence	Gene product	Gene Short name	Primer sequence	Product length [bp]

NM 001040058.1	Secreted phosphoprotein 1 (Osteopontin)	OPN	CAGACCTGACATCCAGTACCC GGTCATCCAGCTGACTCGTT	173
NM 001920.3	Decorin	DCN	CAGCATTCCTCAAGGTCTTCCT GAGGCCATTGTCAACAGCA	150
NM 000088.3	Collagen alpha-1(I) chain	COLIA1	CCCCAGCCACAAAGAGTCTAC TTGGTGGGATGTCTTCGTCT	150
NM 001256799.1	Glyceraldehyde-3-phosphate dehydrogenase	GAPDH	GGGAGCCAAAAGGGTCATCA GCATGGACTGTGGTCATGAGT	198

2.10 Statistical analysis

Results are presented as mean ± standard deviation. The statistical analysis of data was performed using GraphPad Prism 6 software. Statistical analysis was carried out using 2-way ANOVA for significant differences among studied conditions followed by Turkey's multiple comparison test. A minimum of 95% confidence interval was considered for all measurements ($p<0.05$). Statistical significant values and associated degree of confidence ($p<0.05$) are denoted by symbols represented in the graphs.

2.11 References

[1] Silva C, Novoa-Carballal R, Reis RL, Pashkuleva I. Following the enzymatic digestion of chondroitin sulfate by a simple GPC analysis. Analytica Chimica Acta. 2015;885:207-13.

[2] Amini AR, Laurencin CT, Nukavarapu SP. Bone tissue engineering: recent advances and challenges. Critical reviews in biomedical engineering. 2012;40:363-408.

[3] Yang G, Rothrauff BB, Tuan RS. Tendon and Ligament Regeneration and Repair: Clinical Relevance and Developmental Paradigm. Birth defects research Part C, Embryo today : reviews. 2013;99:203-22.

[4] Li Q, Williams CG, Sun DD, Wang J, Leong K, Elisseeff JH. Photocrosslinkable polysaccharides based on chondroitin sulfate. Journal of biomedical materials research Part A. 2004;68:28-33.

[5] Lim JJ, Temenoff JS. The effect of desulfation of chondroitin sulfate on interactions with positively charged growth factors and upregulation of cartilaginous markers in encapsulated MSCs. Biomaterials. 2013;34:5007-18.

[6] Deepa SS, Umehara Y, Higashiyama S, Itoh N, Sugahara K. Specific molecular interactions of oversulfated chondroitin sulfate E with various heparin-binding growth factors. Implications as a physiological binding partner in the brain and other tissues. The Journal of biological chemistry. 2002;277:43707-16.

[7] Honda T, Kaneiwa T, Mizumoto S, Sugahara K, Yamada S. Hyaluronidases Have Strong Hydrolytic Activity toward Chondroitin 4-Sulfate Comparable to that for Hyaluronan. Biomolecules. 2012;2:549-63.

[8] Smith AJ, Greenman J, Embery G. Detection and possible biological role of chondroitinase and heparitinase enzymes produced by Porphyromonas gingivalis W50. Journal of Periodontal Research. 1997;32:1-8.

[9] Reddy LH, Arias JL, Nicolas J, Couvreur P. Magnetic Nanoparticles: Design and Characterization, Toxicity and Biocompatibility, Pharmaceutical and Biomedical Applications. Chemical Reviews. 2012;112:5818-78.

[10] Yuge L, Okubo A, Miyashita T, Kumagai T, Nikawa T, Takeda S, et al. Physical stress by magnetic force accelerates differentiation of human osteoblasts. Biochemical and biophysical research communications. 2003;311:32-8.

[11] Santos LJ, Reis RL, Gomes ME. Harnessing magnetic-mechano actuation in regenerative medicine and tissue engineering. Trends in biotechnology. 2015;33:471-9.

[12] Xu F, Wu CA, Rengarajan V, Finley TD, Keles HO, Sung Y, et al. Three-dimensional magnetic assembly of microscale hydrogels. Advanced materials (Deerfield Beach, Fla). 2011;23:4254-60.

[13] Crespo-Diaz R, Behfar A, Butler GW, Padley DJ, Sarr MG, Bartunek J, et al. Platelet Lysate Consisting of a Natural Repair Proteome Supports Human Mesenchymal Stem Cell Proliferation and Chromosomal Stability. Cell Transplantation. 2011;20:797-811.

[14] Tsay RC, Vo J, Burke A, Eisig SB, Lu HH, Landesberg R. Differential growth factor retention by platelet-rich plasma composites. Journal of oral and maxillofacial surgery : official journal of the American Association of Oral and Maxillofacial Surgeons. 2005;63:521-8.

[15] Santo VE, Duarte ARC, Popa EG, Gomes ME, Mano JF, Reis RL. Enhancement of osteogenic differentiation of human adipose derived stem cells by the controlled release of platelet lysates from hybrid scaffolds produced by supercritical fluid foaming. Journal of Controlled Release. 2012;162:19-27.

[16] Carvalho Ade M, Badial PR, Alvarez LE, Yamada AL, Borges AS, Deffune E, et al. Equine tendonitis therapy using mesenchymal stem cells and platelet concentrates: a randomized controlled trial. Stem cell research & therapy. 2013;4:85.

[17] Santo VE, Gomes ME, Mano JF, Reis RL. Chitosan-chondroitin sulphate nanoparticles for controlled delivery of platelet lysates in bone regenerative medicine. Journal of tissue engineering and regenerative medicine. 2012;6 Suppl 3:s47-59.

[18] Babo P, Santo V, iacute, tor E, Duarte ARC, Correia C, et al. Platelet lysate membranes as new autologous templates for tissue engineering applications. Inflammation and Regeneration. 2014;34:033-44.

[19] Nicodemus GD, Bryant SJ. Cell encapsulation in biodegradable hydrogels for tissue engineering applications. Tissue engineering Part B, Reviews. 2008;14:149-65.

[20] Wang L-F, Shen S-S, Lu S-C. Synthesis and characterization of chondroitin sulfate–methacrylate hydrogels. Carbohydrate Polymers. 2003;52:389-96.

[21] Smeds KA, Pfister-Serres A, Miki D, Dastgheib K, Inoue M, Hatchell DL, et al. Photocrosslinkable polysaccharides for in situ hydrogel formation. Journal of biomedical materials research. 2001;54:115-21.

[22] Tóth IY, Veress G, Szekeres M, Illés E, Tombácz E. Magnetic hyaluronate hydrogels: preparation and characterization. Journal of Magnetism and Magnetic Materials. 2015;380:175-80.

[23] Gupta AK, Curtis ASG. Surface modified superparamagnetic nanoparticles for drug delivery: Interaction studies with human fibroblasts in culture. Journal of Materials Science: Materials in Medicine. 2004;15:493-6.

[24] Barbucci R, Giani G, Fedi S, Bottari S, Casolaro M. Biohydrogels with magnetic nanoparticles as crosslinker: characteristics and potential use for controlled antitumor drug-delivery. Acta Biomater. 2012;8:4244-52.

[25] Kuo JW, Swann DA, Prestwich GD. Chemical modification of hyaluronic acid by carbodiimides. Bioconjugate chemistry. 1991;2:232-41.

[26] Fairbanks BD, Schwartz MP, Bowman CN, Anseth KS. Photoinitiated polymerization of PEG-diacrylate with lithium phenyl-2,4,6-trimethylbenzoylphosphinate: polymerization rate and cytocompatibility. Biomaterials. 2009;30:6702-7.

[27] Bahney CS, Lujan TJ, Hsu CW, Bottlang M, West JL, Johnstone B. Visible light photoinitiation of mesenchymal stem cell-laden bioresponsive hydrogels. Eur Cell Mater. 2011;22:43-55; discussion

[28] Binh VT, Purcell ST, Semet V, Feschet F. Nanotips and nanomagnetism. Applied Surface Science. 1998;130–132:803-14.

[29] Sapir Y, Cohen S, Friedman G, Polyak B. The promotion of in vitro vessel-like organization of endothelial cells in magnetically responsive alginate scaffolds. Biomaterials. 2012;33:4100-9.

[30] Goncalves AI, Rodrigues MT, Carvalho PP, Banobre-Lopez M, Paz E, Freitas P, et al. Exploring the Potential of Starch/Polycaprolactone Aligned Magnetic Responsive Scaffolds for Tendon Regeneration. Advanced healthcare materials. 2015.

[31] Santos L, Silva M, Goncalves AI, Pesqueira T, Rodrigues MT, Gomes ME. In vitro and in vivo assessment of magnetically actuated biomaterials and prospects in tendon healing. Nanomedicine (Lond). 2016;11:1107-22.

[32] Caliari SR, Burdick JA. A practical guide to hydrogels for cell culture. Nat Meth. 2016;13:405-14.

[33] Panyam J, Sahoo SK, Prabha S, Bargar T, Labhasetwar V. Fluorescence and electron microscopy probes for cellular and tissue uptake of poly(d,l-lactide-co-glycolide) nanoparticles. International Journal of Pharmaceutics. 2003;262:1-11.

[34] Thomopoulos S, Zaegel M, Das R, Harwood FL, Silva MJ, Amiel D, et al. PDGF-BB released in tendon repair using a novel delivery system promotes cell proliferation and collagen remodeling. Journal of orthopaedic research : official publication of the Orthopaedic Research Society. 2007;25:1358-68.

[35] Hashimoto Y, Yoshida G, Toyoda H, Takaoka K. Generation of tendon-to-bone interface "enthesis" with use of recombinant BMP-2 in a rabbit model. Journal of orthopaedic research : official publication of the Orthopaedic Research Society. 2007;25:1415-24.

[36] Bi Y, Ehirchiou D, Kilts TM, Inkson CA, Embree MC, Sonoyama W, et al. Identification of tendon stem/progenitor cells and the role of the extracellular matrix in their niche. Nat Med. 2007;13:1219-27.

[37] Feisst V, Meidinger S, Locke MB. From bench to bedside: use of human adipose-derived stem cells. Stem Cells and Cloning : Advances and Applications. 2015;8:149-62.

[38] Rampersad SN. Multiple Applications of Alamar Blue as an Indicator of Metabolic Function and Cellular Health in Cell Viability Bioassays. Sensors (Basel, Switzerland). 2012;12:12347-60.

[39] Livak KJ, Schmittgen TD. Analysis of relative gene expression data using real-time quantitative PCR and the 2(-Delta Delta C(T)) Method. Methods (San Diego, Calif). 2001;25:402-8.

CHAPTER III

MULTIFUNCTIONAL MAGNETIC-RESPONSIVE HYDROGELS TO ENGINEER TENDON-TO-BONE INTERFACES

This chapter is based on the following publication:

Silva ED, Babo P, Costa-Almeida R, Domingues RMA, Mendes B, Rodrigues MT, Granja PL, Gomes ME "Multifunctional Magnetic Responsive Hydrogels to Engineer Tendon-to-Bone Interface"

3. MULTIFUNCTIONAL MAGNETIC-RESPONSIVE HYDROGELS TO ENGINEER TENDON-TO-BONE INTERFACE

3.1 Abstract

Photocrosslinkable natural based hydrogel matrices have received great interest for tissue engineering strategies, especially because they provide versatile systems that can be potentially used in diverse applications. Nevertheless, to engineer complex tissues and/or tissue interfaces, it is necessary to develop systems that can accommodate various functionalities. Such systems could also benefit from the possibility of being remotely controlled and/or further manipulated *ex vivo*. This work reports on the development of a photocrosslinkable magnetic responsive hydrogel based on a methacrylated chondroitin sulfate (met-CS) matrix enriched with platelet lysate (PL), envisioning the generation of tunable hydrogel building blocks to engineer tissue interfaces, such as tendon-bone. To provide magnetic responsiveness, magnetic nanoparticles (MNPs) coated with met-CS (met-CS MNPs) were produced to enable their linkage to the hydrogel matrix. The produced met-CS MNPs were characterized and subsequently incorporated in PL enriched met-CS hydrogel matrices. The actuation of an external magnetic field (EMF) to modulate the properties of the system was then investigated. The application of an EMF was shown to modulate the swelling, degradation and release of growth factors naturally present in the PL. Moreover, the effect of EMF in hydrogels laden with either pre-osteoblasts differentiated from human adipose derived stem cells (pre-Ost) or human tendon cells (hTDCs), was assessed in single and co-culture systems. Both hTDCs and pre-Ost cells were able to proliferate, colonize and express tendon and bone related markers in the developed hydrogels. Moreover EMF seems to impact cell morphology and the synthesis of a tendon- and bone- like ECM, whose effect is highlighted in co-culture systems. Together, these results suggest that developed hydrogel represents a potential cell laden system for tissue engineering in which the properties can be externally modulated through EMF stimulation.

3.2 Introduction

Progresses in regenerative medicine and tissue engineering [1] have been deeply associated to the development of functional biomaterials for guiding tissue regeneration[2],[3]. Nevertheless, these systems could benefit from the addition of functionalities that would allow manipulate and remotely control specific components of the construct. This is of particular importance for bioengineering tissue interfaces such as tendon-to bone, tendon-muscle and osteochondral, that are constituted by distinct cell types and extracellular matrix (ECM) components, with a critical interdependence in terms of structure, function, organization and composition[4], [5]. This requires for approaches that allow engineer constructs enabling to spatially distribute cell populations and establish cell to cell and cell-environmental interactions in a temporal and spatial resolved environment (mechanical and biochemical). In the particular case of tendon-to-bone interface or enthesis, which is severely prone to injury [6], once they are mechano-sensitive tissues [7],[8] the application of a mechanical stimulus that may assist the recapitulation, to some extent, of the forces that are exerted on the cells *in vivo*. The actuation of a magnetic field has shown to provide essential mechanical cues to induce and activate the interactions between cells and ECM via mechanosensing pathways[9]. Furthermore, growing evidence suggests that magnetic forces enhance vital functions of cells including adhesion [10], proliferation and differentiation [11]. Thus, the fabrication of magnetic tendon-specific and bone-specific units with tunable features may assist the development of a gradient-like "tissue", closer mimicking the native interface. In this case, magnetic forces could be used not only to tune the behavior of laden cells[12] but also to externally control the properties of the system, like degradation and swelling.

In this particular point, the incorporation of iron-based magnetic nanoparticles (MNPs) with a 3D cell carrier, such as a hydrogel matrix, may constitute a great option to obtain functional building blocks structures with ability to modulate biochemical, physical and mechanical stimuli. However, strategies currently used to produce mag-gels present several limitations, including the risk of MNPs leaching from the hydrogel upon contact with a liquid environment[13] or in the case of MNPs cross-linked to the matrix the cytotoxicity associated with the process[14]. In the present study we propose to develop a magnetic responsive hydrogel composed of a methacrylated chondroitin sulfate (metCS) matrix enriched with platelet lysate, in which met-CS coated MNPs were covalently linked to the matrix. Therefore, with this incorporation the use of magnetic forces might be used to externally control the properties of the system like and to tune the behavior of

studied cells [12]. Moreover in this case CS was chosen as the main element of the hydrogel matrix because this natural polymer is a crucial component of the extracellular matrix (ECM) in several connective tissues, including tendon and it is also available in bone, and it is known to have a crucial function in maintaining the structural integrity and ECM [15]. Also, CS presents a strong negative charge and thus an inherent ability to attract positively charged matrix molecules like growth factors (GFs) [16]. Once, platelet Lysate (PL) is constituted by a pool of mitogenic molecules that are released from degranulation of platelets to trigger the process of regeneration [17], they could be an effective and cost-effective alternative to have a pool of GF and other bioactive molecules to trigger[18] the orchestration of the regeneration process in such complex interfaces as tendon-to-bone[19]. In addition, the use of an external magnetic field in combination with the presence of MNPs in the matrix could be used to tune the release of GF available in PLs from the hydrogel units.

The developed hydrogels units were used to create 3D magnetic responsive constructs that could be externally manipulated through the use of magnetic field for tendon-to-bone interface and extensively characterized in terms mechanical properties, swelling, degradation profile, the impact of an external magnetic field to modulate these intrinsic properties and also its biological performance. To assess such features, hydrogel units were either encapsulated with human adipose derived stem cells (hASCs) previously osteogenic differentiated for 14 days or with human tendon cells (hTCs) were used. The 3D constructs composed of two interconnected units (bone and tendon units) were assembled and cultured for 21 days upon magnetic stimulation and characterized in terms of proliferation, metabolic activity, osteo and tendon-related genes and protein expression.

3.3 Materials and Methods

3.3.1 Preparation of Platelet Lysate

PL was prepared from platelet concentrate (PC) obtained by plasma apheresis from volunteer blood donors, following a previous established cooperation protocol with Hospital de São João (Porto, Portugal). PC with a platelet count of 10^6 platelets/µL were biologically selected according to the Portuguese legislation (Decreto Lei nº 185/2015) and processed using 10 donnors as previously described[18].

3.3.2 Synthesis of Methacrylated Chondroitin Sulfate

The methacrylation of chondroitin sulfate (CS), (Chondroitin sulfate A sodium salt from bovine trachea, Sigma) was performed following a procedure described elsewhere20. Briefly, the pH of a 1% (w/v) solution of CS was adjusted to 8.5 using a 5 M NaOH solution. The methacrylation process occurred with the addition of 10-fold excess molar of methacrylic anhydride (276685, Sigma) to the CS solution. The pH was adjusted to 8-8.5 for 24h at 4°C. Then, the reaction products were precipitated by adding 3-fold reaction volume of cold ethanol (absolute ethanol at -20oC, E/0650DF/17, Enzymatic). Three subsequent centrifugation steps (6154 g, once for 10 minutes and twice for 5 minutes) using absolute ethanol were performed. The met-CS was then dialyzed (cellulose dialysis membranes, average flat width 33 mm, Mw cut-off 14 kDa, Sigma) against distilled water for one week, with water renewal three times a day. Finally, the solution was filtered (180µm, Millipore), frozen at -80oC and freeze-dried (LyoALfa 10/15 Telstar) for one week.

3.3.3 Production of Methacrylated - Chondroitin sulfate nanoparticles (met-CS MNPs)

3.3.3.1. Production of MNPs by Co-Precipitation method

MNPs were prepared by co-precipitation of Fe^{2+} and Fe^{3+} with ammonium hydroxide (NH_4OH) (05002, Sigma) as previously described [20]. Briefly, $FeCl_3.6H_2O$ (31232, Sigma) and $FeCl_2.4H_2O$ (220299, Sigma) were mixed at a molar ratio of 2:1 (2.25 mmol Fe^{3+}: 1.125 mmol Fe^{2+}) under magnetic stirring and in a nitrogen environment. The mixture was heated up to 80 °C and 25% (v/v) of NH_4OH was added to the salt solution until pH 10.5. The solution was further cooled at room temperature for 15 min and the precipitate was separated from the solution using a permanent magnetic (0.6 T). These particles were washed 3 times with Millipore water and 3 times with absolute ethanol by centrifugation at 8322 rcf for 15 min.

3.3.3.2. Functionalization of MNPs with a met-CS Coating

A 2% (w/v) met-CS solution was added dropwise to the suspension of uncoated MNPs at a solid/liquid ratio of 20 g/L at pH 6.3 ± 0.3 for 24h under magnetic agitation in a nitrogen environment.

The stabilization of the met-CS coating was performed with adipic acid dihydrazide (ADH) (A0638, Sigma) using a well-established carbodiimide (EDCI) (424331, Sigma)-based chemistry22. Briefly, the met-CS MNPs suspension was set to pH 4.75 and a solution containing an excess molar of 2:1

(ADH/EDCI:met-CS) was dropwise added to the suspension. The pH was continuously adjusted to 4.5 with 0.1 M of HCl until no pH variation was observed. The solution was washed 3 times by centrifugation (8322 rcf, 10 min) with Milipore water and dialyzed (cellulose dialysis membranes, , Mw cut-off 14 kDa, Sigma) for one week against Milipore water.

3.3.4 Development of magnetic responsive hydrogels enriched with platelet lysate (met-CS MAGPL Hydrogels)

Photocrosslinkable, met CS hydrogel matrices were produced using the photoinitiator Irgacure 2959 [2-hydroxy-4'-(2-hydroxyethoxy)-2-methylpropiophenone 98%] (410896, Sigma) in the presence of UV light. In brief, Irgacure 2959 (0.25 % (w/v)) was dissolved in either PBS or in a PL solution, obtained as described in section 3.3.1., where a 8% (w/v) met-CS was dissolved afterwards. The solution was vortex and centrifuged (2 minutes at 6000 rpm). Afterwards, met-CS MNPs (100, 200 and 400 µg/mL) were added to the met-CS solution of PBS (met-CS MAG) or PL (met-CS MAGPL) and sonicated for 20 seconds. Hydrogels without met-CS MNPs were also produced as controls.

After assessing the most promising hydrogel formulation with met CS MNPs (200µg/mL) for cellular studies, PL enriched met CS hydrogels were produced as single and double hydrogel units. The single hydrogel units were produced by injecting 50 µL of the solution of met-CS PL with Irgacure in a PDMS mold (5mm×5mm) and UV polymerized for 120 seconds

In the case of double hydrogel units, the first hydrogel unit was prepared as described for the single units and placed into the left side of a second PDMS mold (10mm×10mm) and another 50 µL of solution was added to the right side of this mold. The hydrogels units were physically attached into a double hydrogel unit by UV light polymerization for 120 seconds.

3.3.5 Characterization of met-CS by ^{1}H Nuclear Magnetic Resonance (NMR)

The degree of methacrylation (Dm) of CS was determined by the analysis of ^{1}H NMR spectrum. met-CS were dissolved in deuterium oxide ($^{2}H_2O$, D-020-100, Laborspirit) at 5mg/mL and their spectra recorded (Varian Inova 500) at 70°C with a frequency of 400.13 MHz and a delay of 1s. The Dm was calculated based on the ratio between the relative area of the peaks corresponding to vinyl protons of methacryloyl moiety (at 5.8 and 6.2 ppm) and the methyl protons of the acetyl moiety of CS (at ~2.1 ppm), present in Annex 1.

3.3.6 Characterization of produced MNPs

3.3.6.1Fourier Transform Infrared (FTIR) Spectroscopy

CS, met-CS, uncoated MNPs and met-CS MNPs samples were mixed with potassium bromide, and processed into pellets. The infrared spectra of CS, met-CS, uncoated MNPs and met-CS MNPs were record in an IR-Prestige-21 equipment (FTIR Shimadzu). The spectra were obtained in the range of 400 to 4000 cm^{-1} at a 4 cm^{-1} resolution with 32 scans

3.3.6.2. Electrokinetic Measurement (Zeta Potential) and Hydrodynamic Size

The zeta potential of uncoated MNPs and met-CS MNPs was measured at different pH (3, 5, 7, 10) and the hydrodynamic size was assessed at 7.4., in both cases at room temperature, using a ZetaSize Nano-ZS (Malvern Instruments Ltd).

For that, met-CS MNP and uncoated MNPs solutions (0.005% (w/v)) were prepared in Millipore water and the pH adjusted accordingly to the desired pH (3, 5, 7, 10) before being sonicated for 1 minute at room temperature.

The mean diameter was evaluated using the Stokes-Einstein equation. Triplicate samples were considered and analyzed for a minimum of 10 scans.

3.3.6.3.Thermo Gravimetric Analysis (TGA)

The met-CS coating of met CS MNPs was assessed with a simultaneous thermal analyzer (model STA7200, Hitachi). Met-CS MNPs (2-4 mg) were placed in a stainless steel crucible and an empty stainless steel crucible was used as reference. The sample was exposed to a rising temperature up to 105°C (10°C/min) under an oxygen environment. Then, the temperature was isothermally held for 10 min, increased to 600°C (20°C/min) and isothermally maintained during 20 min under nitrogen environment. The mass was recorded as function of the temperature. The weight percentage of met-CS in the MNPs was calculated comparing the mass loss after water removal and the remaining mass. Uncoated MNPs were used as experimental controls. Four replicates per condition were analyzed.

3.3.6.4.Magnetic Properties of produced MNPs

The magnetization measurements of uncoated MNPs and met-CS MNPs were assessed in a superconducting quantum interference device (SQUID-VSM) magnetometer from Quantum Design, under an applied magnetic field between −20.0 and 20.0 kOe at room temperature. Before the analysis, met-CS MNPs and MNPs were freeze dried (LyoALfa 10/15 Telstar) for three days.

3.3.6.5.Transmission Electron Microscopy (TEM)

The size of the uncoated MNPs and met-CS MNPs were assessed by Transmission Elecron Microscopy TEM (Jeol JEM 1400, Zeiss model EM 10C), upon preparation of solutions with 0.05% of uncoated MNPs and met-CS MNPs in Millipore Water. The Electron Microscopy Service of I3S (Instituto de Investigação e Inovação em Saúde) prepared and performed the analysis.

3.3.7 Characterization of magnetic responsive hydrogels enriched with platelet lysate (met-CS MAGPL Hydrogels)

3.3.7.1. Low Temperature Scanning Electron Microscopy (cryo-SEM) and Transmission Electron Microscopy

The microstructure of magnetic hydrogels enriched with PL (met-CS MAGPL) with 200 and 400 µg/mL of met-CS MNPs (met-CS200 and met-CS400 MAGPL) was assessed by cryo-SEM. Hydrogels without MNPs (met-CS and Met-CS PL hydrogels were used as control).

The Cryo-SEM analysis was performed using a high resolution scanning electron microscope with X-ray Microanalysis with a JEOL JSM 6301F/ Oxford INCA Energy 350/ Gatan Alto 2500 equipment. For that, the hydrogels were rapidly cooled into slush nitrogen and transferred under vacuum to the cold stage of the preparation chamber. Further the specimen was fractured, sublimated ('etched') for 120 sec. at -90°C, and coated with Au/Pd by sputtering for 45 sec. The analysis was performed at a temperature of -150°C.

In order to assess the distribution within the met-CS MAGPL hydrogels transmission electron microscopy (Jeol JEM 1400, Zeiss model EM 10C) was performed, using the same equipment referred above. In these case the formulations were fixed with a specific fixator for TEM (TEM-Fix) and met-CS PL hydrogels as control.

3.3.7.2. Dynamic Mechanical Analysis

DMA was used to measure the mechanical/viscoelatic properties of magnetic met-CS hydrogels enriched with PL with different concentrations of met-CS MNPs (200, 400 µg/mL) using an ATRITEC8000B DMA (Triton Technology, UK) equipped with a compressive mode. Hydrogel without met-CS MNPs were used as control. Hydrogels with approximately 5 × 5 mm and a thickness of 1 mm were assayed. The experiment was performed by applying compression cycles of increasing frequency (0.1-10 Hz) under constant strain amplitude (0.1 µm) using a preload of 0.1 % of the sample thickness. The assays were performed under simulated physiological

conditions by immersion of the samples in a Teflon reservoir with α-MEM medium at 37°C. At least three hydrogels per formulation were tested.

3.3.7.3. Effect of magnetic stimulation in the properties of developed met-CS MAGPL hydrogel

Magnetic stimulation was provided by a magnefect nano device (nanoTherics Ltd, Keele, UK) under an oscillation frequency of 2 Hz and 0.2 mm of displacement conditions composed by an oscillating magnet array system (0.35 T per magnet per scaffold). The magnetic stimulation induced by the oscillation frequency was maintained without interruption during the experimental setup. Samples under static, non-stimulating, conditions were used as experimental negative controls of the magnetic actuation influence.

The influence of an external magnetic field in the swelling and degradation was assessed in cylindrical-shaped met-CS_{200} MAGPL hydrogels (5 mm diameter and 5 mm of height).

For the swelling assay met-CS_{200} MAGPL hydrogels were incubated in 1.5 mL of PBS at 37° C, collected after 3 and 6 h, 7 and 21 days and weighted in an analytical balance (Denver Instrument, Germany) after the removal of excess surface liquid

In the degradation assay, hydrogels were incubated at 37°C in 1.5 ml of a solution of 2.6 U/mL of hyalurodinase (HAse, H2126, Sigma) in PBS or in PBS alone (experimental control) for 3 and 6 hours, 1, 4, 7, 10, 13, 17 and 19 days. At each time point, the formulations were weighed using an analytical balance (Denver Instrument, Germany) after removal of excess surface liquid. Then, the enzymatic solution or PBS was replaced by fresh solutions until the end of the experimental setup.

Samples under static non stimulating conditions were used as experimental controls. The experiments were performed using in a minimum of 3 samples per analyzed condition.

3.3.7.3.1. PDGF-BB release upon Magnetic Stimulation

The release of platelet derived growth factor (PDGF-BB) from hydrogels subjected to EMF stimulation and/or enzymatic degradation was assessed by enzyme-linked immunosorbent assay (ELISA), accordingly to manufacturer's instructions (Pepro Trech). For this, met-CS_{200} MAGPL hydrogels were prepared and incubated in PBS or in a HAse solution at 37°C, and the PDGF

quantified in the incubation media after 15, 45 and 90 minutes, 3 and 6 hours, 1, 2, 4, 7 and 10 days. The PDGF-BB was quantified using a minimum of 3 samples per condition.

3.3.8 Isolation, culture and characterization of cells

Cells used in the present work were isolated from human tissue samples collected under an established protocol with Hospital da Prelada (Porto, Portugal). All samples were obtained under informed consent, according to the Declaration of Helsinki and the protocols were approved by the ethical committee of the Hospital.

3.3.8.1. Human Tendon Derived Cells (hTDCs)

Human tendon derived cells (hTDCs) were collected from tendon samples from patients undergoing orthopedic reconstructive surgeries. Briefly, samples were washed with DPBS containing 10% (v/v) of A/A and surrounding non-tendon tissue was removed. Afterwards, samples were minced and digested with a 0.1% (w/v) collagenase type I solution (Z56.LS004196, Sigma) during 1 hour at 37oC under agitation (200 rpm). The digested tissue was filtered (100 μm), centrifuged (1200 rpm, 5min, 5°C) and the cellular suspension was expanded in basal medium (α MEM supplemented with 10% FBS, 1% A/A and Na2CO3. In all experimental assays, hTDCs were used in passage 2 to 4.

3.3.8.2. Human Adipose Stem Cells (hASCs) and pre osteogenic differentiation

HASCs were isolated from lipoaspirate samples of female donors as previously described [18].The sample was digested with 0.05% (w/v) collagenase type I in PBS under mild agitation during 45min at 37°C. Then, the suspension was filtered (100μm, Sigma), centrifuged (2587rpm, 10 minutes) and washed with lysis buffer before centrifuged at 2587rpm for 10 min. The cellular suspension was expanded in basal medium, cryopreserved and expanded upon needed. Experimental assays were performed with hASCs in passage 3 to 5.

Human ASCs were cultured in standard osteogenic medium for 14 days before being encapsulated in the developed met-CS_{200} MAGPL hydrogel units. The medium was composed of basal medium supplemented with osteogenic factors, namely dexamethaxone (10^{-8} M, Sigma-Aldrich), ascorbic acid (50μg/mL; Sigma-Aldrich) and β-glycerophosphate (10mM; Sigma- Aldrich).

3.3.9 Assessment of the Cytocompatibility of Developed MNPs in the Presence of hASCs

The influence of met CS MNPs in cells were assessed by culturing hASCs in 24-well tissue culture plates at 10^3/cm2 in α-MEM. After 24 h, the culture medium was replaced with α MEM medium containing different concentrations of MNPs (200, 400 μg/mL) cultured for 1, 3 and 7 days and characterized for metabolic activity by Alamar Blue (BUF012B, Arium) and for cellular proliferation using a dsDNA quantification kit (P7589,Alfagene). Met-CS MNPs were compared to uncoated MNPs and to cells cultured in the absence of MNPs.

3.3.10 Biological assessment of cell laden hydrogel units

3.3.10.1. Encapsulation of hTDCs and/ or Pre-Ost in the met-CS MAGPL hydrogel tendon and bone units

The behavior of cells laden in met-CS_{200} MAGPL hydrogels was assessed in single (tendon or bone units) and co-cultures of hTDCs and hASCs pre differentiated into osteoblatic like cells (pre-Ost) (tendon bone interface units).

HTDCs and pre-Ost were detached using tripLE Express (126905-028, Alfagene) and counted using a hemocytometer. Cells were then centrifuged at 1200rpm for 5 minutes and suspended at a density of 2×10^6 /mL in the solution prepared as described in section 3.3.4.

In tendon and bone single units, 50 μL of the prepared solution containing hTDCs or pre-Ost was injected and polymerized as described in section 3.3.4. In the case of the co-culture systems, 50 μL of the solution containing hTDCs was injected in the PDMS mold with 5mm×5mm of dimensions before UV polymerized for 120 seconds. Then, the formed hydrogel (tendon unit) was placed into the left side of a PDMS mold with 10mm×10mm and 50 μL of the prepared solution containing pre-Ost cells was added to the right side of 10mm×10mm mold, and produced as mentioned for the tendon unit, forming a single co-culture tendon-bone interface unit. Both single and co-culture units were gently removed from the mold and cultured in 24 well plate in basal medium during 1, 7, 14 and 21 days in EMF. Formulations cultured in non-stimulating conditions were used as experimental control of magnetic actuation.

3.3.11 Characterization Cell Behavior in the Developed Systems

3.3.11.1. Alamar Blue® assay

The metabolic activity of hASCs in the presence of uncoated and met-CS MNPs was verified after 1, 3 and 7 days while cell-laden met-CS MAGPL hydrogels in single and co-culture units was assessed at 1, 7, 14 and 21 days. Briefly, Alamar Blue solution (AB, 10 % (V/V)) was prepared in α-MEM medium. Samples were washed twice in PBS and incubated with 800 µL of the AB solution previously prepared for 5 hours at 37°C.The fluorescence was read in a microplate reader (Synergy HT, BIO-TEK) with an excitation of 530 nm and an emission of 590 nm. At least 3 biological replicates were considered for each condition per time point

3.3.11.2. Cellular Content Assay (dsDNA quantification)

The cell content of hASCs cultured with different concentrations of met-CS MNPs was assessed after 1, 3 and 7 days and after 1, 7, 14, 21 days in single (bone or tendon) and co-culture (tendon-bone units)

The samples were washed twice with PBS, 1 mL of ultra-pure water was added and the samples were frozen at -80°C. Prior to the analysis, the samples were thawed and milled in an ultrasonic processor (VCX-130PB-220, Sonics). The quantification of dsDNA was performed using a Quant-Ti PicoGreen dsDNA Assay Kit (Thermo Fisher Scientific) accordingly with manufacturer´s instructions. At least 5 biological replicates were considered for each condition per time point.

3.3.11.3. Immunolabelling of tendon and bone related proteins:

Immunolabelling for Collagen I (*COLIA1*) (ab90395), Osteopontin (*OPN*) (ab14175) and Tenascin-C (*TEN*) (ab6393) was performed in single units after 7 and 21 days and co-culture cell hydrogel units after 21 days in culture. All antibodies were purchased to Abcam. The antibodies were diluted as 1:200, 1:100 and 1:200 for collagen I, osteopontin and tenascin-C respectively and incubated 1 hour at room temperature. The fluorescent secondary antibody Alexa Fluor 488 (A21206, alfagene) was incubated for 1 hour at room temperature followed by DAPI (4', 6-diamidino-2-phenylindole) (1:1000, 40009, VWR) and Phalloidin Red (Phalloidin–Tetramethylrhodamine B isothiocyanate) (1:200, P1951, Labodidactica) stains. After, the samples were analyzed in an inverted confocal microscope (TCS SP8, LEICA) equipped with argon/He-Ne laser sources.

3.3.11.4. Gene Expression Analysis by Real-Time Polymerase Chain Reaction (RT-PCR)

The expression of the genes *COLAI*, *DCN* and *TEN* was assessed by real-time polymerase chain reaction (RT-PCR) on RNA isolated from hTDCs and pre-Ost and co-cultures 7, 14 and 21 days after the encapsulation in met-CS MAGPL hydrogels. In tendon-bone units, hydrogels were sectioned in three parts: tendon unit: the section with the hydrogel encapsulating hTDCs, the interface between the hydrogel encapsulating hTDCs and pre-Ost and the bone unit where pre-Ost were laden in the hydrogel. Four independent biological replicates were analyzed for each time point.

Total RNA was isolated from cells laden in the hydrogel using the TRI Reagent® RNA Isolation Reagent (733-1089, Sigma-Aldrich) according with the manufacturer's instructions. The yield and purity of RNA isolation was determined by spectrometry using the NanoDrop 1000 Spectrophotometer (ThermoScientific). The cDNA was synthesized using 100 pg of RNA as template and the qScript™ cDNA Synthesis Kit (733-1175, VWR). The primers, listed in Table 3.1 were designed using the primer-BLAST tool available at http://www.ncbi.nlm.nih.gov/tools/primer-blast. Target genes were normalized to the reference housekeeping *GAPDH* gene according to Livak's method[21]. The analysis was performed on a real time Polymerase Chain Reaction (RT-PCR) Mastercycler (Realplex, Eppendorf).

Table 3.1: List of primers used for RT-PCR expression analysis of osteogenic and tendon related genes. The primers were designed using the primer-BLAST web tool.

NCBI Reference Sequence	Gene product	Gene Short name	Primer sequence	Product length [bp]
NM 001040058.1	Secreted phosphoprotein 1 (Osteopontin)	SPP1	CAGACCTGACATCCAGTACCC GGTCATCCAGCTGACTCGTT	173
NM 001920.3	Decorin	DCN	CAGCATTCCTCAAGGTCTTCC T GAGGCCATTGTCAACAGCA	154

NM 000088.3	Collagen alpha-1(I) chain	COLIA1	CCCCAGCCACAAAGAGTCTAC TTGGTGGGATGTCTTCGTCT	150
NM 001256799.1	Glyceraldehyde-3-phosphate dehydrogenase	GAPDH	GGGAGCCAAAAGGGTCATCA GCATGGACTGTGGTCATGAGT	198

3.3.12 Statistical Analysis

Results are presented as mean ± standard deviation. The statistical analysis of data was performed using GraphPad Prism 6 software. Statistical analysis was carried out using 2-way ANOVA for significant differences among studied conditions followed by Turkey's multiple comparison test. A minimum of 95% confidence interval was considered for all measurements ($p<0.05$). Statistical significant values and associated degree of confidence ($p<0.05$) are denoted by symbols represented in the graphs.

3.4 Results

3.4.1 Production and Characterization of Uncoated MNPs and Met-CS MNPs

In this work, iron oxide magnetic nanoparticles (MNPs) were successfully produced by a co-precipitation method. The developed MNPs were further coated with CS modified with methacrylated groups and stabilized via a crosslinking reaction with ADH promoted by carbodiimide. These MNPs were further characterized and their physicochemical, morphologic and magnetic properties are described below.

3.4.1.1. Physicochemical characterization of met-CS MNPs

FTIR analysis of uncoated and met-CS MNPs was performed to confirm the presence of the met-CS coating (Figure 3.1).

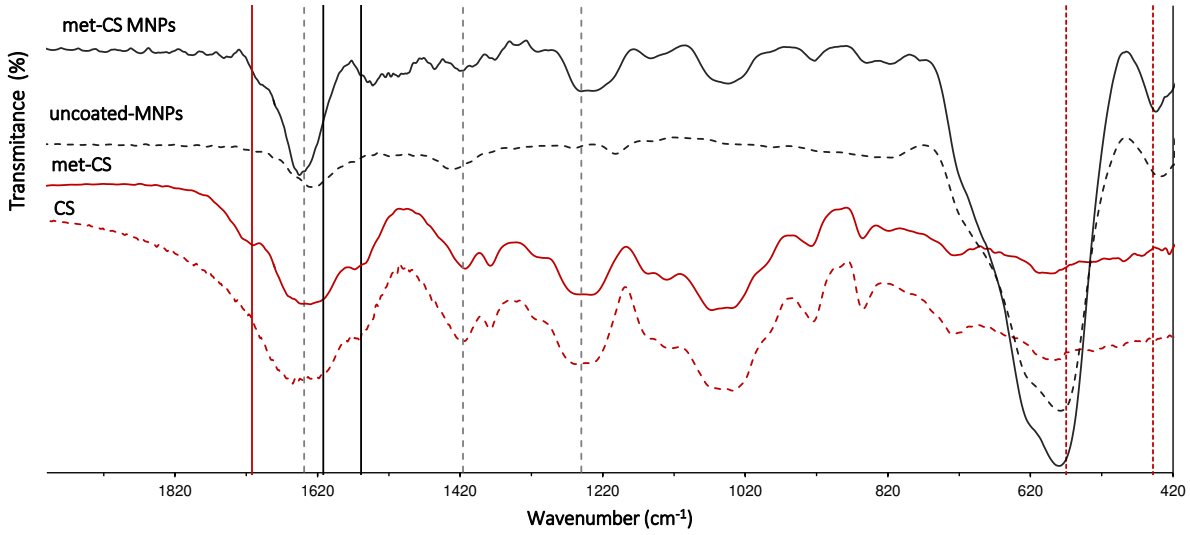

Figure 3.1: FTIR transmittance spectra of uncoated magnetic nanoparticles (MNPs, dashed black line), chondroitin sulphate (CS, red dashed line), methacrylated chondroitin sulfate (met-CS, red line) and MNPs coated with met-CS (met-CS MNPs, black line). Red line corresponds to the anhydrous aldehyde (R-C=O) stretch at ~ 1715cm^{-1}. The dashed grey line indicates the amide stretch at ~ 1639cm^{-1} and sulphate group at 1250 cm-1. The black lines matches with to the amide (R-C=O-NH-R') NH vibrational bending at ~1569cm^{-1} and C=O stretch of the carboxylic group at ~1612cm^{-1}. The dashed red lines correspond to the iron III oxide peaks at ~ 570 and 453 cm^{-1}.

The FTIR spectrum of CS (non-methacrylated) displays the typical bands associated with this polymer at ca. 1639 and 1416 cm^{-1}, which are assigned to the asymmetric and symmetric axial deformations of the carboxylate anion (–COO^{-} stretching) and the peak related to the sulfate group at 1250 cm^{-1} (represented with grey dashed lines). The presence of the methacrylic group on met-CS was confirmed by the ester absorption peak at 1715 cm^{-1}, which corresponds to pendant vinyl groups (–CH=CH2) not detectable in the CS polymer (red line).

The iron III oxide absorption bands at 460 and 540 cm^{-1} were observed in uncoated and met-CS MNPs spectra (red dashed lines). The met-CS MNPs spectrum showed the typical bands of met-CS polymer and of MNPs, confirming the presence of CS polymer in met-CS coated MNPs (met-CS), which are not observed in the uncoated MNPs spectrum. The successful crosslinking with carbodiimide and EDCI to stabilize the met CS coating of met-CS MNPs was detected by the

disappearance of the characteristic asymmetric vibration of R-COO⁻ at approximately 1612 cm-1 and the presence of NH bending from the secondary amide at 1569 cm-1 (black lines).

Additionally, the weight percentage (wt %) of polymeric coating in the met-CS MNPs was quantified by TGA analysis performed under an oxygen atmosphere.

A5.9 ± 0.25 % wt of organic phase was detected in met-CS MNPs, which corresponds to the polymer coating. This value was calculated by subtracting the percentage of weight loss obtained for the uncoated MNPs to the value of met-CS present in the met-CS MNPs.

The stability of met-CS MNPs in aqueous conditions was assessed by measuring the electrokinetic potential at different pH and compared to uncoated MNPs (Table 3.2).

Table 3.2: Assessment of Zeta Potential of (A) uncoated MNPs and (B) met-CS MNPs obtained at different pH- SD represents the standard deviation.

A

pH	Zeta Potential	SD
3	31.57	1.87
5	22.80	1.22
6.5	12.07	0.12
7.2	0.20	0.86
12	-46.87	4.72

B

pH	Zeta Potential	SD
3	-8.15	0.41
5	-21.93	0.73
7	-26.73	1.03
10	-31.50	0.20

The electrophoretic mobility of MNPs showed a positive net surface charge at pH up to 7.2, necessary to assure the formation of the met-CS coating (negatively charged) (Table 3.2). After the coating of MNPs with met-CS, the net surface charge became negative in the range of studied pH values. These results indicate that the formation of a colloidal stable suspension of uncoated MNPs was only possible at strongly acidic pH or strongly basic pH. At physiological pH, uncoated MNPs presented low electrostatic repulsion, which relates to less stable suspensions, while met-CS MNP suspensions were more stable. The stability of MNPs in suspension was also confirmed by the sedimentation rate at physiological pH (Figure 3.2).

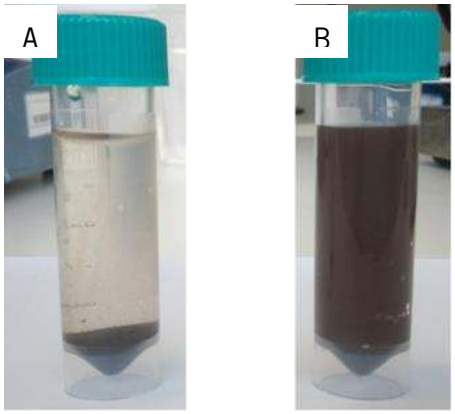

Figure 3.2: Sedimentation rate of A) Uncoated MNPs; B) met-CS MNPs after 20h in Millipore water at pH 7 and room temperature.

As observed in Figure 3.2 a suspension of uncoated MNPs (Figure 3.2A) showed a faster sedimentation rate than a suspension of met-CS MNPs (Figure 3.2B).

The hydrodynamic size of met-CS MNPs was measured at pH=7, showing an average size of 210.8 ± 0.225 nm with a polydispersity index (PI) of 0.225 ± 0.009.

Furthermore, the dimensions and shape of developed MNPs was also assessed by TEM (Figure 3.3).

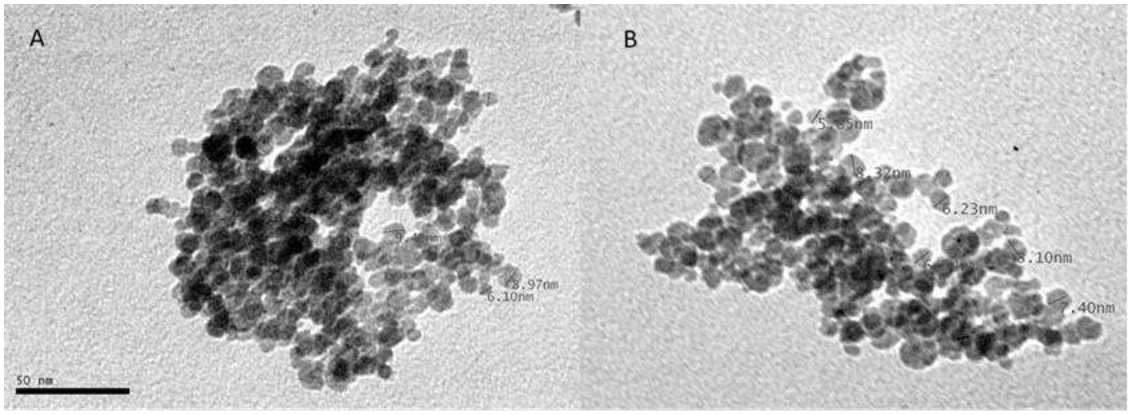

Figure 3.3: Assessment of MNP dimensions. TEM images of A) Uncoated MNPs and B) met-CS MNPs. The scale bar represents 50 um.

TEM images showed that the produced MNPs have a typical round-shape morphology and an average diameter of 6.9 ± 1.0 nm that is not affected by the presence of a met CS coating.

3.4.1.2. Magnetic characterization of met-CS MNPs

Magnetic properties of met-CS MNPs were evaluated using a SQUID-VSM magnetometer and are represented in the Figure 3.4.

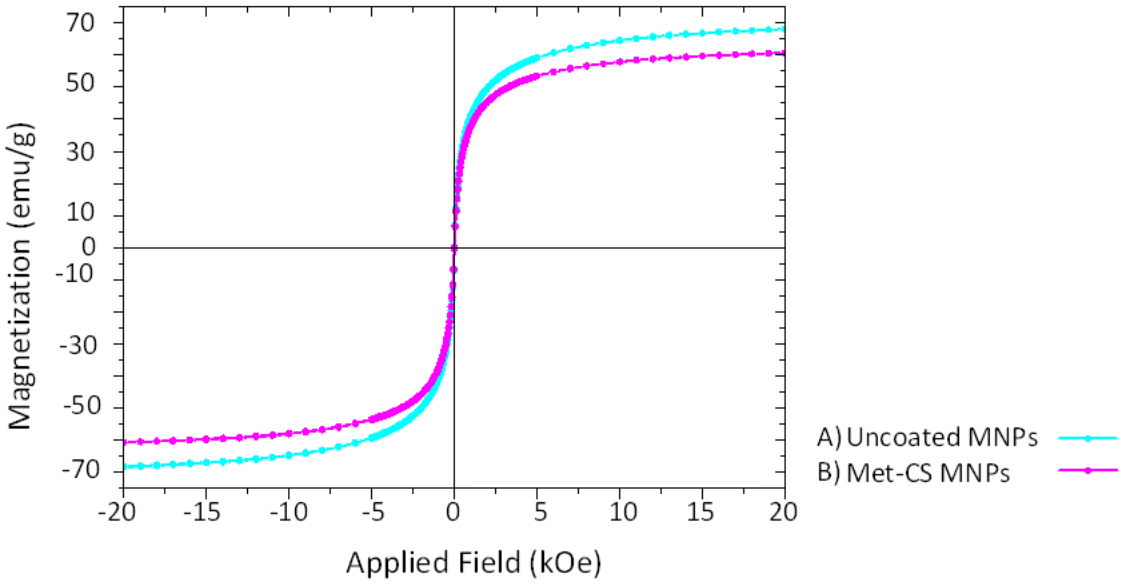

Figure 3.4: Hysteresis loop of A) Uncoated MNPs b) Met-CS MNPs under an applied magnetic field between −20.0 and 20.0 kOe at room temperature.

The absence of remaniscence and coercive forces at zero magnetic field confirms the superparamagnetic behaviour of MNPs at room temperature. The magnetic saturation values were found to be 68.12 emu/g for uncoated MNPs and 60.66 emu/g for met-CS MNPs. The magnetic saturation values of met-CS MNPs were then normalized with the weight percentage of met CS coating (5.9 ± 0.25 %) determined by TGA, showing no loss of magnetic saturation with the coating process.

3.4.1.3. Cytocompatibility assessment of developed MNPs

To incorporate met-CS MNPs into 3D constructs aiming at TE approaches, the evaluation of their cytocompatibility is of critical importance. Thus, the effect of the concentration of MNPs on the viability and proliferation of human adipose derived stem cells (hASCs) was followed-up for 7 days (Figure 3.5).

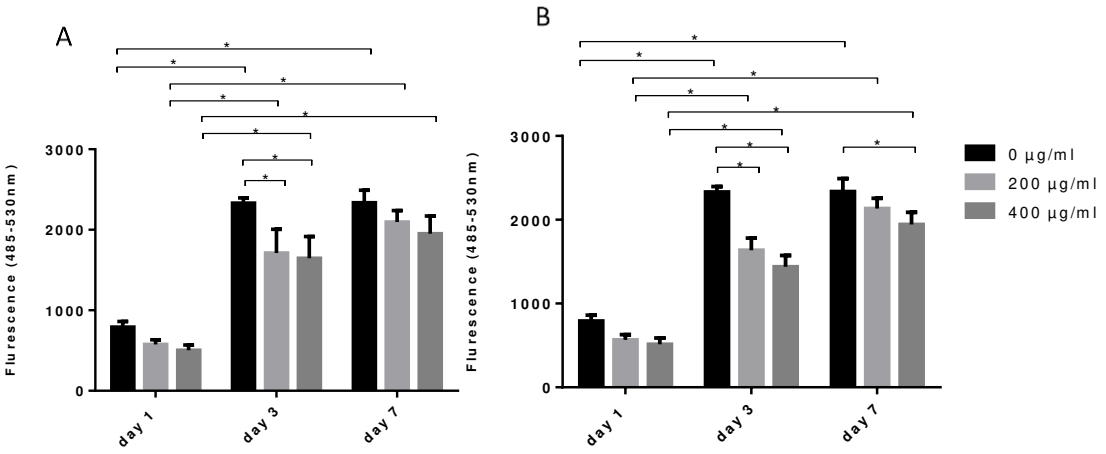

Figure 3.5: Metabolic activity of hASCs cultured in the presence of different concentrations of MNPs (0, 200, 400 µg/mL) after 1, 3 and 7 days in basal culture medium. a) Uncoated MNPs and b) Met-CS MNPs. Symbol (*) denote statistically significant differences ($p<0.05$).

The profile of the metabolic activity of hASCs cultured in the presence of MNPs was similar in both uncoated MNPs and met CS MNPs with a tendency to increase with the time in culture, suggesting that the presence of MNPs does not negatively affect the viability of these cells. However, hASCs cultured in the presence of uncoated MNPs and metCS MNPs show lower metabolic activity after 3 days of culture in comparison with cells cultured without MNPs ($p<0.05$). However, after 7 days, only the highest concentration of met CS MNPs (400 µg/mL) resulted in a lower metabolic activity in comparison to cells cultured without MNPs ($p<0.05$).

Furthermore, the quantification of dsDNA of cells in the presence of MNPs supports the results of metabolic activity (Figure 3.6).

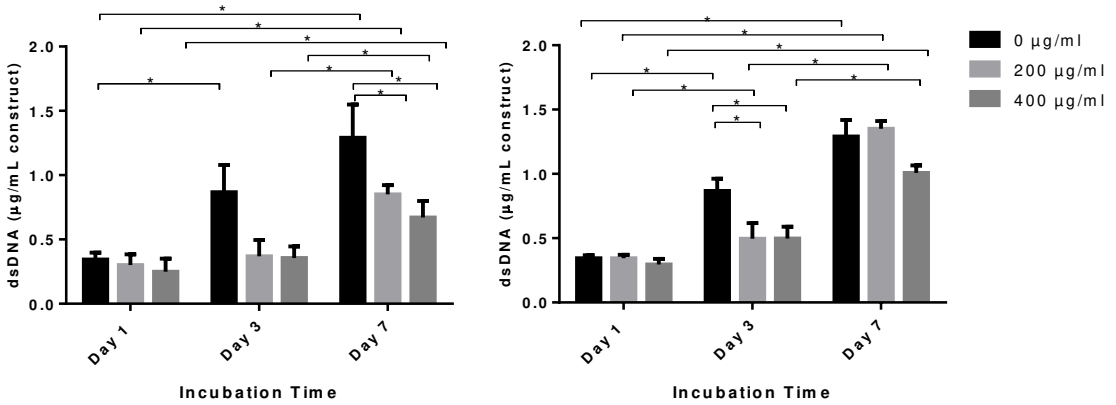

Figure 3.6: Cellular Content quantification of hASCs cultured in the presence of different concentrations of MNPs (0, 200, 400 µg/mL) after 1, 3 and 7 days in basal culture medium. a) Uncoated MNPs and b) Met-CS MNPs. Symbol (*) denote statistically significant differences ($p<0.05$).

An increase of cell content was observed in the presence of both uncoated MNPs and met-CS MNPs over the time in culture (Figure 3.6). A decrease of DNA content of hASCs cultured for 3 in the presence of metCS MNPs and for 7 days in the presence of uncoated MNPs when comparing to hASCs cultured in the absence of MNPs (0 µg/mL). In the case of metCS, this decrease in cell content is overcome at 7 days when dsDNA values are similar to the ones from hASCs without MNPs.

3.4.2 Production and Characterization of Methacrylated Chondroitin Sulfate Magnetic Hydrogels Enriched with Platelet Lysate (met-CS MAGPL hydrogels)

After the production and characterization of met-CS MNPs, they were further incorporated into photocrosslinkable met-CS MAG hydrogels enriched with PL. The met-CS MAGPL hydrogels were produced with different concentrations of met-CS MNPs, namely0, 200 and 400 µg/mL (Figure 3.7).

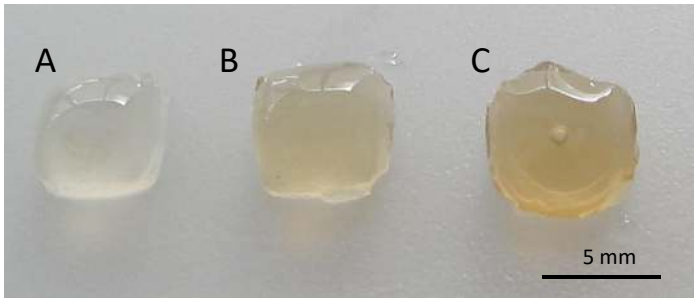

Figure 3. 7: Macroscopic images of the hydrogels produced A) met-CS PL hydrogel; B) met-CS_{200} MAGPL hydrogel and; C) met-CS_{400} MAGPL hydrogel.

The increase in the metCS MNPs concentration incorporated in the hydrogels is detected by a darker color of the met-CS MAGPL hydrogel. Overall, no macroscopic aggregates of MNPs were detected in the formulations assessed.

To confirm the crosslinking of met-CS MNPs to the met-CS hydrogel matrix, hydrogels with 2% (w/v) of met-CS containing 400 μg/mL of either uncoated or met-CS MNPs were incubated with osmotized water (10mM NaCl) at pH 8 and placed in contact with a magnet. Hydrogels produced with both types of MNPs were responsive to the application of a magnetic field. The release of MNPs was observed from hydrogels incorporating uncoated MNPs, unlike the met-CS MNPs incorporated within met-CS MAGPL hydrogels, which remained entrapped in the hydrogel matrix (data not shown).

3.4.2.1. Morphological Characterization of Met-CS MAGPL Hydrogels

The distribution of met-CS MNPs and their influence in the arrangement of magnetic met-CS MAGPL hydrogel microstructure were assessed by TEM (Figure 3.8) and cryo-SEM (Figure 3.9).

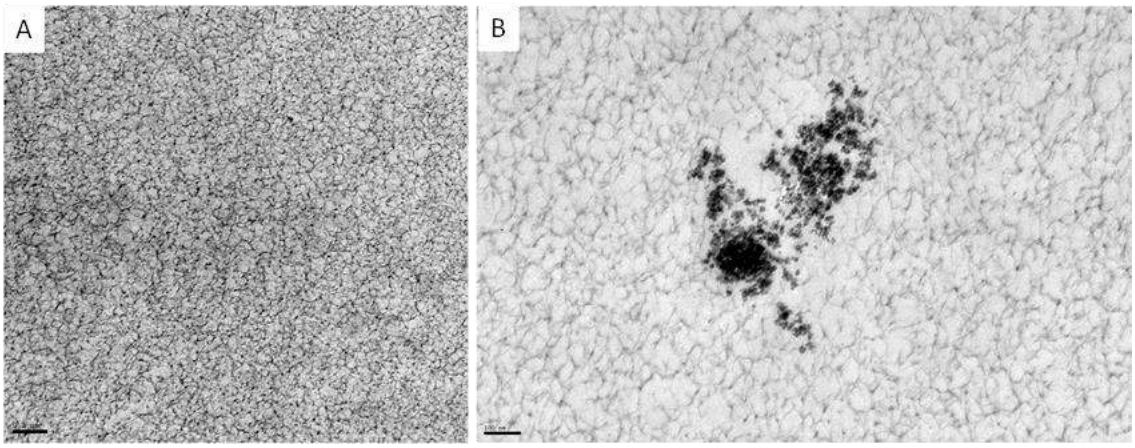

Figure 3.8: TEM images of A) met-CS PL Hydrogel B) met-CS_{200} MAGPL Hydrogel. The scale bar represents 100µm

TEM micrographs of met-CS_{200} MAGPL hydrogel matrices showed spherical met-CS MNPs randomly organized in aggregates within the met CS MAGPL hydrogel matrix.

The CryoSEM micrographs of the met-CS, met-CS with PLs and met-MAGPL hydrogel formulations (200 and 400µg/ml of metCS MNPs) are shown in Figure 3.9 A, B,C and D respectively.

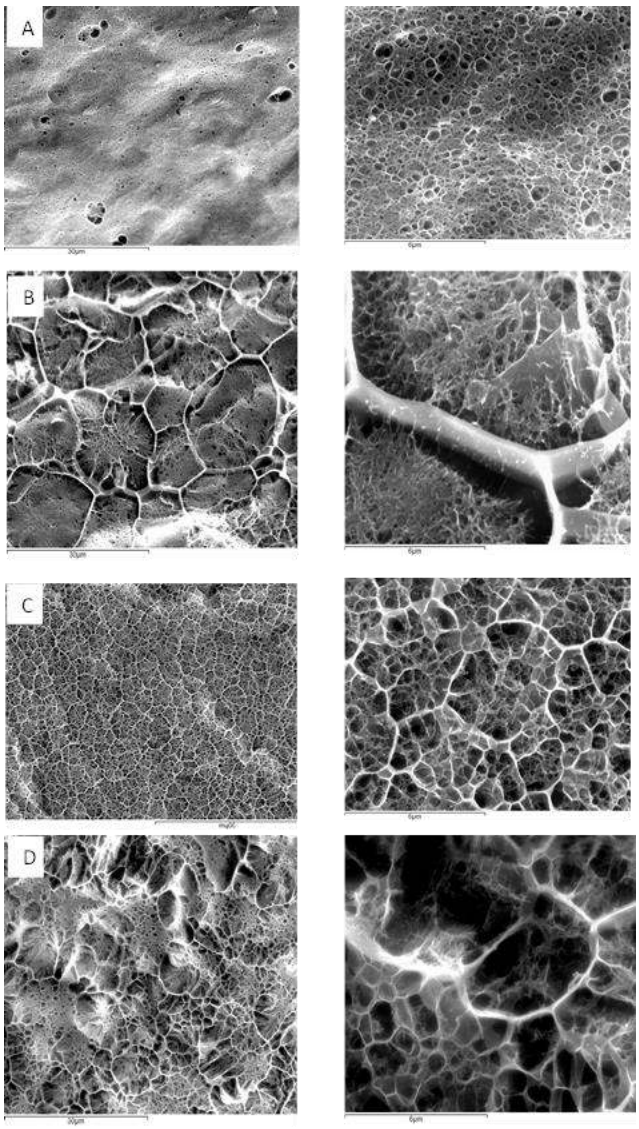

Figure 3.9: Cross-section cryo-SEM images of A) met-CS; B) met-CS PL; C) met-CS_{200} MAGPL; C) met-CS_{400} MAGPL. The scale bar represents in the images of the left 30 µm and the right 6 µm.

Significant differences were observed in the microstructure of the developed hydrogels in terms of micropore dimensions, interconnectivity and micropore distribution within the matrix. Met CS Mag hydrogel presented a condensed matrix with smaller pores homogeneously distributed within the matrix. The PL enrichment to the matrix change the morphology of the hydrogel matrix creating a homogenous distribution of trabecular structures (not present in met-CS MAG hydrogels) containing smaller pores with similar dimensions and shape to the ones observed in met CS hydrogels. The incorporation of met CS MNPs within the hydrogels also influenced the morphology of the matrix, reducing the dimensions of the trabecular structures observed in PL enriched hydrogels. This morphological modification seems to be related to the concentration of met CS MNPs incorporated in the matrix. Hydrogels with met-CS $MNPs_{200}$ exhibited a homogeneous distribution of small pores randomly dispersed within the larger traberculi-like structures. The metCS $MNPs_{400}$ formulation showed a more random microstructure characterized by the presence of regions with larger pores, similar to those observed in the met-CS $MNPs_{200}$ formulation interspersed with small pores matrix.

3.4.2.2. Mechanical Characterization of met-CS MAGPL Hydrogels

The mechanical/viscoelastic properties of met-CS PL and met-CS MAGPL hydrogels (200, 400µg/mL) were analysed by dynamic mechanical analysis at simulated physiological conditions. (Figure 3.10).

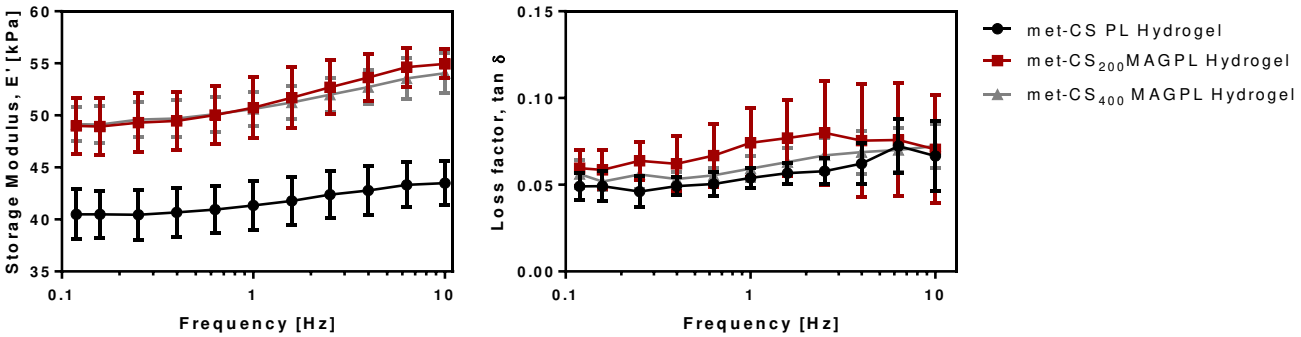

Figure 3.10: Storage modulus (E´) and loss factor (tan δ) of met-CS MAGPL hydrogels produced with different concentrations of met-CS MNPs (0, 200, 400 µg/mL).

The incorporation of met-CS MNPs into the hydrogel matrix led to an increase in the values of storage modulus (E´) in comparison with the hydrogels without met-CS MNPs ($p<0.05$). The increment in the MNP concentration from 200 to 400 µg/ml does not influence the values of

storage modulus of the hydrogels ($p>0.05$). The values of E´ were 41 KPa in the case of met-CS PL hydrogels and in met-CS MAGPL hydrogels ranged from 48 to 54 kPa.

The tan δ provides information about the damping properties of the produced material and shows that hydrogels independently of the presence of met-CS MNPs, presented tan δ values ranging between 0.049 to 0.07 that are an indication of the high elastic properties and low energy dissipation potential of the produced materials. The presence of met-CS MNPs did not affect the tan δ values ($p>0.05$) of the produced hydrogels.

The hydrogel formulation with 200 μg/mL met-CS MNPs (met-CS_{200} MAGPL hydrogel) showed the most promising outcomes considering the results obtained from the MNPs characterization including those concerning the metabolic activity and DNA content of hASCs cultured with different concentrations of met-CS MNPs and from the met-CS MAGPL hydrogel characterization, namely DMA analysis, Cryo-SEM and therefeore this formulation was selected for further studies.

3.4.2.3. Influence of Magnetic field in the Swelling and Degradation Profiles

The swelling properties of the met-CS_{200} MAGPL hydrogels as a function of the incubation time were monitored in PBS at 37ºC (Figure 3.11).

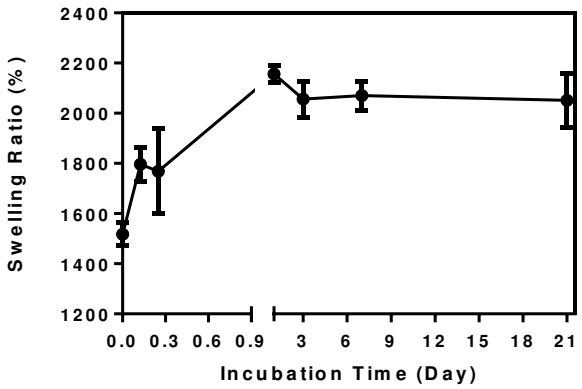

Figure 3.11: Swelling profile of metCS_{200} MAGPL Hydrogels in PBS at 37°C for 21 days

Overall, the swelling ratio, which correlates to the time of liquid immersion, presented a maximum mass increase of 2156 ± 32.8 %. Afterwards, the hydrogel swelling remained almost unaltereted during the experimental setup (21 days).

The impact of magnetic field in the weight loss profile of the hydrogel was assessed as a function of incubation time in the presence/absence of an enzymatic solution of HAse (Figure 3.12).

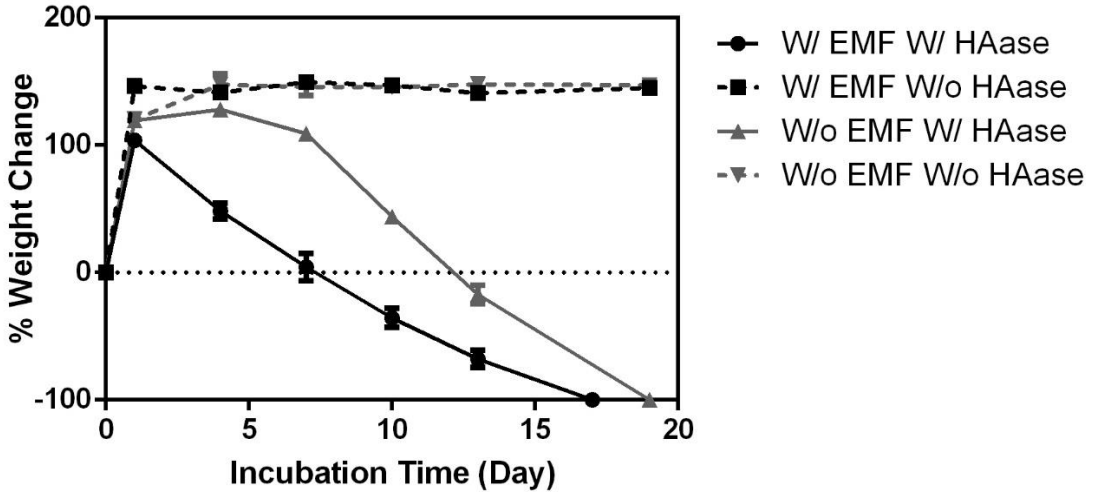

Figure 3.12: Weight loss profile of met-CS_{200} MAGPL hydrogels in a solution of 2.6U/mL hyaluronidase and under the application of an external magnetic field (EMF) in PBS at 37°C for up to 20 days. Continuous black line and grey line represents respectively under EMF , with HAse and without EMF with HAse. Dashed black line represent with EMF without HAse and dashed grey line represents without EMF without HAse.

Herein, met-CS_{200} MAGPL hydrogels incubated under the actuation of an external magnetic field (EMF) reached the maximum sweeling ratio after 1 day of incubation (Figure 3.12).

Hydrogels cultured in static conditions (without EMF) the maximum swelling was acchieved by day 3. The integrity of hydrogels incubated in PBS was mantained during the experimental setup.

Moreover, the impact of magnetic field and the influence of hyalurodinase (HAase) in the degradation of the hydrogel profile were also assessed as a function of incubation time (Figure 3.12).

Met-CS_{200} MAGPL hydrogels incubated in the presence of HAse under EMF stimulation degraded faster than the formulation in static conditions with HAse. In the presence of EMF stimulation and enzymatic solution the degradation was complete after 17 days. In the absence of EMF and in the presence of HAse, hydrogels reaching a complete degradation after 19 days.

3.4.2.4. Influence of Magnetic field in GF release of met-CS MAGPL hydrogel

The release profile of PDGF-BB from met-CS_{200} MAGPL hydrogels under the presence/ absence of magnetic stimulation and in the presence/absence of HAse during 10 days is represented in Figure 3.13.

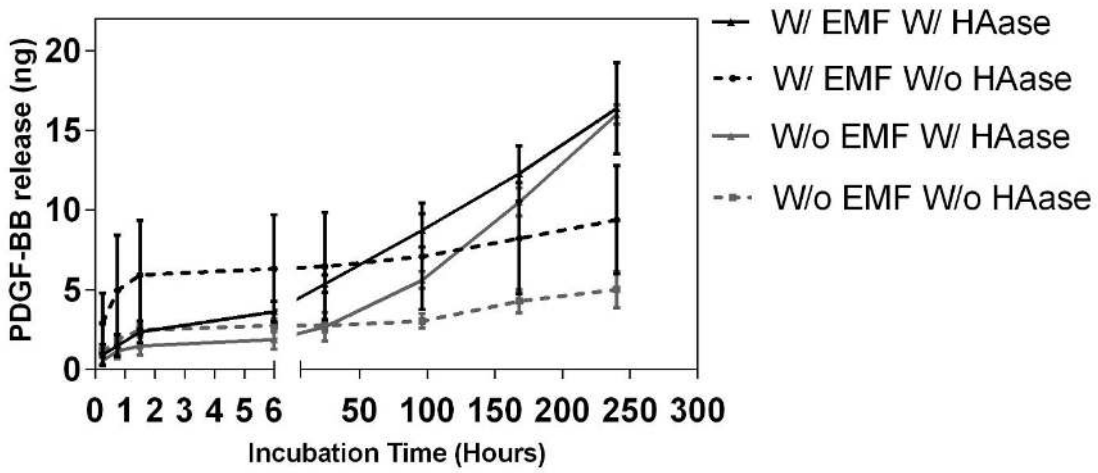

Figure 3.13: ELISA quantification of PDGF-BB release from met-CS200 MAGPL hydrogels to a solution of 2.6U/mL hyaluronidase under the application of an external magnetic field (EMF) in PBS at 37°C for up to 10 days. Continuous black line and grey line represents respectively under EMF , with HAse and without EMF with HAse. Dashed black line represent with EMF without HAse and dashed grey line represents without EMF without HAse.

Independently of the presence/absence of magnetic stimulation and HAse solution, the release of PDGF-BB was caracterized by an initial burst. In the absence of HAse the release of PDGF-BB followed a sustained delivery up to 10 days. Moreover, the presence of magnetic field led to an aparent increase in the release of PDFG-BB in the absence of HAse as early as 2 days of incubation. Independently of the EMF, in the presence of HAse, the release was continuously increased, being once again apparently higher under EMF stimulation in comparison with the formulation without EMF.

3.4.3 Biological assessment of cell-laden hydrogel systems

To assess the ability of developed metCS_{200} MAGPL hydrogels to act as a cell carrier for tendon bone interface strategies, (hTDCs) and hASCs pre-differentiated into osteoblast-like cells (pre-Ost) were laden in the met-CS MAGPL hydrogels, either in single hydrogel units or as double hydrogel units, co-culturing hTDCs and pre-Ost under magnetic stimulation.

3.4.3.1. Metabolic Activity and Cellular content

The metabolic activity and cellular content of cells laden in metCS$_{200}$ MAGPL hydrogels were assessed in single units as well as in the co-culture system after 1, 7,14 and 21 days (Figure 3.14 and 3.15).

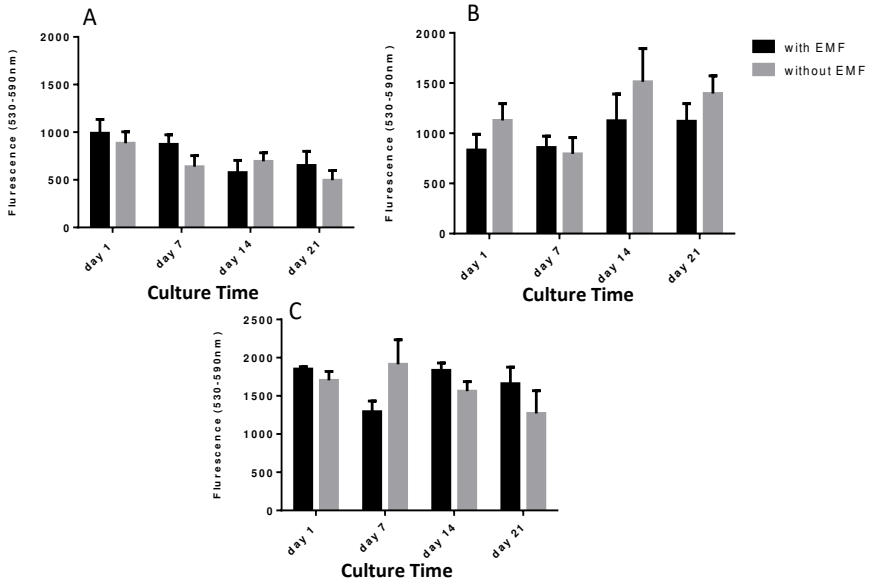

Figure 3.14: Metabolic activity of cell encapsulated in the metCS$_{200}$ MAGPL hydrogel in the presence (with EMF) or absence (without EMF) of magnetic stimulation. A) Human tendon derived cells (hTDCs); B) hASCs pre differentiated into osteoblastic like cells; C) Co-culture of hTDCs and hASCs pre differentiated into osteoblastic like cells encapsulated in the met-CS$_{200}$ MAGPL hydrogels. Symbols (*) denote statistically significant differences ($p<0.05$).

HTDCs and pre-Ost encapsulated in single or double hydrogel units maintained metabolic activity with the time in culture and were not afected by the actuation of an external magnetic field ($p<0.05$).

The results of dsDNA quantification for cells laden in metCS$_{200}$ MAGPL hydrogels are indicated in Figure 3.15.

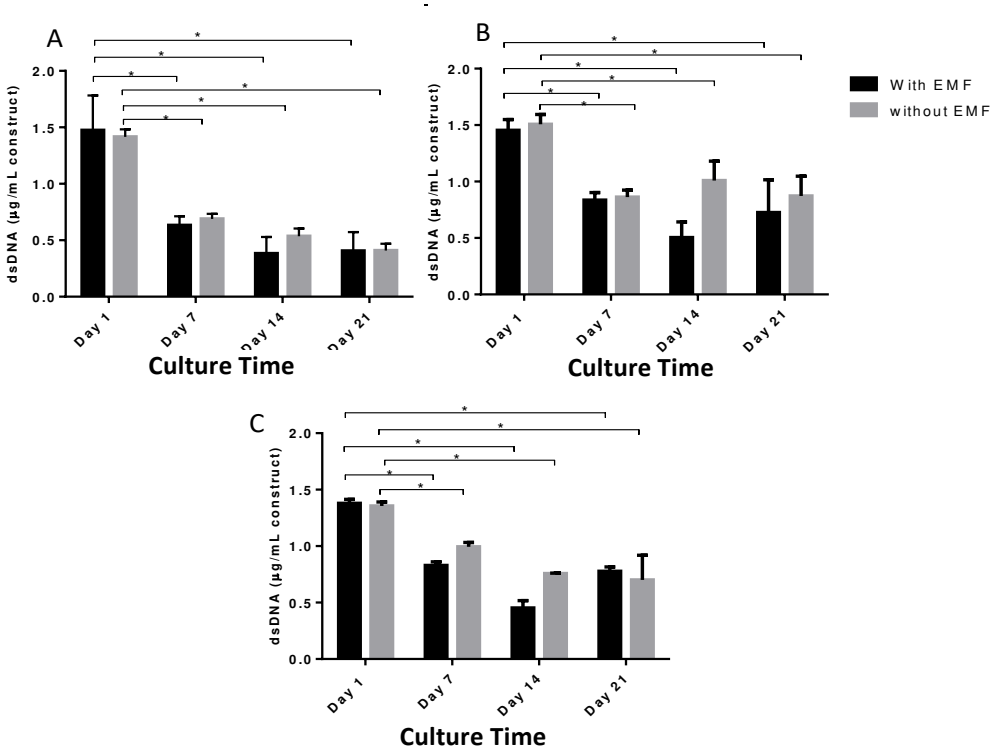

Figure 3.15: dsDNA content of cell encapsulated in the metCS$_{200}$ MAGPL hydrogel in the absence (without EMF) and under magnetic (with EMF) conditions. A) Human tendon derived cells (hTDCs); B) hASCs pre differentiated into osteoblastic like cells; C) Co-culture of hTDCs and hASCs pre differentiated into osteoblastic like cells encapsulated in the met-CS$_{200}$ MAGPL hydrogels. Symbols (*) denote statistically significant differences ($p<0.05$).

HTDCs and pre-Ost cells laden in met-CS MAGPL hydrogels evidenced a significant decrease in cell content from day 1 to day 7 ($p<0.05$), independently of the EMF stimulation or if they are cultured in single or co-culture units. Beyond day 7, cellular content values were kept stable and are maintained during the experimental setup, without significant variations up to 21 days ($p>0.05$).

Overall the results showed that the actuation of an EMF does not negatively influence cell viability and proliferation, in comparison to non-magnetic stimulation.

3.4.2.2. The Role of Magnetic Stimulation in tendon-to-bone interfacial units

The morphology and distribution of cells laden in met-CS$_{200}$ MAGPL hydrogels were evaluated by confocal microscopy as well as the the presence and organization of ECM proteins namely Tenascin-C (*TEN*) (Figure 3.16), collagen I (*COLAI*) (Figure 3.17 and 3.18),) and osteopontin (*OPN*)

(Figure 3.19). Single and double hydrogel units were investigated in the presence or absence of magnetic stimulation.

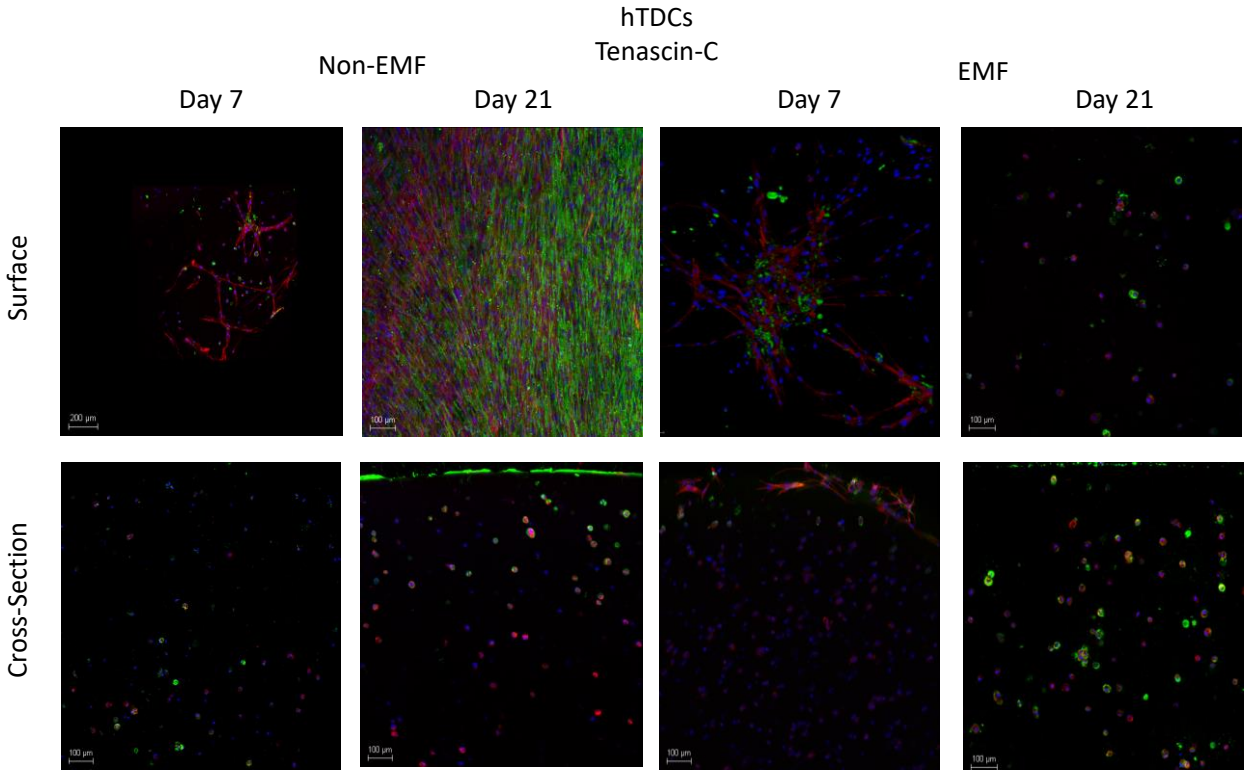

Figure 3.16: Tenascin-C immunolocation in hTDCs laden in met-CS_{200} MAGPL hydrogels, cultured for 7 and 21 days under EMF or static culture (non-EMF). DAPI (blue) stains cell nucleus; Phaloidin (red) represents F-actin and Tenascin-C is represented in green. Scale bar represents 100 μm.

After 7 days ofculture, tendon units exhibited hTDCs both at the surface and in the inner sections of the hydrogel. Human TDCs exhibited a fusiform fibrobastic-like morphology at the surface of the hydrogels in static conditions. Moreover, at the surface of the hydrogel, the actuation of an EMF seems to favor a round morphology of the laden cells with the time in culture.

The presence on Tenascin C is mildly detected as ealy as 7 days in culture, especially at the surface of the hydrogel, independently of the magnetic stimulation (Figure 3.16) Nevertheless, Tenascin C was also observed inside the hydrogel, especially after 21 days under EMF. Also by 21 days, the presence of tenascin-C was highly pronounced at the surface of hydrogels cultured in non EMF conditions. (Figure 3.16).

The collagen I was also assessed in hTDCs laden in metCS_{200} MAGPL hydrogels (Figure 3.17)

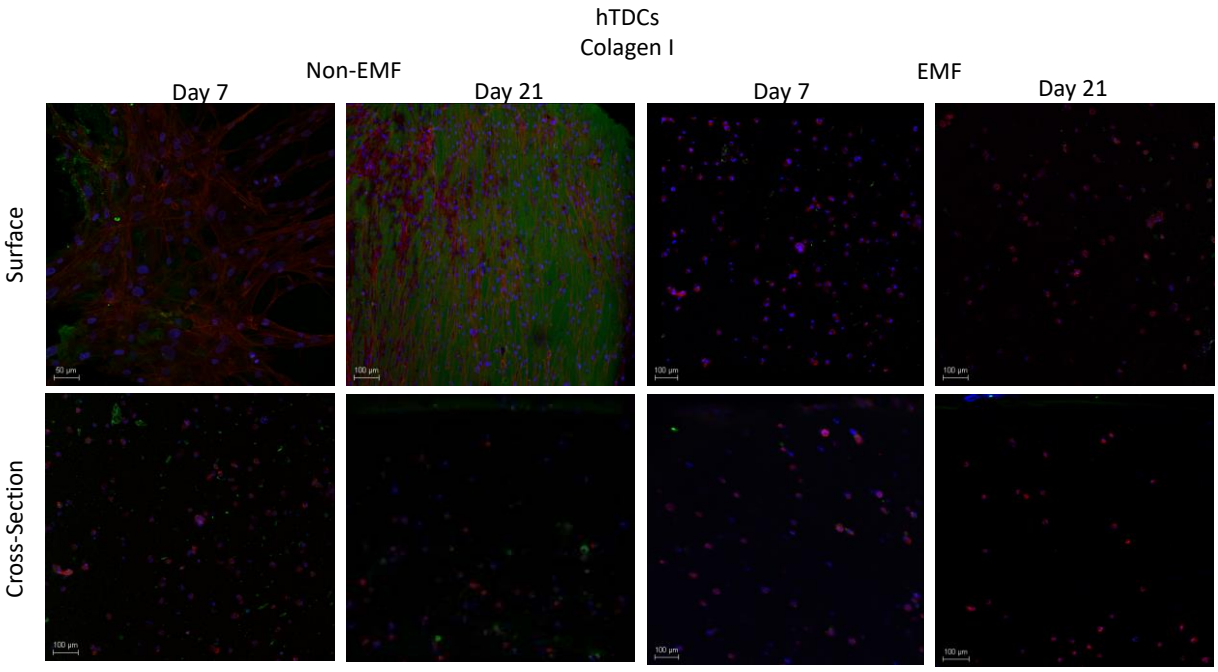

Figure 3.17: Collagen I immunolocation in hTDCs laden in met-CS_{200} MAGPL hydrogels, cultured for 7 and 21 days under EMF or in static culture (non-EMF). DAPI (blue) stains cell nucleus; Phaloidin (red) represents the cell cytoskeleton and collagen type I is identified in green. Scale bar represents 100 μm.

The presence of Collagen I was mildly detected by hTDCs in non-EMF conditions at day 7 and apparently was not found under EMF stimulation (Figure 317). By 21 days, the increment in the amount of collagen I detected was evident, especially at the surface of the hydrogel under static conditions. Although at a minor extent, collagen I was detected inside the hydrogel and tended to increase over the time in culture (Figure 3.17).

In the case of pre-Ost cells laden in single units, the fusiform morphology is also observed at the surface of the single units (Figure 3.18).

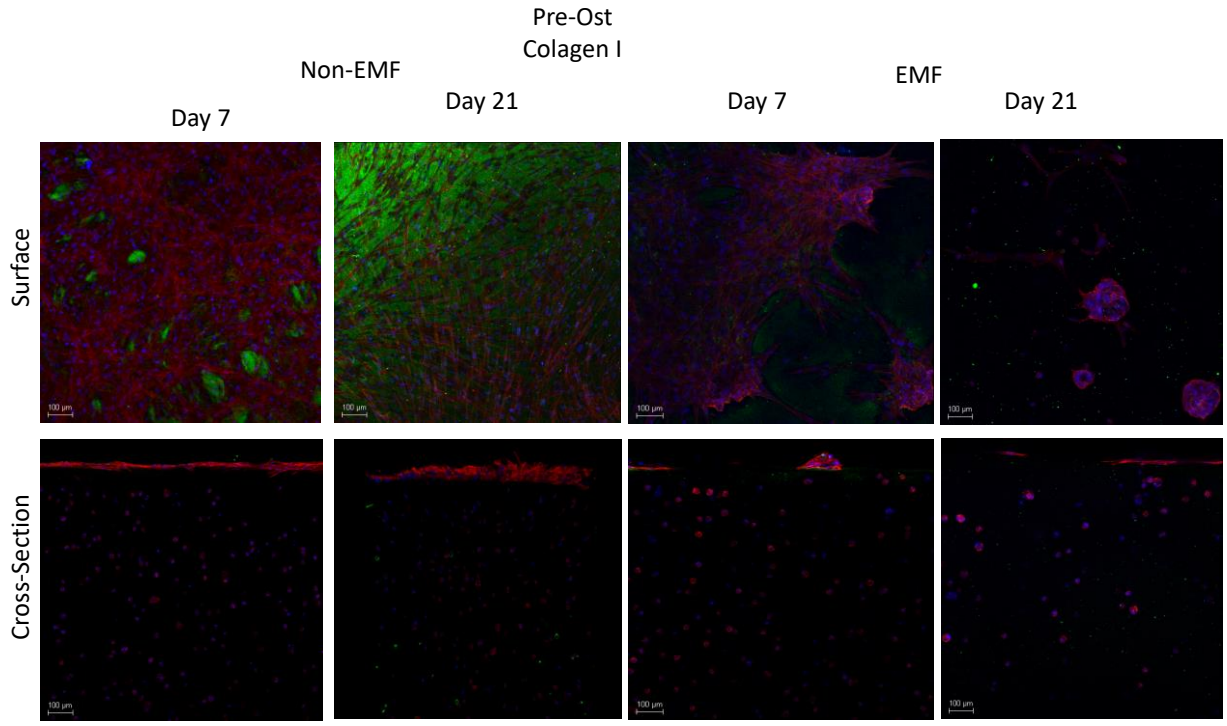

Figure 3.18: Collagen I immunolocation in pre-Ost laden in met-CS_{200} MAGPL hydrogels, cultured for 7 and 21 d under EMF or static culture (non-EMF). DAPI (blue) stains cell nucleus; Phaloidin (red) represents cytoskeleton and Collagen I is represented in green. Scale bar represents 100 µm.

Although the colonization of the surface of the hydrogel by pre-Ost cells is considerably higher in comparison to hTDCs after 7 days, a cell monolayer covering a significant area of the hydrogel surface was observed in both types of cells after 21 days in non-EMF cultures. Also, the cross section image shows a thick cell layer covering the surface of the hydrogel. However, under magnetic stimulation, cells tended to be preferencially round shaped as occurs with hTDCs, both at the surface and inside the hydrogel. A few fusiform cells are also observed at the surface of the hydrogels under EMF although in less extent than the ones cultured in static conditions. Interestingly, it is the detection of cluster-like structures after 21 days in culture by pre-ost cells.

After 7 days of culture, it was possible to detect the presence of collagen I at the surface of the hydrogel in both EMF and non-EMF conditions, that becomes more evident by day 21 in static cultures. Within the hydrogels, the presence of of collagen I is residual .

As for hTDCs, EMF does not seem to promote the colonization of cells at the surface of the hydrogels for longer periods of culture.

The presence of osteopontin was also assessed in pre-Ost cells laden in developed hydrogels (Figure 3.19).

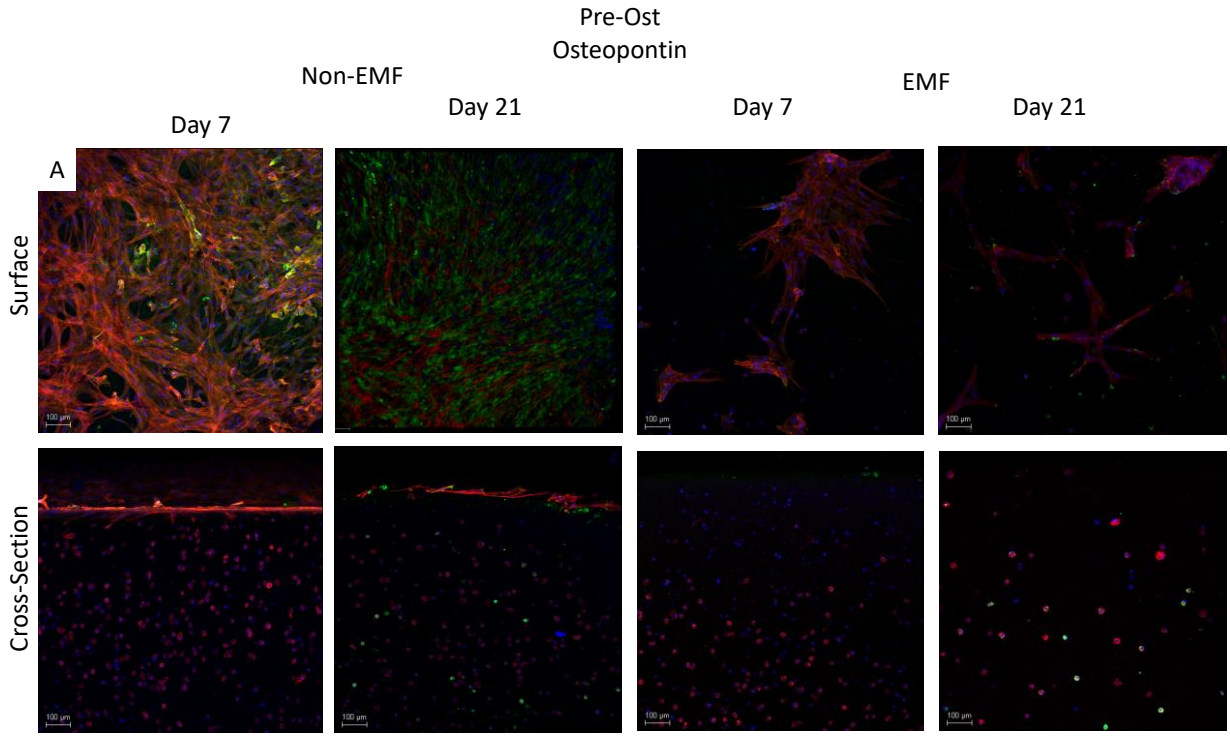

Figure 3.19: Osteopontin immunolocation in pre-Ost laden in met-CS_{200} MAGPL hydrogels, cultured for 7 and 21 d under EMF or static culture. DAPI (blue) stains cell nucleus; Phaloidin (red) represents F-actin and Osteopontin represents the tendon ECM protein. Scale bar represents 100 µm.

Considering the outcomes of cell morphology and protein expression observed in single unit cultures, we investigated the morphology of hTDCs and pre-Ost as well as their ability to synthethize ECM in co-culture systems 21 days after encapsulation in a double hydrogel unit (Figure 20-22). In the co-culture system, a single unit was laden with hTDCs and another with pre-Ost cells and the two units physycally assembled by a second polymerization process.

Matrix deposition and distribution was assessed in different areas of each hydrogel: namely the tendon zone, the interface between the tendon zone and bone zone, where the hydrogel units combine and finally the bone part as represented in Figure 3.1.

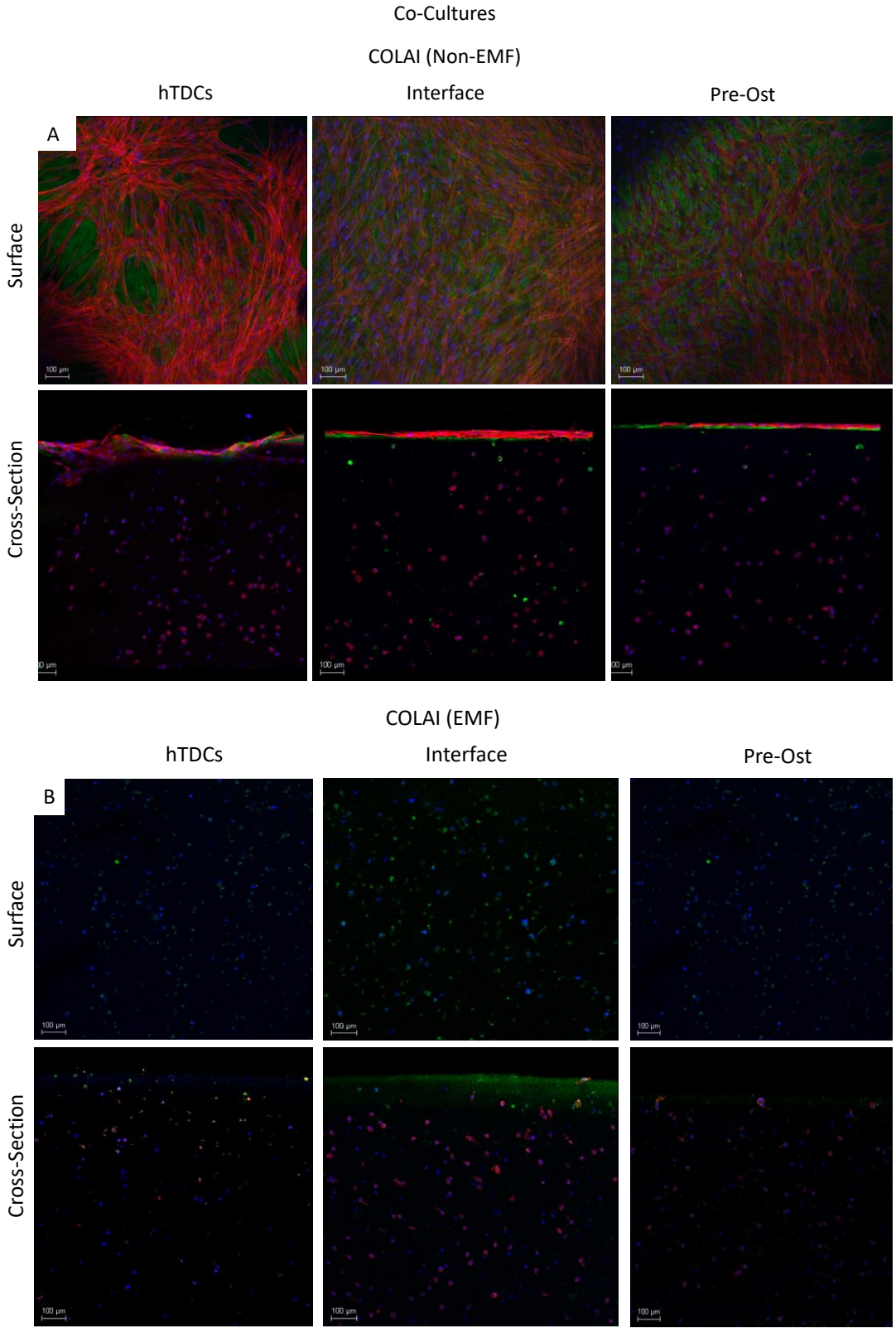

Figure 3.20: Collagen I immunolocation in co-culture met-CS_{200} MAGPL hydrogels, cultured for 21 day A) static culture or B) under EMF. DAPI (blue) stains cell nucleus; Phaloidin (red) stains cytoskeletum Collagen I represents the tendon ECM protein. Scale bar represents 100 μm.

In the particular case of the collagen I, this protein seems to be present in hight amounts at the surface of the co-culture systems in non-EMF conditions and cells exhibit a fusiform morphology. Similarly to cells cultured in single units, co-cultured cells displayed a rounded morphology within the hydrogel independently of the hydrogel zone and EMF stimulation.

When Tenascin C was investigated, the results obtained were different both in terms of morphology and protein detection(Figure 3.21)

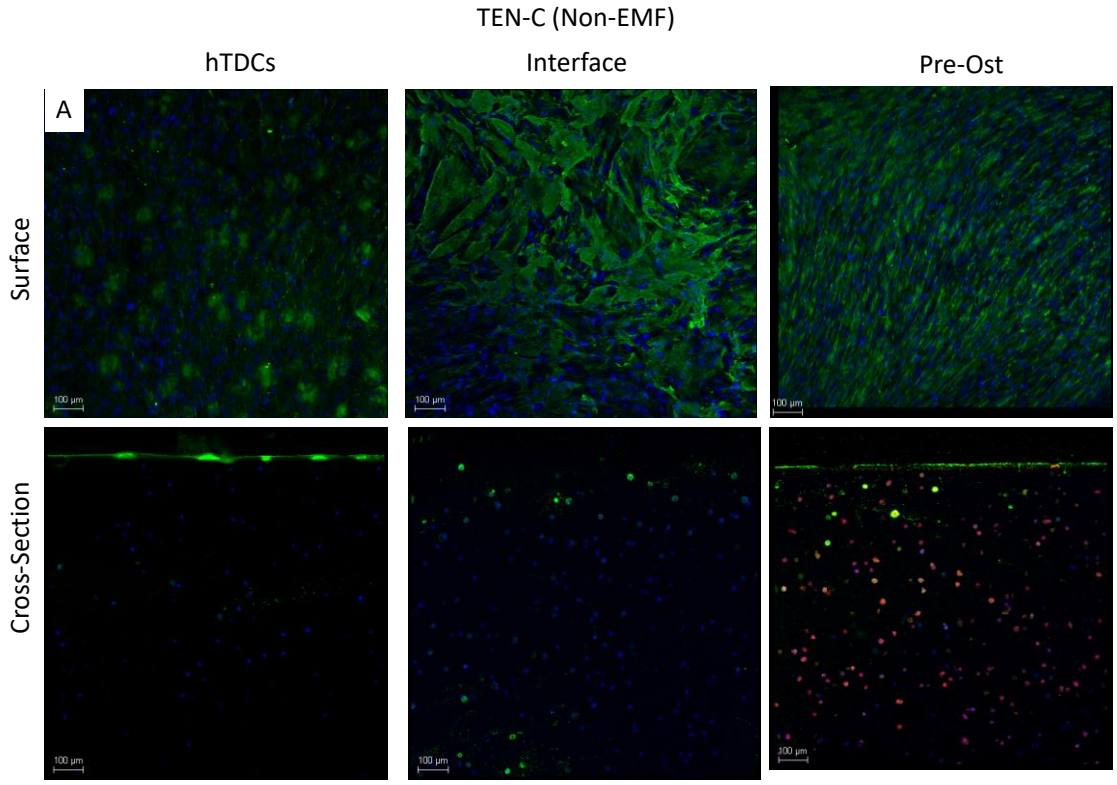

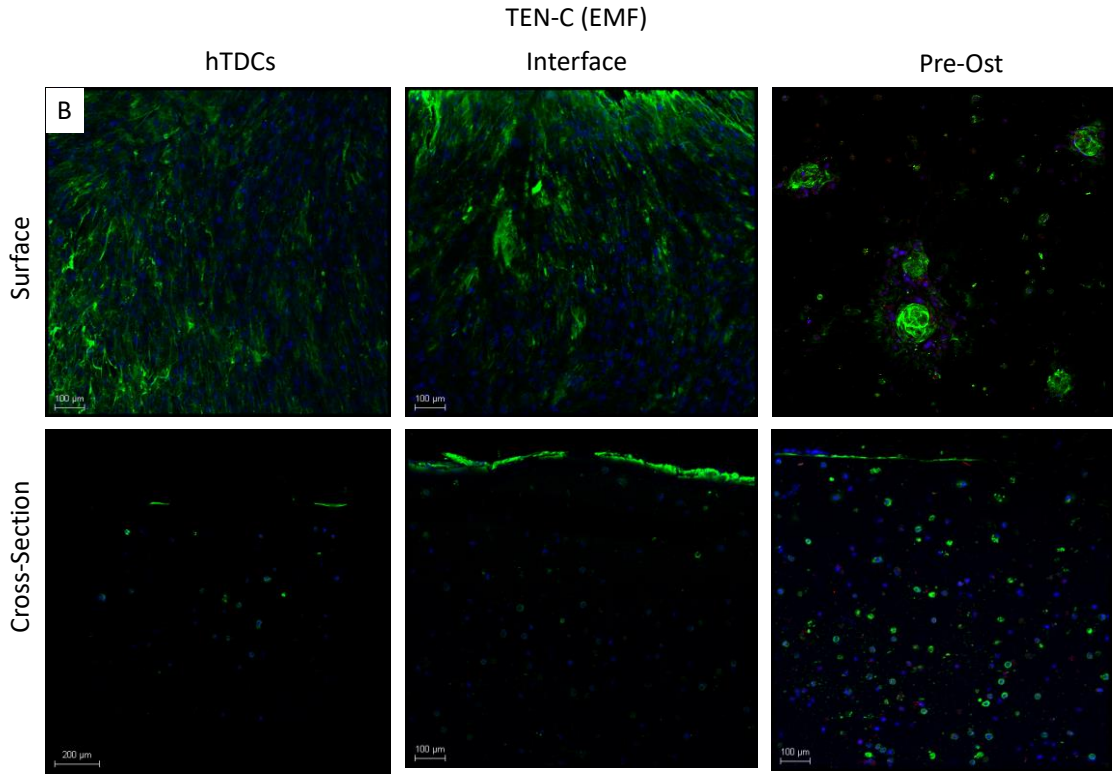

Figure 3.21: Tenascin-C immunolocation in co-culture met-CS_{200} MAGPL hydrogels, cultured for 21 d under EMF or static culture. DAPI (blue) stains cell nucleus; and Tenascin-C represents the tendon ECM protein. Scale bar represents 100 µm.

In both EMF and non-EMF conditions, cells are considerably abundant at the suface of the hydrogel independently of the zone with a fusiform fibrobastic-like morphology and a high amount of of tenascinC was detected. In the inner sections of the hydrogel, the presence of tenascinc is favourably influenced by the EMF. Once again the formation of cluster like organization in the "bone" unit of the system is observed and that are similar in shape and dimensions to the clusters observed in pre-Ost single units under magnetic stimulation (Figure 3.21).

The immunolabeling of osteopontin was also assessed in the co-culture systems (Figure 3.22)

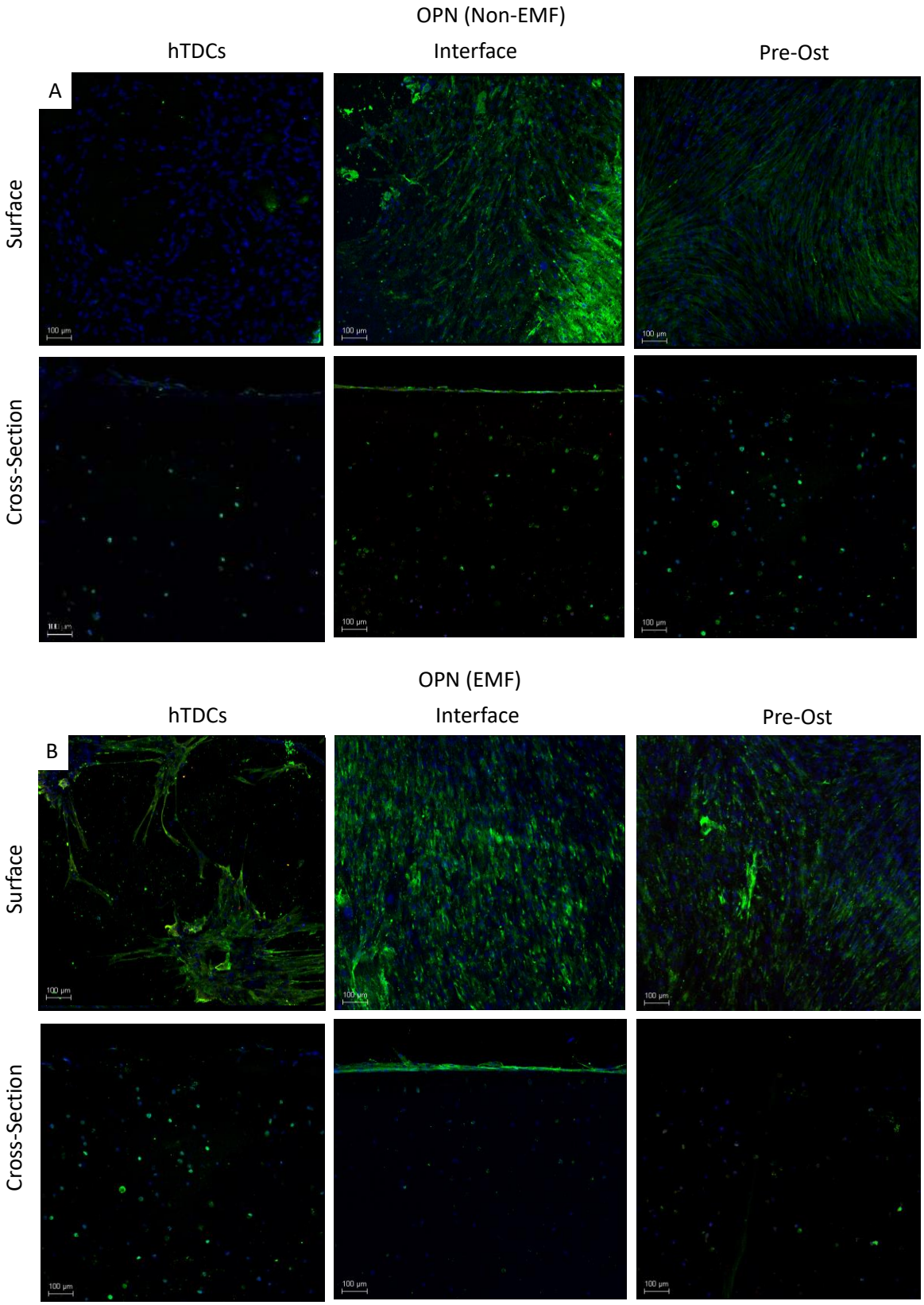

Figure 3.22: Osteopontin immunolocation in co-culture met-CS_{200} MAGPL hydrogels, cultured for 21 d under EMF or static culture. DAPI (blue) stains cell nucleus; and Osteopontin represents the osteo ECM protein. Scale bar represents 100 μm.

OPN, a bone related protein, seems to be present in higher amount in the interface and bone zones of the hydrogel, especially at the surface, although is also detected in the inner sections. Independently of the EMF, cells tend to be fusiform at the surface of the hydrogel.

Overall, non-magnetic condition seems to benefits the fusiform morphology of both cell types. The actuation of a EMF seems to influence hTDCs and pre-osteoblast like cells into a rounder shape after 21 days in culture, and stimulate the formation of clusters in hASCs cells.

The co-culture system evidenced a good cell colonization in all zones of the double hydrogel unit,). Moreover, cells were able to produce ECM, being possible to detect the presence of characteristic proteins , namely collagen I, tenascin C and osteopontin on the surface of the hydrogels resulting in a exuberant layer of cells and matrix in both EMF and non-EMF conditions. Also the presence of these proteins seems to be higher in their specific part of the hydrogel. Therefore, in both conditions tended to form tissue like matrix at the surface construct.

3 Gene expression of Tendon and bone Markers

The expression of bone and tendon markers, namely Decorin (DCN), Osteopontin (OPN) and Colagen type I (COLIA1) in hTDCS and/or pre-Ost encapsulated in met-CS_{200} MAGPL hydrogels under static or EMF conditions was evaluated after 7, 14 and 21 days by quantitative RT-PCR assay. The gene expression of the target genes, normalized to the reference housekeeping GAPDH gene according to Livack's method [21], are represented in Figure 3.23 and 3.24.

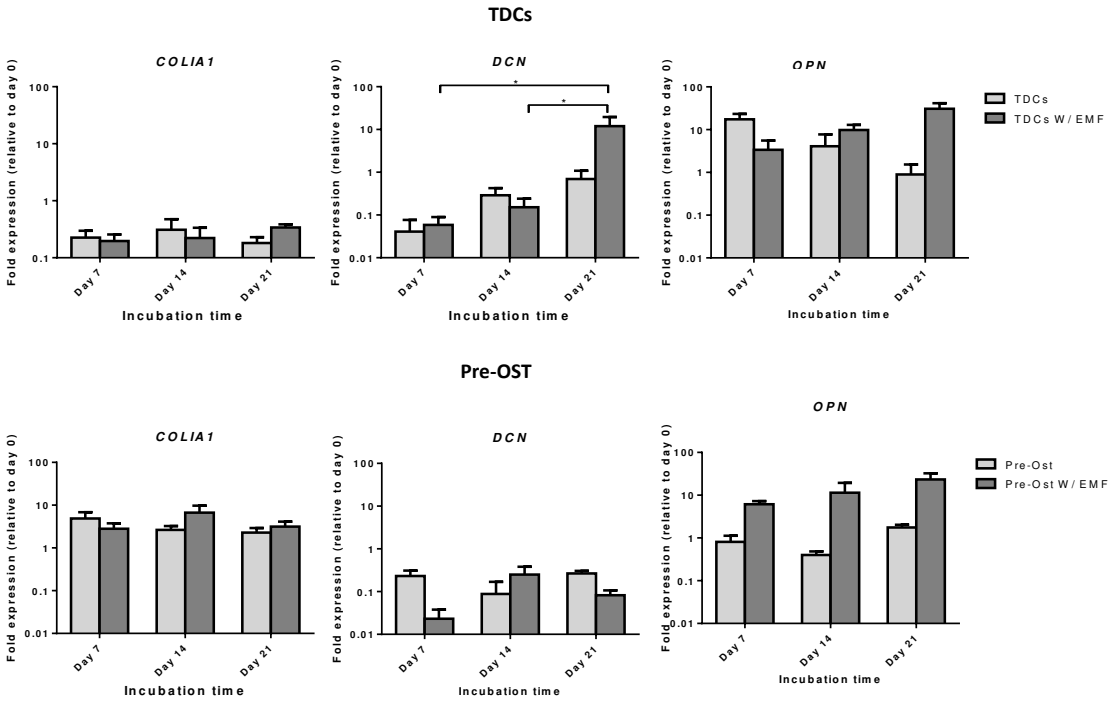

Figure 3.23: Expression of tendon and bone genes in the single units after 7, 14 and 21 days by RT- PCR. Symbols (*) denote statistically significant differences ($p<0.05$). Collagen AI (*COLIA1*); Decorin (*DCN*), Osteopontin (*OPN*).

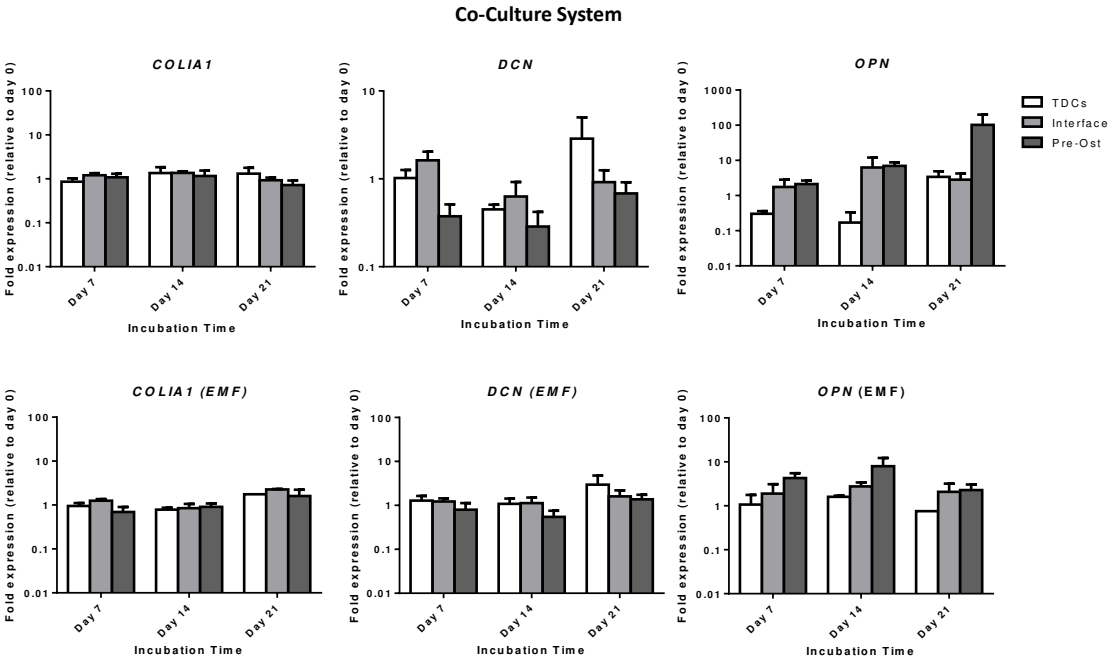

Figure 3.24: Expression of tendon and bone genes in the co-culture system after 7,14 and 21 days by RT-PCR. Collagen AI (COLIA1); Decorin (DCN), Osteopontin (OPN).

The expression of the tendon marker DCN in hTDCs laden single units was enhanced over time independently of the the magnetic stimulation ($p<0.05$) although EMF presented higher expression values ($p>0.05$). However, while cells under magnetic stimulation reached an DCN gene expression 10 fold higher after 21 days in comparison of to cells of the day 0, cells that were not exposed to EMF after the same culture period expressed DCN in same range of values of the day 0. The expression of the other genes assessed, namely osteopontin and colagen type I showed no significant variations with the time of culture nor with the EMF stimulation ($p>0.05$).

Regarding the pre-ost cells incorporated in the hydrogels, despite the tendency to increase the expression of OPN with the time in culture, the gene expression was maintained independently of the EMF conditions. The expression of the other genes assessed, namely decorin and colagen type I showed no significant variations with the time of culture nor with the EMF stimulation ($p>0.05$).

The gene expression was also evaluated in a co-culture system intended to simulate a tendon-bone junction, therefore composed by the combination of: a) the afore evaluated pre-osteoblast-laden hydrogel ("bone" side) and the d) TDCs-laden hydrogel ("tendon" side). The expression of the genes analysed were not altered in both conditions and were stable during the experimental setup (Figure 3.24).

3.5 Discussion

Envisioning the unfulfilled need for tissue engineered constructs with improved functionalities, meeting the requirements of complex tissues and/or tissue interfaces, we proposed the development of a magnetic responsive hydrogel made of a methacrylated chondroitin sulfate-matrix enriched with platelet lysate. To render magnetic responsiveness, magnetic nanoparticles (MNPs) coated with met-CS were used to permit the integration of these MNPs within the hydrogel matrix, thus allowing the tunability and remote control of hydrogel properties upon implantation under the actuation of an external magnetic field (EMF). These properties include the release of growth factors naturally available in PL[22], the degradation rate and the swelling profile of the met CS hydrogel which may be manipulated in a precise manner when controlled magnetic forces are applied. In addition, the magnetic field can also be used to modulate the behavior of cells, once magnetic stimulus has been reported to impact biologic processes by itself or by the activation of

MNPs incorporated within an hydrogel matrix[9]. In both situations, the magnetic field can induce a cellular response likely by the recapitulation of the mechanical forces required for healthy mechano-sensitive tissues such as tendon and bone[9]. Moreover, the inclusion of PL within the met CS hydrogel matrix may also mimic the microenvironment that occurs during the process of tissue healing once PL is constituted by a pool of mitogenic and bioactive molecules, known to modulate tissue repair during tissue injury[17].

This versatile system can be of particular interest for interfaces tissues, highly prone to injury as tendon-to-bone interface[23]. Due to the limited knowledge on this interface, including the cell to cell communication from different tissues, cell-microenvironment interactions and the complexity of gradients in composition and structure, the challenge stands for recreating this structure in a functional interface-like substitute[24].

Based on that in the first part of this work, met-CS MNPs were produced through a co-precipitation method and further coated with met-CS, followed by a chemical stabilization of the met-CS coating. The functionalization of MNPs with methacrilic groups, confirmed by FTIR, is of utmost importance when envisioning the incorporation of magnetic nanoparticles into matrices, as the presence of methacrylate groups available in the met-CS coating enables the linkage to the matrix through photopolymerization[20].

The crosslinking of the coating with ADH, confirmed by FTIR, allowed the stabilization of the met-CS coating that permit the direct binding to the surface of MNPs which otherwise would be leached from the MNPs surface and could overcome the lack of functional groups in natural polymers[20]. Furthermore, the negative charge (-26.8 ± 1.03 mV) of the met-CS coating produced MNPs at physiological conditions, is consistent with the anionic character of the met-CS polymer which is associated to the carboxylic and sulfate groups present in this polymer[25]. As an additional advantage, the met-CS coating may prevent the agglomeration of met-CS MNPs in suspension, as confirmed by the electrokinetic measurements and by the dispersitivy at physiological pH in comparison with the uncoated MNPs.

Another important feature of the developed MNPs is their intrinsic superparamagnetic behaviour at room temperature, with values of magnetization of saturation in the range of 68.12 and 60.66 emu/g for uncoated MNPs and met-CS MNPs, respectively, that are in accordance in which the literature reports for SPIONs magnetization values [20]. This behaviour allows their application as an on/off mechanism, i.e., upon the actuation/removal of magnetic stimulation [20].

Envisioning the use of met CS MNPs to be incorporated into more complex 3D systems as hydrogel matrices in biomedical applications, the biological performance of the produced met-CS MNPs was investigated as a first screening of cytocompatibility. For this purpose, hASCs were seeded and cultured in the presence of uncoated and met-CS MNPs (200 and 400 μg/mL) for 1, 3 and 7 days. Although uncoated and met-CS MNPs is affected the metabolic activity and proliferation of the cells at a concentration of 400 μg/mL, overall MNPs seem not to negatively influence the viability of the cells. In fact, this is in accordance with several studies that have reported the use of iron-based particles for tissue engineering namely cell sheets[11], or cell labeling aiming at bone and chondrogenic differentiation, without particularly affecting cell viability or functionality up to 400 μg/mL. Moreover, several studies have reported that iron oxide MNPs are among the safest particles to grant magnetic responsiveness to biomaterials, with no measurable harmful effect on cell viability [26].

In brief, the MNPs were successfully produced and the functionalization of these MNP with met CS was also successfully achieved. Moreover, the developed met-CS MNP were shown to exhibit promising features, namely stability in aqueous suspensions at physiologic conditions, superparamagnetic behaviour, and high values of Ms and do not affect the viability and proliferation of hASCs etc.

The functionalized met-CS MNPs were therefore subsequently incorporated into a more complex 3D system, a met-CS matrix to develop a versatile magnetic responsive hydrogel enriched with PL by a photopolymerization process in the presence of a photoinitiator. The importance of CS as backbone of ECM is well-known[27] as well as its role in the inflammatory process[28]. Due to its strong negative charge, CS establishes electrostatic interactions with positively charged molecules, such as GFs available at the PL enriched met CS hydrogel matrix, being further released in a controlled manner with the activation of the met-CS MNPs incorporated in the matrix under EMF actuation[29].

The incorporation of MNPs displaying methacrylate moieties allowed the stabilization of the MNPs in the matrix of the hydrogel, an issue that is normally one of the biggest concerns of these systems[30] . Therefore, at pH 8, and unlike uncoated MNPs, the met-CS MNPs were not released from the matrix because they were bonded to it. In fact that was observed into 2% (w/v) met-CS hydrogels incorporating 400 μg/mL of uncoated MNPs at pH 8, released MNPs after contacting with a permanent magnetic field, which was not observed in hydrogels incorporating 400 μg/mL of met-CS MNPs. This is explained by the fact that, at pH=8 both the uncoated MNPs and the met-

CS MNPs were negatively charged and the electrostatic interactions that could occur between the MNPs and the CS matrix would disappear (see table 3.1). At pH 8, the only factor avoiding the release of nanoparticles from the hydrogels incorporating met-CS MNPs was their linkage to the matrix.

Moreover, met-CS MNPs incorporated in met-CS MAGPL hydrogels were showed to be distributed in small aggregates. This spatial rearrangement of the MNPs within the met CS matrix is in accordance to studies published with magnetic hydrogels produced by the blending method highlighting the challenge of having an uniform MNP distribution within the hydrogels that is mainly affected by the high viscosity of the hydrogel precursor solution[3].

In this study the incorporation of met-CS MNPs and PL within the met CS matrices led to alterations in the microstructure and mechanical reinforcement of the hydrogel matrices. Met-CS hydrogels presented a homogenous condensed porous matrix that is associated to the structure of the polymeric met-CS matrix. Although this condensed porous matrix was also observed in PL enriched hydrogels, with the incorporation of PL, larger trabecular like structures were detected and integrated with the met-CS matrix that filled the interior of these structures. The presence of these larger trabecular like structures interconnected with the smaller pores may relate to the presence of structural proteins such as fibrin or vitronectin from PL that have the capacity to form networks and also to interact with glycosaminoglycan for the ECM formation during wound healing [31].

The incorporation of MNPs within the met CS matrix generated hydrogels with a more heterogeneous polymeric matrix, exhibiting areas with a microstructure similar to that observed for PL-enriched hydrogels and other regions where the polymeric matrix was more loosely organized and more evident in hydrogels with higher amounts of MNPs being probably formed by the MNP agglomerates shown by TEM images.

The dynamic mechanical analysis of the hydrogels indicated an increase in the storage modulus (E´) in the formulation containing met-CS MNPs that can be attributed to the presence of the met-CS MNPs bonded to the hydrogel matrix. A similar behavior was observed in other hydrogel matrices as the carboxymethylcellulose hydrogels that upon the incorporation of iron magnetic nanoparticles in concentrations of 0.5g of nanoparticles per gram of polymer demonstrated an increase in the storage modulus in rheometer analysis[32].[30]. Therefore, the iron core of MNPs behaves as an elastic material, which leads to an equivalent increase in the storage modulus as well as the energy dissipating potential, thus maintaining the range of values of tan δ of the formulations without nanoparticles. The low values of the loss factor of the hydrogel matrices are

indicative of the high elastic properties of these hydrogels suggesting a low energy dissipating potential. Overall the produced met CS hydrogels, independently of the presence of MNPs, displayed mechanical properties within the range of other hydrogel systems applied for tissue engineering including tendon regeneration and cartilage [33],[34].

Considering all the results obtained for MNPs including the biocompatibility assay, and metCS hydrogel matrix, the concentration of 200 μg/mL met-CS MNPs was chosen (met_{200} MAGPL hydrogels) for further engineering a magneto-responsive hydrogel with tunable features.

In order to understand the response of the hydrogel, in terms of degradation and swelling profile as well as if these properties can be remotely controlled by the application of an EMF, met_{200} MAGPL hydrogels were incubated under magnetic stimulation with 2.6 U/mg of HAse solution. HAse is one of the enzymes responsible for the *in vivo* degradation of CS [35], available at physiological concentrations ranging from 0.0059 U/mL in human plasma to 38.5 U/mL in human ovaries. Moreover it is present in plasma at concentrations of 2.6 U/mL[36]. The degradation of met-CS_{200} MAGPL hydrogel was completed in at least 17 days in the presence of HAse. In addition within this study, it was possible to confirm that the presence of magnetic field enhances the enzymatic degradation of the hydrogels. Studies on the CS degradation showed a complete degradation after one a two days in works with 0.02 U enzyme/mg of CS [37], thus suggesting that the incorporation of PL assisted the integrity of the hydrogel matrix. The influence of PL may be related to the presence of structural proteins that are not degraded by HAse.

Moreover, the stimulation of met-CS MNPs integrated in the matrix by EMF is likely to cause a temporary cyclic destabilization of the matrix, increasing the permeability of the matrix and consequently the capacity of HAse penetration as well as the diffusion of the aqueous solution into the hydrogel. This hypothesis is supported by the time frame necessary to hydrogels incubated without an enzymatic solution to reach the swelling equilibrium under magnetic stimulation. In fact the time that is needed to achieve the maximum swelling was lower in the case of EMF stimulation without affecting the integrity of the system.

Since the developed magnetic responsive hydrogels are also envisioned to be used as a GF delivery matrix, the release profile of PDGF-BB was assessed under static and EMF conditions.

The release profile of PDGF was chosen because it is one of the most interesting factors present in PL. This GF presents mitogenic and chemotactic effects which is of utmost importance for the recruitment of progenitor cells to the defects and for the stimulation of their proliferation aiming regenerative medicine approaches[17]. As expected, in the conditions with HAse solution, the

release occurs faster and it relates to the profile of degradation. Also, under magnetic stimulation the PDGF-BB release is apparently higher than in non-EMF conditions. This is in accordance to the work by Barbucci et all who showed the release of Doxorubicin incorporated in nanocellulose hydrogels was faster in the formulations under magnetic stimulation in hydrogels where the MNPs were physically incorporated in the matrix [30].

The modulation and sustained release of bioactive molecules such as GF available in PL, is one of the most investigated parameters for tissue regeneration. The system herein presented is therefore expected to allow the adjustment of the release accordingly with the needs of the applications, thus fitting the complex requirements of the regenerative process. In fact as hypothesized GFs as PDFGF establish linkages with matrix of GAG, and the growth factor release depend on the degradation rate of the polymer. Accordingly with Zavan and colleagues the GF interacts with GAGs and the release of these molecules it is just driven by the degradation of the material. Other transport phenomena such as the diffusion process within the polymeric matrix and in the aqueous solution did not affect the release rate. Thus it was proven in this case that the EMF could impact the release of bio-molecules[38].

Envisioning a therapeutic application of this versatile system, we proposed the biological assessment of the developed magnetic responsive 3D matrix having the tendon-to-bone interface as a potential target. Indeed, tendon-to-bone are roughly defined as an interconnection between two completely different tissues. Ideally, tissue engineering strategies should focus in replicating their complex cellular and biochemical composition reflecting the gradient of cells, biomolecules and ECM structural cues Therefore, met-CS_{200} MAGPL hydrogels hydrogel were designed as a two unit system, a "tendon" unit and a "bone" unit in a single and finally co-culture system, homing in one side, cells that would potentially promote the regeneration of new tendon, hTDCs, and in the other side, cells with potential for bone regeneration.

Human TDCs were chosen to be encapsulated in the tendon unit once they constitute a heterogeneous population of tendon resident cells which include mesenchymal stem cells known to mediate the reparative process after tendon injury[39]. For the bone unit hASCs pre differentiated into osteoblast like cells (pre-Ost) were chosen due to their recognized potential to differentiate into osteoblast like cells using standard differentiation protocols [40]. Moreover, hASCs were already proven to have the capacity for *in vivo* bone formation [41]. These units were produced and assessed as single units, and thus laden with hTDCs (tendon units) or with pre-Ost (bone units)

and as co-culture units with co-cultures of hTDCs and pre-Ost cells combining a tendon unit and a bone unit in a physical bond.

The biological performance of this system for interfacial strategies was firstly evaluated as single units. Herein, the proliferation and metabolic activity of tendon and bone units under EMF showed values similar to the ones obtained with non-magnetic stimulation conditions. This is an expected result, since magnetic forces do not negatively influence biological processes of the cells and is in line with other investigations showing that cells hTDCs seeded onto a magnetic constructs of starch poly-ε-caprolactone (SPCL) under EMF do not evidenced changes in metabolic activity and proliferation [10]. Contrarily the cell morphology and deposition of proteins related to an ECM in the single hydrogels units was influenced by cellular location on the hydrogel, at the surface or in the inner sections, but also by the type of cells and EMF stimulation.

Therefore, in the absence of EMF, the deposition of a tissue-like layer with spread cells enriched with ECM proteins was observed on the surface of the hydrogel. Inside the hydrogel, cells were rounded. In the core, cells maintained the viability, with a reduced deposition of ECM. Under magnetic stimulation cells remained with a rounded shape during the entire experiment being pre-Ost cells organized in clusters of cells visualized 21 days after the encapsulation. The deposition of matrix proteins, including tenascin-C and Osteopontin was apparently denser in the core of the hydrogel when compared to hydrogels cultured in non EMF conditions.

This results suggests that this versatile system can be used as a reservatory of cells with the capacity to adhere, proliferate and synthetize matrix in non-EMF conditions. Since the colonization without EMF increases with the time in culture, cells seem to be able to identify adhesion points in the matrix of the hydrogel to adhere and proliferate, principally at the surface. In fact Lamer and colleagues revealed that the adhesion of cells to the matrix needs time to maturate. In the case of EMF stimulation the adhesion locals are in “constant movement” due to the matrix destabilization as demonstrated in this work, and thus cells probably do not have time to maturate the adhesion to the surface and thus remained rounded [42].

Moreover as shown in this work, the presence of magnetic field impact the properties of the system, increasing its permeability which consequently improves the solutes diffusion and consequently the availability of nutrients and oxygen within the hydrogel. With this more “suitable” environment, cells were more prone to colonize and deposit matrix within the hydrogel core, forming the clusters of cells observed in the case in the case of pre-Ost. Interesting is the fact that EMF seems to stimulate the deposition of TNC by hTDCs and OPN by pre-Ost within the hydrogel.

Indeed this modulation of ECM synthesis within the core of the hydrogel can also be related with the activation of mechanotransduction pathways through the magnetic actuation in the cells[9]. Once tendon and bone are mechanically responsive tissues, EMF may induce local deformations in the cells by itself or through the vibration of the met-CS MNPs present in the matrix, and activate multiple intracellular processes namely expression of specific genes etc[9]. This hypothesis was confirmed by the quantification of gene expression, which suggest that the expression of specific genes related with tendon (tenascin-C) and osteogenesis (Osteopontin) tended to be enhanced after 21 days in the presence of magnetic field in the respective single unit. In fact, Gonçalves et al demonstrated that EMF led to an increase in the expression of tendon related genes under magnetic stimulation[11]. Also it was demonstrated that the stimulation with pulsed electromagnetic field led to an increase in deposition of bone ECM related proteins as well as calcium deposits[43].

Thus, considering the results obtained, the cell laden hydrogel matrices where produced as a co-culture hydrogel composed by a tendon unit and a bone unit to investigate the applicability of this versatile systems for tendon-to bone interface. As demonstrated for the single units, the metabolic activity of the co-culture systems was not affected by the magnetic stimulation. These results confirm that the produced hydrogel is suitable for encapsulating different types of cells and for further application in co-culture systems. Moreover contrary to single units in the developed co-culture systems it is clear the communication and interplay between the hTDCs and hASC in which after 21 days, both type of cells were spreaded at the surface of the hydrogel independently of the magnetic stimulation. In fact, cells produced deposits of ECM related markers of bone and tendon (*OPN, TEN*) after 21 days in culture. Once more, in the studied conditions both cell types displayed a round morphology during the entire experiment within the hydrogel. Moreover the deposition of bone and tendon related proteins was more evident in the bone and tendon zones, respectively of the co-culture system, which favors a "gradient" of matrix deposition As presented in the single units, the deposition of ECM related matrix seems to be higher inside of the hydrogel in EMF. This apparent proliferative and protein expression effect verified by immunolabeling assays is probably associated to the paracrine communication established between hTDCs and pre-Ost. Some reports demonstrated that cells secrete trophic factors that may stimulate tendon and bone ECM production and tissue remodeling[44]. Both type of cells likely produce a variety of cues, like release of cytokines that may have a crucial contribution for tissue maintenance and tissue regeneration [45], [46].

Nevertheless the interactions between these two type of cells in terms of paracrine signaling and extracellular matrix cues and how these cells influence each other behavior remains to be elucidated and should be deeply investigated in future studies.

The analysis to the expression of tenogenesis or osteogenesis-related genes from the cells present in the "bone", "tendon" or interface regions, revealed that the expression of tendon and bone related genes was apparently higher after 21 days in the correspondent unit of the hydrogel in non-magnetic conditions following the gradient of expression as also demonstrated by immunofluorescence. Under magnetic stimulation the gene expression was maintained constant over time without the formation of a clear gene expression of tendon-bone gradient.

Overall, the magnetic field has an impact in the modulation of the properties of the met-CS_{200} MAGPL hydrogels including the profile of swelling, degradation and release of biomolecules. Moreover in single hydrogel constructs, the EMF stimulate the expression of DCN and OPN in hTDCs and pre-Ost, respectively with the time in culture, while without EMF the cells were able to colonize and produce matrix. In the co-cultre system, the cells were able to colonize and produce matrix independently of the EMF stimulation and the gene expression seems to be stabilized and maintained along the time and independently of the type of cells. Again these results may be due to the interactions established between such different cells as hTDCs and pre-Ost. Moreover, the mechanisms involved in the overexpression and upregulation of genes in a co-culture system may be associated to multiple processes the cells respond to, and to the complex stimulatory environment provided by EMF (mechanical), PL (biochemical), met-CS matrix (topographical) from our systems.

3.6 Conlusions

The produced magnetic hydrogel was demonstrated to be multifunctional, enabling the possibility of controlling several intrinsic properties of the system, including degradation and swelling through the use of EMF. Besides, the release of GF from the construct could also be tuned through the use of this stimulation. Moreover, the developed system can be used as a cell carrier for different types of cells, thus demonstrating its applicability envisioning different applications in the field of TE. In fact, this versatile magnetic hydrogel was demonstrated to support the colonization of human tendon cells and pre-osteoblasts, proving its potential for the use in tissue interfaces, particularly tendon-to-bone

3.7 References

[1] Perea H, Aigner J, Heverhagen JT, Hopfner U, Wintermantel E. Vascular tissue engineering with magnetic nanoparticles: seeing deeper. Journal of tissue engineering and regenerative medicine. 2007;1:318-21.

[2] Li Q, Williams CG, Sun DD, Wang J, Leong K, Elisseeff JH. Photocrosslinkable polysaccharides based on chondroitin sulfate. Journal of biomedical materials research Part A. 2004;68:28-33.

[3] Li Y, Huang G, Zhang X, Li B, Chen Y, Lu T, et al. Magnetic Hydrogels and Their Potential Biomedical Applications. Advanced Functional Materials. 2013;23:660-72.

[4] Phillips JE, Burns KL, Le Doux JM, Guldberg RE, García AJ. Engineering graded tissue interfaces. Proceedings of the National Academy of Sciences. 2008;105:12170-5.

[5] Seidi A, Ramalingam M, Elloumi-Hannachi I, Ostrovidov S, Khademhosseini A. Gradient biomaterials for soft-to-hard interface tissue engineering. Acta Biomater. 2011;7:1441-51.

[6] Rees JD, Wilson AM, Wolman RL. Current concepts in the management of tendon disorders. Rheumatology. 2006;45:508-21.

[7] Galloway MT, Lalley AL, Shearn JT. The Role of Mechanical Loading in Tendon Development, Maintenance, Injury, and Repair. The Journal of bone and joint surgery American volume. 2013;95:1620-8.

[8] Klein-Nulend J, Bacabac R, Mullender M. Mechanobiology of bone tissue. Pathologie biologie. 2005;53:576-80.

[9] Santos LJ, Reis RL, Gomes ME. Harnessing magnetic-mechano actuation in regenerative medicine and tissue engineering. Trends in biotechnology. 2015;33:471-9.

[10] Santos L, Silva M, Goncalves AI, Pesqueira T, Rodrigues MT, Gomes ME. In vitro and in vivo assessment of magnetically actuated biomaterials and prospects in tendon healing. Nanomedicine (Lond). 2016;11:1107-22.

[11] Goncalves AI, Rodrigues MT, Carvalho PP, Banobre-Lopez M, Paz E, Freitas P, et al. Exploring the Potential of Starch/Polycaprolactone Aligned Magnetic Responsive Scaffolds for Tendon Regeneration. Advanced healthcare materials. 2016;5:213-22.

[12] Mattix B, Olsen TR, Gu Y, Casco M, Herbst A, Simionescu DT, et al. Biological magnetic cellular spheroids as building blocks for tissue engineering. Acta Biomaterialia. 2014;10:623-9.

[13] Shin MK, Kim SI, Kim SJ, Park SY, Hyun YH, Lee Y, et al. Controlled Magnetic Nanofiber Hydrogels by Clustering Ferritin. Langmuir. 2008;24:12107-11.

[14] Schexnailder P, Schmidt G. Nanocomposite polymer hydrogels. Colloid Polym Sci. 2009;287:1-11.

[15] Taskesen A, Ataoglu B, Ozer M, Demirkale I, Turanli S. Glucosamine-chondroitin sulphate accelerates tendon-to-bone healing in rabbits. Eklem hastaliklari ve cerrahisi = Joint diseases & related surgery. 2015;26:77-83.

[16] Lindahl U, Hook M. Glycosaminoglycans and their binding to biological macromolecules. Annual review of biochemistry. 1978;47:385-417.

[17] Crespo-Diaz R, Behfar A, Butler GW, Padley DJ, Sarr MG, Bartunek J, et al. Platelet Lysate Consisting of a Natural Repair Proteome Supports Human Mesenchymal Stem Cell Proliferation and Chromosomal Stability. Cell Transplantation. 2011;20:797-811.

[18] Babo P, Santo V, iacute, tor E, Duarte ARC, Correia C, et al. Platelet lysate membranes as new autologous templates for tissue engineering applications. Inflammation and Regeneration. 2014;34:033-44.

[19] Font Tellado S, Balmayor ER, Van Griensven M. Strategies to engineer tendon/ligament-to-bone interface: Biomaterials, cells and growth factors. Adv Drug Deliv Rev. 2015;94:126-40.

[20] Reddy LH, Arias JL, Nicolas J, Couvreur P. Magnetic Nanoparticles: Design and Characterization, Toxicity and Biocompatibility, Pharmaceutical and Biomedical Applications. Chemical Reviews. 2012;112:5818-78.

[21] Livak KJ, Schmittgen TD. Analysis of relative gene expression data using real-time quantitative PCR and the 2(-Delta Delta C(T)) Method. Methods (San Diego, Calif). 2001;25:402-8.

[22] Chen L, Zhang H, Li L, Yang Y, Liu X, Xu B. Thermoresponsive hollow magnetic microspheres with hyperthermia and controlled release properties. Journal of Applied Polymer Science. 2015;132:n/a-n/a.

[23] Apostolakos J, Durant TJS, Dwyer CR, Russell RP, Weinreb JH, Alaee F, et al. The enthesis: a review of the tendon-to-bone insertion. Muscles, Ligaments and Tendons Journal. 2014;4:333-42.

[24] Shearn JT, Kinneberg KRC, Dyment NA, Galloway MT, Kenter K, Wylie C, et al. Tendon Tissue Engineering: Progress, Challenges, and Translation to the Clinic. Journal of musculoskeletal & neuronal interactions. 2011;11:163-73.

[25] Václavíková E, Kvasnička F. Quality control of chondroitin sulphate used in dietary supplements. Czech Journal of Food Sciences. 2015;33:165-73.

[26] Lima J, Gonçalves AI, Rodrigues MT, Reis RL, Gomes ME. The effect of magnetic stimulation on the osteogenic and chondrogenic differentiation of human stem cells derived from the adipose tissue (hASCs). Journal of Magnetism and Magnetic Materials. 2015;393:526-36.

[27] Wang L-F, Shen S-S, Lu S-C. Synthesis and characterization of chondroitin sulfate–methacrylate hydrogels. Carbohydrate Polymers. 2003;52:389-96.

[28] Vallieres M, du Souich P. Modulation of inflammation by chondroitin sulfate. Osteoarthritis and cartilage / OARS, Osteoarthritis Research Society. 2010;18 Suppl 1:S1-6.

[29] Lim JJ, Temenoff JS. The effect of desulfation of chondroitin sulfate on interactions with positively charged growth factors and upregulation of cartilaginous markers in encapsulated MSCs. Biomaterials. 2013;34:5007-18.

[30] Barbucci R, Giani G, Fedi S, Bottari S, Casolaro M. Biohydrogels with magnetic nanoparticles as crosslinker: characteristics and potential use for controlled antitumor drug-delivery. Acta Biomater. 2012;8:4244-52.

[31] LeBoeuf RD, Raja RH, Fuller GM, Weigel PH. Human fibrinogen specifically binds hyaluronic acid. The Journal of biological chemistry. 1986;261:12586-92.

[32] Giani G, Fedi S, Barbucci R. Hybrid Magnetic Hydrogel: A Potential System for Controlled Drug Delivery by Means of Alternating Magnetic Fields. Polymers. 2012;4:1157.

[33] Domingues RM, Silva M, Gershovich P, Betta S, Babo P, Caridade SG, et al. Development of Injectable Hyaluronic Acid/Cellulose Nanocrystals Bionanocomposite Hydrogels for Tissue Engineering Applications. Bioconjugate chemistry. 2015;26:1571-81.

[34] Popa E, Santo V, Rodrigues M, Gomes M. Magnetically-Responsive Hydrogels for Modulation of Chondrogenic Commitment of Human Adipose-Derived Stem Cells. Polymers. 2016;8:28.

[35] Honda T, Kaneiwa T, Mizumoto S, Sugahara K, Yamada S. Hyaluronidases Have Strong Hydrolytic Activity toward Chondroitin 4-Sulfate Comparable to that for Hyaluronan. Biomolecules. 2012;2:549.

[36] Yeo Y, Highley CB, Bellas E, Ito T, Marini R, Langer R, et al. In situ cross-linkable hyaluronic acid hydrogels prevent post-operative abdominal adhesions in a rabbit model. Biomaterials. 2006;27:4698-705.

[37] Silva C, Novoa-Carballal R, Reis RL, Pashkuleva I. Following the enzymatic digestion of chondroitin sulfate by a simple GPC analysis. Analytica Chimica Acta. 2015;885:207-13.

[38] Zavan B, Vindigni V, Vezzu K, Zorzato G, Luni C, Abatangelo G, et al. Hyaluronan based porous nano-particles enriched with growth factors for the treatment of ulcers: a placebo-controlled study. Journal of materials science Materials in medicine. 2009;20:235-47.

[39] Bi Y, Ehirchiou D, Kilts TM, Inkson CA, Embree MC, Sonoyama W, et al. Identification of tendon stem/progenitor cells and the role of the extracellular matrix in their niche. Nat Med. 2007;13:1219-27.

[40] Jaiswal N, Haynesworth SE, Caplan AI, Bruder SP. Osteogenic differentiation of purified, culture-expanded human mesenchymal stem cells in vitro. Journal of cellular biochemistry. 1997;64:295-312.

[41] Amini AR, Laurencin CT, Nukavarapu SP. Bone tissue engineering: recent advances and challenges. Critical reviews in biomedical engineering. 2012;40:363-408.

[42] Lamers E, te Riet J, Domanski M, Luttge R, Figdor CG, Gardeniers JG, et al. Dynamic cell adhesion and migration on nanoscale grooved substrates. Eur Cell Mater. 2012;23:182-93; discussion 93-4.

[43] Tsai MT, Li WJ, Tuan RS, Chang WH. Modulation of osteogenesis in human mesenchymal stem cells by specific pulsed electromagnetic field stimulation. Journal of orthopaedic research : official publication of the Orthopaedic Research Society. 2009;27:1169-74.

[44] Beredjiklian PK, Favata M, Cartmell JS, Flanagan CL, Crombleholme TM, Soslowsky LJ. Regenerative versus reparative healing in tendon: a study of biomechanical and histological properties in fetal sheep. Annals of biomedical engineering. 2003;31:1143-52.

[45] Chen L, Tredget EE, Wu PYG, Wu Y. Paracrine Factors of Mesenchymal Stem Cells Recruit Macrophages and Endothelial Lineage Cells and Enhance Wound Healing. PloS one. 2008;3:e1886.

[46] Shin L, Peterson DA. Human mesenchymal stem cell grafts enhance normal and impaired wound healing by recruiting existing endogenous tissue stem/progenitor cells. Stem cells translational medicine. 2013;2:33-42.

CHAPTER IV Conclusions and Final Remarks

4. Conclusions and Final Remarks

The main goal of this work was to develop a versatile photopolimerizable hydrogel based on a matrix of chondroitin sulfate functionalized with methacrylated groups enriched with platelet lysate that could be remotely controlled or further manipulated ex vivo under the actuation of an external magnetic field. Herein this system was proposed to meet a major challenge for tissue regeneration which is the possibility to tune the intrinsic properties of a construct to the needs of tissue microenvironment and to the complex process of regeneration.

Based on that, a magnetic met-CS hydrogel enriched with platelet lysate incorporating met-CS MNPs within the matrix was successfully produced. In this system we observed that properties as the swelling profile orthe rate of degradation could be externally manipulated by the application of ECM. Moreover the sustained release of growth factors (GFs) such as PDGF-BB from the PL confirms the potential of using the developed hydrogel as a GF delivery system for tissue regeneration strategies. Indeed, EMF was shown to increase the rate of PDGF-BB released from the hydrogels and likely improve the solutes diffusion and consequently the availability of nutrients and oxygen within the hydrogel. However it is not clear if this effect is due to the activation of met CS MNPs incorporated within the hydrogel through the stimulation of EMF or if it is just the presence of the magnetic field by itself. Thus, it could be important to assess the profile of GF release just with the use of the hydrogel without met-CS MNPs.

Moreover the *in vitro* studies performed to assess the impact of this versatile system envisioning tendon-to-bone interfaces reveled that hTDCs and pre-Ost cultured alone in single hydrogel units or in co-culture in a hydrogel composed of two units were able to colonize and produce matrix thus forming tissue-like structures. The application of EMF in this system stimulated the genetic expression of DCN in hTDCs with the time in culture. Once the system permit the cell colonization and production of specific ECM proteins synthesized by different type of cells especially at later time points and the EMF stimulation increased the genetic expression of tendon genes, it could be interesting to assess the possible impact of alternating the application of EMF or just keep the actuation of the EMF for shorter periods of time. In fact this type of short EMF application in already applied in physiatrist patients with problems in musculoskeletal tissues, where a pulsed electromagnetic field is commonly used to bridge a non- or delayed bone fracture.

Neverthess, this system reveled to be a versatile construct that can fit their use for diverse areas of tissue regeneration including tissue interfaces like tendon-to-bone interface. In the co-culture system the two type of cells were able to proliferate and synthetize matrix in both conditions but the values of gene expression were maintained constant during the experience. In this particular case of tendon-to-bone interface it is important to perform further investigations in order to understand the interactions between these two types of cells in terms of paracrine signaling and extracellular matrix cues and how these cells influence each other and to understand the possible impact of EMF in native enthesis. To our knowledge the impact of EMF for tendon-to-bone interface has not been properly assessed and further studies on mechanosensing and mechanotranslation mechanisms of cells in response to EMF would greatly benefit the interfacial strategies towards interface tissue regeneration. Moreover this system can offer a possibility of being injectable directly into a defect and further polymerized, thus being and additional advantage using minimally invasive procedure. Once this system possess magnetic responsiveness, hydrogel may be used as magnetic building blocks in order to create 3D structures with increased complexity towards recreating or producing tissue-like structures for biomedical applications.

Overall, the results reported in this Thesis, show that this magnetic responsive hydrogel represents a valuable resource for tissue engineering, not only as a controllable source of GF from PL in which the properties of the system could be externally modulated through EMF stimulation but also as a cell carrier.

Synthesis and characterization of methacrylated chondroitin sulfate

CS was successfully modified through a reaction with methacrylic anhydride (MA) (Figure 3.1), originating methacrylic groups in its backbone. The efficiency of the modification process was evaluated by NMR spectroscopy (Figure A.1). The degree of substitution which corresponds to the methacryloyl groups per disaccharide repeat unit, was calculated from the NMR spectrum as the ratio between the relative peak integrations of the methacrylate protons (δ 5.77 – 6.20 ppm) and the methyl protons of CS (δ 2.05 ppm). The degree of substitution of methacrylated CS polymer was was 24%.

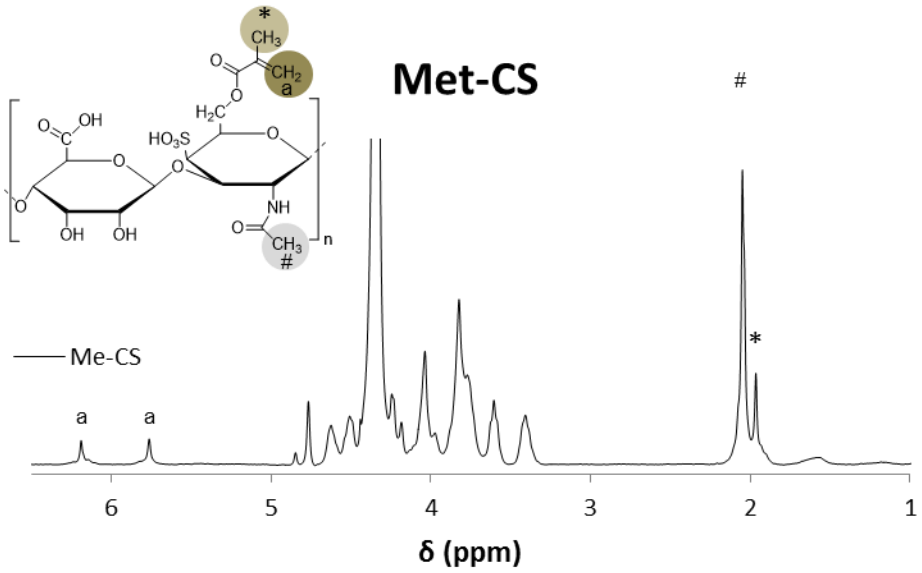

Figure A.1: ^{1}H NMR spectrum of methacrylated chondroitin sulfate (met-CS)